



THE UNIVERSITY OF QUEENSLAND
AUSTRALIA

Characteristics of unification: exploring the tension between quantum and gravitational physics

C. T. Marco Ho
BSc (Hons), BSc

*A thesis submitted for the degree of Doctor of Philosophy at
The University of Queensland in 2019
School of Mathematics and Physics*

Abstract

Ever since the bifurcation of classical physics into general relativity and quantum physics, physicists have sought a unified theory of quantum gravity. However, the profound mathematical and conceptual difference between the two theories has meant little success. Despite this, the partial unification achieved in quantum field theory in curved spacetime (QFTCS) has yielded novel phenomena such as Hawking radiation and raised conceptual questions such as the problem of time and the black hole information paradox. While proposed grand syntheses such as string theory and loop quantum gravity approach the problem from a top-down perspective, toy theories and in particular, the continued study of QFTCS—constituting the bottom-up approach—address problems of unification with a stronger empirical basis. Recently, a new field known as relativistic quantum information has applied techniques and concepts from quantum optics & computing to QFTCS and toy theories. In this thesis, I utilise relativistic quantum information as well as standard techniques from QFTCS to investigate four projects.

In the first project, we consider the black hole information paradox and the associated firewall paradox and suggest a modification of the standard black hole theory. We propose that the vacuum state of a scalar field around a black hole is a modified Unruh vacuum. In (1+1) dimensions, we show that a free-faller close to an event horizon can be modelled as an inertial observer in a modified Minkowski vacuum. The modification allows for information-leaking correlations at high frequencies. Using a Gaussian detector centred at k_0 , we find that the expectation value of the number operator for a detector crossing the horizon is proportional to $1/|k_0|$, implying that the free-faller will observe unbounded numbers of high energy photons, i.e. a firewall.

In the second project, we derive the theory of a scalar field in Minkowski spacetime and its coupling with gravitational waves. Using Feynman diagrammatic techniques, we identify the reason why particles are not created by linear plane gravitational waves up to arbitrary orders in Feynman diagrams. We then extend our theory to second order gravitational waves & diagrams and show how non-linear waves could create particles. Finally, we show how the gravitational quasinormal modes (QNMs) of a Schwarzschild black hole play the role of a multimode squeezer that can generate particles. For a minimally coupled scalar field, the QNMs “squeeze” the initial state of the scalar field and produce scalar particles.

In the third project, we examine acausal quantum mechanics and causal inequalities. Processes with an indefinite causal structure may violate a causal inequality, which quantifies quantum correlations that arise from a lack of causal order. We show that when the inequalities are analysed with a Gaussian-localised field theoretic definition of particles and labs, the causal indeterminacy of the fields themselves allows a causal inequality to be violated within the causal structure of Minkowski spacetime. We also quantify the violation of the inequality and determine the optimal ordering of observers.

Finally, in the fourth project, we derive the theory for the levitation of a mirror by a laser. Using a Fabry-Pérot cavity oriented vertically, a laser maintains a circulating steady state ‘bed’ of photons that supports a freely floating upper mirror. The fluctuations of the mirror-cavity system around the steady state then act as a linearised quantum optomechanical system. We analyse the stability of the system

and conclude that for experimentally accessible parameters, the mirror must be 'blue detuned' and would normally be considered in optomechanics as weakly coupled to the cavity. However, when we calculate the entanglement between the mirror and cavity using the covariance matrix and we find fairly strong entanglement (15 ebit peak) between them. Finally, we find that the mirror's position is squeezed below shot noise.

Declaration by author

This thesis is composed of my original work, and contains no material previously published or written by another person except where due reference has been made in the text. I have clearly stated the contribution by others to jointly-authored works that I have included in my thesis.

I have clearly stated the contribution of others to my thesis as a whole, including statistical assistance, survey design, data analysis, significant technical procedures, professional editorial advice, financial support and any other original research work used or reported in my thesis. The content of my thesis is the result of work I have carried out since the commencement of my higher degree by research candidature and does not include a substantial part of work that has been submitted to qualify for the award of any other degree or diploma in any university or other tertiary institution. I have clearly stated which parts of my thesis, if any, have been submitted to qualify for another award.

I acknowledge that an electronic copy of my thesis must be lodged with the University Library and, subject to the policy and procedures of The University of Queensland, the thesis be made available for research and study in accordance with the Copyright Act 1968 unless a period of embargo has been approved by the Dean of the Graduate School.

I acknowledge that copyright of all material contained in my thesis resides with the copyright holder(s) of that material. Where appropriate I have obtained copyright permission from the copyright holder to reproduce material in this thesis and have sought permission from co-authors for any jointly authored works included in the thesis.

Publications included in this thesis

1. [1] Ho, C. M. *et al.* Black hole field theory with a firewall in two spacetime dimensions. *Physical Review D* **94**, 081502 (Oct. 10, 2016)
2. [2] Su, D. *et al.* Black hole squeezers. *Physical Review D* **96**, 065017 (Sept. 25, 2017)

Submitted manuscripts included in this thesis

1. [3] Ho, C. T. M. *et al.* Violation of a causal inequality in a spacetime with definite causal order. *arXiv:1804.05498 [quant-ph]*. arXiv: 1804.05498 (Apr. 16, 2018)

Other publications during candidature

1. [4] Su, D. *et al.* Quantum circuit model for non-inertial objects: a uniformly accelerated mirror. *New Journal of Physics* **19**, 063017 (2017)

Contributions by others to the thesis

No contributions by others

Statement of parts of the thesis submitted to qualify for the award of another degree

No works submitted towards another degree have been included in this thesis.

Research involving human or animal subjects

No animal or human subjects were involved in this research.

Acknowledgments

Firstly, thanks go to my family for supporting me throughout my studies and for suffering quietly. To my supervisors Tim and Robb, thanks for the guidance and help throughout the PhD. To my office-mates and friends, David Cavanagh and Amie Khosla, thanks for listening to my complaints and for sanity preserving tea breaks. Thanks also go to my co-authors, Daiqin Su, Christina Giarmatzi and Fabio Costa for their helpful collaboration and technical assistance. Finally, to my Wednesday dinner buddies, Elise Kenny and Ben Duffus, thanks your company and friendship during our much needed mid-week breaks.

Financial support

This research was supported by the Australian Government Research Training Program (RTP) Scholarship, the Natural Sciences and Engineering Research Council of Canada and the Australian Research Council Centre of Excellence for Quantum Computation and Communication Technology (Project No. CE170100012)

Keywords

Quantum gravity, relativistic quantum information, black holes, firewall, particle creation, gravitational waves, particle creation, causal inequalities, levitating mirror, quantum optomechanics.

Australian and New Zealand Standard Research Classifications (ANZSRC)

ANZSRC code: 020105, General Relativity and Gravitational Waves, 35%

ANZSRC code: 020602, Field Theory and String Theory, 40%

ANZSRC code: 020604, Quantum Optics, 25%

Fields of Research (FoR) Classification

FoR code: 0201, Astronomical and Space Sciences 35%

FoR code: 0206, Quantum Physics, 65%

For my family who still look puzzled whenever I talk about my thesis,
for my friends, without whom this thesis would've been finished earlier,
and finally for my supervisors, without whom there would be no thesis.

Contents

Abstract	ii
Contents	ix
List of figures	xii
List of Tables	xiii
List of conventions, abbreviations and symbols	xv
1 Introduction	1
2 Canonical quantisation in curved spacetime	5
2.1 Renormalisation group and the action for a scalar field	5
2.2 Positive frequency modes	8
2.3 General formulation for modes	10
2.3.1 Bogolyubov transformations between sets of modes	11
2.4 The Unruh effect	11
2.4.1 Derivation of the Unruh effect	15
2.4.2 Correlations in the Minkowski vacuum	16
2.5 Quantum field theory around a Schwarzschild black hole	17
2.5.1 An analogy to Unruh modes	19
2.5.2 Hawking radiation	22
2.6 Unitary inequivalence	23
2.7 Conclusion	24
3 Black hole field theory with a firewall	25
3.1 Unitarity and Black hole complementarity	26
3.2 Firewall	28
3.3 Boulware and Unruh vacua, and Black Holes	29
3.4 Correspondence between Schwarzschild and Rindler metrics	30
3.5 Motion of the falling observer	31

3.6	Number expectation for an observer coupling to Minkowski modes in the modified Minkowski vacuum	32
3.7	Position dependent response to the firewall	34
3.8	Cutoff	35
3.9	Squeezing	36
3.10	Correlations and leaking information	37
3.11	Conclusion	37
4	Particle creation by gravitational waves	39
4.1	Linear gravitational waves in Minkowski spacetime	39
4.2	Path integral formalism	41
4.2.1	Path integrals for fields	42
4.2.2	Correlation/Green's functions	43
4.2.3	Φ^4 Interactions	45
4.2.4	Vacuum bubbles	47
4.2.5	Momentum space Feynman diagrams	47
4.3	Scalar field in gravitational waves	48
4.4	Particle creation from classical electromagnetic field	51
4.5	Diagrams and gravitational waves to second-order	52
4.6	Particle creation by quasi-normal modes	55
4.6.1	Coupling between QNMs and the scalar field	55
4.6.2	Gravitational quasi-normal modes	57
4.6.3	Time-evolution with quasi-normal modes	57
4.7	Conclusion	59
5	Violation of a causal inequality in a spacetime with definite causal order	61
5.1	Causal inequalities	62
5.2	Gaussian field modes	63
5.3	Definition of a closed lab	64
5.4	Physical setup and violation of inequality	65
5.5	The mode selective mirror	68
5.6	Measurements with different timing precision than the mode	69
5.7	Feedback loop for a CNOT gate	70
5.8	Conclusion	72
6	Optical levitation of a mirror	75
6.1	Quantum Optomechanics	76
6.2	Hamiltonian of the system	77
6.3	Markov approximation for cavity and mirror coupled to separate baths	78
6.3.1	The Langevin parameters and optical cavity	78

6.4	Equations of motion	79
6.5	Conditions on parameters and Detuning	80
6.5.1	Detuning of the steady state solutions	81
6.6	Standard optomechanical theory	82
6.6.1	Strong coupling	83
6.7	Linearised Hamiltonian	83
6.8	Numerical study	85
6.8.1	Stability	85
6.8.2	Damping	87
6.9	Frequency space solution to linearised equations of motion	88
6.9.1	Covariance matrix	92
6.9.2	Entropy of entanglement	95
6.9.3	Diagonalisation of the Covariance matrix	96
6.9.4	Quadrature variances	96
6.10	Conclusion	97
7	Conclusion	99
	Bibliography	101
8	Floating Mirror covariance matrix elements	115

List of figures

2.1	Minkowski spacetime with Minkowski and Rindler coordinates.	12
2.2	Penrose diagram of the maximally extended, eternal black hole.	20
3.1	A cartoon of the information paradox and the firewall.	28
3.2	Correspondence between Schwarzschild and Minkowski inertial trajectories	31
3.3	Firewall as a function of position and cutoff.	34
3.4	Left moving and right moving modes of the Firewall.	35
5.1	Inequality violation laboratory setup.	65
5.2	Three regimes of maximal inequality violation.	67
5.3	Probability of success as a function of wavepacket width.	68
5.4	The derivative of the probability of success.	68
5.5	Mode selective mirror.	69
5.6	Cnot gate with a cross Kerr non-linearity.	70
5.7	CNOT gate with zero-time feedback.	71
6.1	The floating mirror.	82
6.2	Energy level diagram for the floating mirror system.	86
6.3	Stability analysis of the floating mirror.	86
6.4	Steady state parameters of the floating mirror as a function of dimensionless power.	87
6.5	The ‘mirror’ damping as a function of dimensionless power.	88
6.6	The ‘mirror’ frequency as a function of dimensionless power.	89
6.7	The ‘cavity’ damping as a function of dimensionless power.	89
6.8	The ‘cavity’ frequency as a function of dimensionless power.	90
6.9	Entropy of entanglement between the mirror and the cavity.	95
6.10	3D plots of the variance of cavity Q and P quadratures.	96
6.11	3D plots of the variance of mirror Q and P quadratures.	97

List of Tables

List of conventions, abbreviations and symbols

Natural units are used except where noted. In these units, Boltzmann's constant k_B , the speed of light c , the universal gravitational constant G and the reduced Planck's constant \hbar are all equal to 1.

Einstein notation is used throughout. Repeated superscript and subscript indices are to be summed over.

Latin indices i, j, k &c. range over spatial coordinates, i.e. $A^i B_i = (A^1 B_1 + A^2 B_2 + A^3 B_3)$.

Greek indices μ, ν , &c. range over spatial and time coordinates. The time coordinate is denoted by the index, 0. I.e.,

$$A^\mu B_\mu = (A^0 B_0 + A^1 B_1 + A^2 B_2 + A^3 B_3).$$

The time derivative of an object is sometimes denoted using the overdot notation. i.e., $\dot{\phi} = \frac{\partial \phi}{\partial t}$.

Other partial derivatives are sometimes denoted by ∂_μ , occasionally, a notation is used where the coordinate variable is used in place of the index. For example, the partial derivatives of the coordinates (t, x, y, z) can be represented by ∂_0 or ∂_t , ∂_1 or ∂_x , ∂_2 or ∂_y and ∂_3 or ∂_z .

Covariant derivatives are denoted by ∇_σ and are defined for arbitrary tensors with rank (k, l)

$$\begin{aligned} \nabla_\sigma T^{\mu_1 \mu_2 \dots \mu_k}_{\nu_1 \nu_2 \dots \nu_l} = & \partial_\sigma T^{\mu_1 \mu_2 \dots \mu_k}_{\nu_1 \nu_2 \dots \nu_l} \\ & + \Gamma^{\mu_1}_{\sigma \lambda} T^{\lambda \mu_2 \dots \mu_k}_{\nu_1 \nu_2 \dots \nu_l} + \Gamma^{\mu_2}_{\sigma \lambda} T^{\mu_1 \lambda \dots \mu_k}_{\nu_1 \nu_2 \dots \nu_l} + \dots + \Gamma^{\mu_k}_{\sigma \lambda} T^{\mu_1 \mu_2 \dots \lambda}_{\nu_1 \nu_2 \dots \nu_l} \\ & - \Gamma^\lambda_{\sigma \nu_1} T^{\mu_1 \mu_2 \dots \mu_k}_{\lambda \nu_2 \dots \nu_l} - \Gamma^\lambda_{\sigma \nu_2} T^{\mu_1 \mu_2 \dots \mu_k}_{\nu_1 \lambda \dots \nu_l} - \dots - \Gamma^\lambda_{\sigma \nu_l} T^{\mu_1 \mu_2 \dots \mu_k}_{\nu_1 \nu_2 \dots \lambda} \end{aligned}$$

The transpose, complex conjugate and the hermitian conjugate of a vector, operator or complex function A is denoted, A^T , A^* and A^\dagger respectively.

Bold letters—e.g. $\mathbf{A} = (A^x, A^y, A^z)^T$ —denote spatial components of vectors.

$\delta_\nu^\mu, \delta_{ij}$ are examples of the Kronecker delta.

For an n -dimensional coordinate system (x_1, x_2, \dots, x_n) , the n -dimensional Dirac delta function is denoted by $\delta^{(n)}(\mathbf{x} - \mathbf{y}) = \delta(x_1 - y_1) \delta(x_2 - y_2) \cdots \delta(x_n - y_n)$.

The sign convention for various General Relativity tensors are defined below.

The Minkowski metric tensor is denoted by $\eta_{\mu\nu}$. The signature we will use for metrics is $(-, +, +, +)$. The metric in coordinate based geometric notation is,

$$\mathbf{g} = g_{\mu\nu} \mathbf{d}x^\mu \otimes \mathbf{d}x^\nu.$$

Christoffel symbol

$$\Gamma_{\mu\nu}^\rho = \frac{1}{2} g^{\rho\lambda} \left(\partial_\mu g_{\nu\lambda} + \partial_\nu g_{\mu\lambda} - \partial_\lambda g_{\mu\nu} \right)$$

Riemann curvature tensor

$$R^\sigma{}_{\rho\mu\nu} = \left(\partial_\mu \Gamma^\sigma{}_{\nu\rho} + \Gamma^\sigma{}_{\mu\kappa} \Gamma^\kappa{}_{\nu\rho} \right) - \left(\partial_\nu \Gamma^\sigma{}_{\mu\rho} + \Gamma^\sigma{}_{\nu\kappa} \Gamma^\kappa{}_{\mu\rho} \right)$$

Ricci tensor

$$R_{\mu\nu} = R^\sigma{}_{\mu\sigma\nu}$$

Ricci scalar

$$R = R_{\mu\nu} g^{\mu\nu}$$

Geodesic equation

$$\frac{d^2 X^\rho}{dl^2} + \Gamma^\rho{}_{\mu\nu}(X(l)) \frac{dX^\mu}{dl} \frac{dX^\nu}{dl} = 0$$

Abbreviations	
QFT	Quantum Field Theory
QFTCS	Quantum Field Theory on curved spacetime
QNM	Quasi-normal modes
GR	General Relativity
EFE	Einstein field equations
h.c.	Hermitian conjugate

Symbols	
Φ	Scalar field
$g_{\mu\nu}$	Metric tensor

$\eta_{\mu\nu}$	Minkowski metric
g	Determinant of the metric
\Re	Real part
\Im	Imaginary part

Chapter 1

Introduction

Since the synthesis of Special Relativity (SR) and Quantum Mechanics (QM) into Quantum Field Theory (QFT) and the formulation of the electromagnetic, weak and strong interactions as quantum field theories, physicists have searched for a quantum description of gravity. There are two leading motivations. The first motivation is a philosophical belief among some physicists that a singular, parameter-free, ‘theory of everything’ is the final goal of physics. In this respect, the disparate nature of QM and General Relativity (GR) and their separate areas of applicability is highly undesirable. This motivation was born from the successes⁵ of QFT in explaining the electrodynamic, weak and strong interaction; in particular, the unification^{6,7} of the electrodynamic and weak interaction into a single interaction have led to suggestions of a grand unification with the strong interaction and a belief in a ‘theory of everything’ encompassing gravitation. The second motivation is the conflicting mathematical formulation of GR and QM and philosophical conflicts between their postulates and interpretation. Take one particular example: QM or QFT is always formulated on a fixed background of spacetime. QFT in flat spacetime relies vacuum states and particles which—as we will see in a later chapter—are observer dependent. Much of the techniques such as path integrals and Fourier analysis depend on a global techniques possible only because of a static Minkowski spacetime. Even the extension of QFT to curved spacetime relies on a classical background spacetime and the mathematical formulation relies on slicing spacetime into constant-time hypersurfaces. Meanwhile, GR posits that spacetime is dynamic and curved and its evolution is given by the non-linear Einstein field equations (EFE),

$$R_{\mu\nu} - \frac{1}{2}Rg_{\mu\nu} = \frac{8\pi G}{c^4}T_{\mu\nu}. \quad (1.1)$$

$R_{\mu\nu}$ is the Ricci tensor, R is the Ricci scalar, both of which are built from the metric, $g_{\mu\nu}$ which quantifies distances in the spacetime. $T_{\mu\nu}$ is the Energy-Momentum tensor that quantifies the energy of matter in the universe. As far as we know the matter in the universe appears to be explained by quantum physics so $T_{\mu\nu}$ must be an operator on the Hilbert spaces of matter. But if this were so then the Ricci and metric tensors must also be operators. However it is no simply matter to quantise gravity. The different dynamics and the roles that time plays in QFT and GR is known as the problem of time;

this conceptual conflict is particularly evident when attempting to quantise gravity.*

QFT can usually be applied in a straightforward manner to a classical field. One might think that to quantise gravity, we should view the metric as a field that could be canonically quantised. This naive quantisation treats the metric $g_{\mu\nu}$ as the dynamic object in our QFT and quantises it using the canonical formalism or the path integral formalism. The Einstein field equations are non-linear, in the language of QFT, we say that the metric is self-interacting. One way to make sense of interacting theories is to require them to be perturbatively renormalisable⁷. Unfortunately, canonical quantum gravity has been shown to be perturbatively non-renormalisable.^{5,10,11} There are now attempts^{12–14} to understand non-perturbative theories but this is still a nascent field. String theory and Loop quantum gravity have been proposed to alleviate these difficulties but both have major unsolved problems. String theory, in particular, is prolific in predictions but bereft of uniqueness.^{15,16} Loop quantum gravity is still unable¹⁷ to provide a semiclassical limit to GR. So far these proposals have not borne out their initial promises.

As Nicolai *et al.*¹⁷ persuasively puts, the major questions in quantum gravity are,

... what does one mean when one speaks of a consistent theory of quantum gravity? And what are the basic properties that such a theory should satisfy?

These are questions that one can ask even without a theory of quantum gravity. Perhaps we can find some answers to these questions with a quantum theory of fields on a classical curved spacetime. In trying to quantise gravity, we seek to understand how quantum fields affect gravity. The complementary quest is understanding is how gravity affects quantum fields. As was discovered by Fulling,¹⁸ Davies,¹⁹ Hawking²⁰ and others, even without quantising gravity, Quantum Field Theory on Curved Spacetime (QFTCS)—by looking at how classical gravity affects quantum fields—introduces novel physics and allows us to examine in detail the conflicts between the two theories as well as raising a number of important questions we must resolve. The Unruh effect—where radiation is observed by an accelerating detector—and Hawking radiation—where black holes thermally radiate at a temperature inversely proportion to their mass—are two examples of quantum effects in a classical curved spacetime. Hawking radiation, in particular, provokes multifarious questions, including, but not limited to: What is the state of quantum fields around black holes?^{21,22} Do black holes completely evaporate^{23–26} from Hawking radiation? Do black holes even form?²¹ These are important questions that may be answerable using QFTCS. The motivation for this research project is that there are unresolved problems in this arena that may shed some light on quantum gravity.

* In the Hamiltonian formulation⁸ of general relativity, the Hamiltonian is a constraint that must vanish ($H = 0$). If we were to naively quantise⁵ general relativity, we get the Wheeler-DeWitt equation $H|\Psi\rangle = 0$. In classical and quantum theory, we know that the Hamiltonian generates time translation (evolution). If we forget about quantum for the moment, in what sense does $H = 0$ mean in general relativity? General relativity—often called classical—is nonetheless a significant modification of our classical conception of dynamics. The solution to the classical problem of time is found by weakening the concept of time and incorporating it into spacetime. A solution of the Einstein field equations determines a ‘spacetime’ that exists as a single entity. I.e., there is no conception of time as a separate entity. In contrast, in QFT, time and space are external parameters. This is in keeping with special relativity where the conception of spacetime also exists but is not dynamic. In a fixed Lorentz (inertial) frame, time evolution of QFT using the variable $t = x^0$ is possible. However, in the Wheeler-DeWitt equation, time doesn’t appear at all. For more details on this point, see Kiefer⁵ pg. 136 or Oriti⁹ pg. 6.

Recently, a new field known as relativistic quantum information²⁷ has incorporated techniques and concepts from quantum optics & computing to analyse the fascinating intersection between gravity and quantum theory. So far it has proven promising with results ranging from using completely positive maps to study causal orders²⁸ to how entanglement^{29,30} can be ‘harvested’ from the entanglement of vacuum states to allow communication without a quantum channel.

In this thesis I have used these techniques as well as the methods first sketched by Fulling, Davies, Hawking and others when QFTCS was first laid out. I will focus on the conflict between QFT and GR in the arena of the black hole and explore how the techniques of quantum optics and relativistic quantum information can be applied to investigate other regimes where quantum physics and gravity overlap, in particular: indefinite causal ordering and the optical levitation of mirrors.

In Chapter 2 I introduce the basic concepts of canonical quantisation in curved spacetime, quantising the field in Minkowski spacetime using both Rindler and Minkowski approaches and show the observer dependence of particles and vacuum. We then explore the quantisation of the field in Schwarzschild spacetime and the Hawking effect, noting the issue of unitary inequivalence.

I discuss the black hole information paradox and the firewall in Chapter 3 and I analyse the behaviour of a new black hole field theory that I propose based on unitary inequivalence and the firewall paradox.

Then in Chapter 4, using Feynman diagrammatic techniques I show how linear plane gravitational waves in flat spacetime cannot cause any particle creation through its coupling to a scalar field. Extending to second order diagrams and second order gravitational waves does not lead to particle creation. Finally I discuss our paper where we showed the particle creation due to gravitational waves around a Schwarzschild black hole.

In Chapter 5 I investigate the process matrix formalism and causal inequalities. I show that when the inequalities are analysed with a Gaussian-localised field theoretic definition of particles and labs, the causal indeterminacy of the fields themselves allows a causal inequality to be violated within the causal structure of Minkowski spacetime. I quantify the violation of the inequality and determine the optimal ordering of observers.

Finally in Chapter 6 I derive the theory for a floating mirror levitated by a mirror, study the steady state solutions and their stability, analyse the linearised perturbations around the steady state and quantify the entanglement in the system.

Chapter 2

Canonical quantisation in curved spacetime

In this chapter we will review quantisation in curved spacetime. Many concepts will need to be clarified, generalised and distinguished from the flat space. I will assume that the reader is acquainted with general relativity and has some familiarity with Quantum Field Theory in Minkowski spacetime.* We will consider the action of a scalar field and its quantisation in curved spacetime. Then we will introduce the concepts of positive frequency modes and Bogolyubov transformations.

In the second half of this chapter, we will look at the Unruh effect. While Quantum Field Theory in Curved spacetime (QFTCS) is not strictly necessary for the Unruh effect, its close analogy with the Hawking effect will serve to elucidate concepts of QFTCS. This will serve as motivation and analogy for deriving the scalar field theory around an eternal black hole. From this, we will discuss the Hawking effect and unitary inequivalence.

2.1 Renormalisation group and the action for a scalar field

Let us consider a scalar field $\Phi(x)$ from which we want to form an action that is invariant under general coordinate transformations, also known as general invariance or general covariance. This means that we must have an action of the form $S = \int d^4x \sqrt{|g|} (\dots)$. The determinant of the metric is g and the terms in the brackets must be scalars. As a starting point, any derivative of the field must be a covariant derivative.** To determine the Lagrangian for our field, we need to appeal to two main ideas.

The first is the renormalisation group method⁷ which can give us constraints on the form of the Lagrangian. The renormalisation group approach assumes that there is a fundamental high energy cutoff Λ_{cutoff} , given by unknown physics at some fundamental scale.[†] Renormalisation theory says that an arbitrarily complicated theory at fundamental scale, simplifies to a low-energy effective theory. The coupling constants of terms with higher powers of Φ than 4, (e.g. Φ^5 , Φ^6 , &c.) and higher powers of the

* In a later footnote I will describe how to obtain the flat space theory as a special case of the curved space theory presented in this chapter.

** For scalar fields, this step is actually unnecessary as the covariant derivative of a scalar is the same as the partial derivative.

[†] Perhaps due to some fundamental quantised nature of spacetime, usually considered to be the Planck length.

first derivatives (e.g. $(\nabla_\mu \Phi \nabla^\mu \Phi)^2$, $(\nabla_\mu \Phi \nabla^\mu \Phi)^3$, &c.) become negligible at lower energies/momenta ($\sqrt{p_\mu p^\mu} \ll \Lambda_{\text{cutoff}}$). This allows us to ignore such terms in our effective theory for the scalar field.

The other idea is the constraint is that we must prevent higher order derivatives (e.g. $\nabla_\mu \nabla_\nu \Phi \nabla^\mu \nabla^\nu \Phi$) of the field from appearing because they lead^{31,32} to a lack of lower-energy bound (i.e. the energy can go infinitely negative) and to more degrees of freedom which requires more initial Cauchy data.*

Actually, both of these constraints can and should be questioned. First, the renormalisation group methods must be extended to curved spacetime. This has been done by Hollands and Wald³³ but they did not analyse the higher order terms.** There has been some work^{31,32,37} in trying to include higher derivatives of the field without the usual drawbacks mentioned.

Although we are trying to work in a regime of low energy, fields are believed to pervade all spacetime. Certainly there are always regions (e.g. near the singularity of the black hole) where there are incredibly large curvatures and at these points a low energy effective theory is not adequate. How does this affect predictions using the effective theory? No one knows. Think back to the early 20th century, before quantum theory. Who would have thought that the quantum nature of electromagnetism was the key to the ultraviolet catastrophe? Certainly our rules of thumb on where quantum mechanics/field theory is important seem to fail us. Another example is the spin of the electron, a relativistic effect, manifesting in decidedly non-relativistic regimes.

We must keep these caveats in mind as we continue with defining the theory. If we accept the renormalisation group and the higher order derivative argument, then the only terms that we can add to the scalar field Lagrangian are Φ , Φ^3 and Φ^4 . The last two are commonly studied as interacting scalar field theories. They are both renormalisable^{7,38} in 4 spacetime dimensions or less and cannot be discounted by the renormalisation group argument. Renormalisability is a requirement for perturbation theory in regimes where the momentum is much less compared to the fundamental cutoff Λ . Due to their complexity, we are not interested in interacting field theories (but perhaps we should be) so we only have the Φ term to deal with. The Euler-Lagrange equation tells us that the coefficient associated with this term becomes[†] a source term. It makes the equation of motion inhomogeneous. We are not interested in sources and sinks for the field either so we can also neglect this term.

We do not want to modify the coefficient of the first derivative term of the Lagrangian as that dictates the dynamics. However, we can modify the Φ^2 term. We are adding in gravity, so we can couple Φ with the Ricci scalar R , which is formed from the Riemann tensor. Thus, the action for the scalar field that is coupled directly to curvature (gravity) is,

$$S = \int d^4x -\frac{1}{2}\sqrt{|g|} \left(g^{\mu\nu} \nabla_\mu \Phi \nabla_\nu \Phi + m^2 \Phi^2 + \xi R \Phi^2 \right). \quad (2.1)$$

$g^{\mu\nu}$ is the inverse metric; ξ is the coupling constant to curvature. Given an action $S = \int d^4x \sqrt{|g|} \mathcal{L}(\Phi, \nabla\Phi, g_{\mu\nu})$,

* That is to say, solutions to the equation of motion require more than the initial value of the field and its first derivative.

** There have been suggestions^{5,10,34-36} besides string theory¹⁷ that GR should be viewed as an effective field theory, i.e., the term in the Einstein-Hilbert action is the first in an infinite series of terms with higher derivatives and powers of the Ricci scalar, tensor and Riemann tensor.

† The flat space example is $S = \int d^4x \mathcal{L} = \int d^4x (\frac{1}{2} \eta^{\mu\nu} \partial_\mu \Phi \partial_\nu \Phi - \frac{1}{2} m^2 \Phi^2 + J(x)\Phi)$. The equation of motion would be $(\partial_\mu \partial^\mu + m^2) \Phi = J(x)$.

the Euler-Lagrange equation* $\nabla_\mu \frac{\partial \mathcal{L}}{\partial \nabla_\mu \Phi} - \frac{\partial \mathcal{L}}{\partial \Phi} = 0$ gives the equation of motion for the scalar field,

$$g^{\mu\nu} \nabla_\mu \nabla_\nu \Phi - m^2 \Phi - \xi R \Phi = 0. \quad (2.2)$$

The coupling term can be neglected when we work in Minkowski spacetime or the Schwarzschild metric because R is zero in these metrics. Our scalar field is intended to model one of the degrees of freedom of the electromagnetic field without the additional complication of gauge symmetry; therefore we will only consider massless fields. When we quantise a field, we expand the field in terms of a complete set (basis) of modes (e.g. $\{f_k(x^\mu)\}$) that satisfy the field equations. As is the case in flat spacetime, solutions to the Klein-Gordon equation satisfy a generalised Klein-Gordon scalar product. The scalar product, being an integral over only spatial coordinates, must be evaluated^{39,40} on a space-like hyper-surface** Σ with an induced metric γ_{ij} .[†] This space-like hyper-surface has a unit vector n^μ normal to the surface and is typically chosen to be future-directed. The scalar product (also known as the Klein-Gordon inner product) is generalised to,

$$(f_1, f_2) \equiv i \int d^3x \sqrt{|\gamma|} n^\mu \left(f_1^* \overleftrightarrow{\nabla}_\mu f_2 \right). \quad (2.3)$$

Where $f_1 \overleftrightarrow{\nabla}_\mu f_2 \equiv f_1 \nabla_\mu f_2 - f_2 \nabla_\mu f_1$. Because $f_1^* \overleftrightarrow{\nabla}_\mu f_2$ is a conserved current, it can be shown^{39,41} that the scalar product does not change with time and does not depend on the hyper-surface we choose. Therefore if we find a set of solutions (modes) $\{f_i(x^\mu)\}$ to Eq. (2.2) that is orthonormal[‡] $(f_i(x^\mu), f_j(x^\mu)) = \delta_{ij}$, it will remain so for all time.

The equal-time commutation relations, $[\Phi(\mathbf{x}, t), \Pi(\mathbf{x}', t)] = i\delta(\mathbf{x} - \mathbf{x}')$ are generalised with the Schwinger action principle.^{41,43} First we choose a coordinate system, (x^0, x^1, x^2, x^3) and define the conjugate field on a constant time hyper-surface,

$$\Pi(\mathbf{x}, x^0) = \frac{\partial \mathcal{L}}{\partial (\partial_0 \Phi(\mathbf{x}, x^0))}, \quad (2.4)$$

and the canonical energy-momentum tensor,

$$\Theta^\mu{}_\nu = \frac{\partial \mathcal{L}}{\partial (\nabla_\mu \Phi)} \nabla_\nu \Phi - \delta^\mu{}_\nu \mathcal{L}. \quad (2.5)$$

Now consider a variation of the coordinates and the field,

$$x^\mu \rightarrow x'^\mu = x^\mu + \delta x^\mu, \quad (2.6)$$

$$\Phi(x) \rightarrow \Phi'(x) = \Phi(x) + \delta_0 \Phi(x), \quad (2.7)$$

* The Euler-Lagrange equation are obtained by varying the action with respect to Φ and setting that variation to zero. A note of caution. Some people absorb $\sqrt{|g|}$ into their definition of \mathcal{L} which yields a slightly different results.

** Often chosen as a constant time space-like hyper-surface.

† If we introduce Gaussian normal coordinates where the metric can be written as $\mathbf{g} = \mathbf{d}x^0 \otimes \mathbf{d}x^0 + \gamma_{ij} \mathbf{d}x^i \otimes \mathbf{d}x^j$ then $\sqrt{|g|} = \sqrt{|\gamma|}$. While these coordinates may not hold throughout all of spacetime, they can always be chosen to be well defined on the hyper-surface. See Carroll⁴⁰ Appendix D for further details.

‡ Here I am using big box normalisation⁴² where the modes are discrete and labelled by i .

where $\delta_0\Phi(x)$ vanishes on the constant time hyper-surfaces that bound the action and where $g'_{\mu\nu}(x) = g_{\mu\nu}(x)$. The total variation of the field and the coordinate transform is written as $\delta\Phi(x) = \Phi'(x') - \Phi(x) = \delta_0\Phi(x) + \partial_\mu(\Phi(x))\delta x^\mu$. Then variational calculus gives a total divergence,⁴¹

$$\delta S = G(t_2) - G(t_1), \quad (2.8)$$

where

$$G(t) = \int d^{n-1}x \sqrt{|\gamma|} [\Pi\delta\Phi - \Theta^0_\nu\delta x^\nu], \quad (2.9)$$

and $\sqrt{|\gamma|}$ is the induced metric on the constant time hyper-surface. Schwinger's action principle says if F is a functional of $\Phi(x)$ and $\Pi(x)$ and $\delta_0 F = F[\Phi + \delta_0\Phi, \nabla(\Phi + \delta_0\Phi)] - F[\Phi, \nabla(\Phi)]$, then,

$$i\delta_0 F = [F, G]. \quad (2.10)$$

This generalises the equal-time commutation relations. While the above presentation is quite a general formalism, in practice, we usually exploit the symmetries of a given background spacetime which allows a more simplified canonical commutation relation. Symmetric spacetimes often allow for a complete set of solutions (modes) $\{f_\alpha\}$ to the field equations. We can expand our field in terms of these modes and their associated mode operators $\Phi \sim \sum_\alpha a_\alpha f_\alpha + a_\alpha^\dagger f_\alpha^*$. We quantise by imposing simplified commutation relations, e.g. $[a_i, a_j^\dagger] = \delta_{ij}$ which must obey the equal-time commutation relations (themselves obeying the Schwinger action principle). For the spacetimes we usually consider, the commutation relations of this form and so the Schwinger action principle is rarely needed. In addition, the modal expansion lets us define a vacuum state $|0_A\rangle$ by requiring $a_\alpha |0_A\rangle = 0, \forall\alpha$ and associate 'particles' with excitations of the mode operator, for example, a single 'particle' state would be $a_\alpha^\dagger |0_A\rangle$. So far this is very similar to the usual method of quantisation in Minkowski spacetime, however, the choice of modes is not unique. There are many ways we could quantise! If we have another set of modes $\{g_i(x^\mu)\}$ we can expand our field in terms of these modes, $\Phi \sim \sum_\alpha b_\alpha g_\alpha + b_\alpha^\dagger g_\alpha^*$. The vacuum defined by $a_\alpha |0_A\rangle = 0$ is not always the same vacuum defined by $b_\alpha |0_B\rangle = 0$. In most cases they are different.* This is the mathematical reason^{41,44,45} for the Unruh effect, Hawking effect, cosmological particle creation,⁴⁶ dynamic Casimir effect,⁴⁷ etc.

2.2 Positive frequency modes

In flat space we have the added convenience of a separable field equation where the 'time' (\mathcal{T}) dependence can be separated from the space components. This advantage exists for any spacetime metric that obeys,⁴⁰

$$\partial_0 g_{\mu\nu} = 0 \quad \text{and} \quad g_{0i} = 0. \quad (2.11)$$

* The usual definition of the vacuum is equivalent to defining the vacuum as a ground state (a state of minimum energy) with respect to time translation. In general relativity, physical theories must have general invariance (covariance). This is also the case in classical mechanics, but only with respect to the three spatial coordinates and the time coordinate separately. General invariance means the action of the physical theory must be invariant under general coordinate transformations. $S = \int d^4x \mathcal{L}(x) = \int d^4x' \mathcal{L}(x')$. This means there is no preferred time coordinate to define our time translations.

In Minkowski space, a unique vacuum state is chosen by requiring that the state is invariant under Poincaré transformations.³³

As the metric is independent of the ‘time’ coordinate, this means that a time-like Killing vector* (field) $\mathbf{K} = \partial_{\mathcal{T}}$ exists^{40,48}. In component form $K^\mu = \delta_{\mathcal{T}}^\mu$. This allows us to write Eq. (2.2) as,

$$\partial_0^2 f = - \left(g^{00} \right)^{-1} \left[g^{ij} \partial_i \partial_j + \frac{1}{2} g^{00} g^{ij} (\partial_i g_{00}) \partial_j - g^{ij} \Gamma_{ij}^k \partial_k - \left(m^2 + \xi R \right) \right] f, \quad (2.12)$$

where Γ_{ij}^k is the Christoffel symbol. You may observe that all of the time dependence is on the left side of the equation. This suggests that we can find separable solutions of the form,

$$f_\omega(x^\mu) = e^{-i\omega\mathcal{T}} \tilde{f}_\omega(\mathbf{x}), \quad (2.13)$$

where ω is the separation constant which we will call the frequency of f_ω . We call $f_\omega(x^\mu)$, a positive frequency mode with respect to time \mathcal{T} , while its complex conjugate will be called a negative frequency mode. If we want to write this expression** in coordinate-invariant form we can make use of the Killing vector so that,

$$K^\mu \partial_\mu f_\omega(x^\mu) = -i\omega f_\omega(x^\mu). \quad (2.14)$$

The Killing vector can be thought^{40,48} of as giving rise to one parameter diffeomorphisms[†] (ϕ_t). If we consider a point in the manifold p , any one-parameter diffeomorphisms, e.g. ϕ_t , map this point to a curve on the manifold parametrised by t . In this way, the one-parameter diffeomorphism arising from our Killing vector field forms a set of curves that fill the manifold and the Killing vector field is the set of tangent vectors to these curves.

Since there is an ambiguity with the choice of basis modes, how do we know which to choose? Clearly we should choose modes that make sense to an observer. In general, if an observer is travelling along a curve,[‡] they should measure using frequencies according to their proper time so they would define positive frequency modes via,

$$\frac{dx^\mu}{d\tau} \nabla_\mu f_k = -i\omega_k f_k, \quad (2.15)$$

where $\frac{dx^\mu}{d\tau}$ is the tangent vector to the path of the detector. $\frac{dx^\mu}{d\tau} \nabla_\mu$ is called the directional derivative along the path x^μ . If our observer happens to be travelling along a curve of the Killing vector[§] field then the tangent vector of the path should be proportional to the Killing vector field, i.e., $\frac{dx^\mu}{d\tau} \propto K^\mu = \delta_{\mathcal{T}}^\mu$.

A concrete example may be more easily understood. In Minkowski spacetime the positive frequency modes for inertial observers are the plane wave modes because they are positive frequency with respect to the time coordinate t which is also the proper time of an inertial observer. We have the time-like Killing vector $K^\mu = \delta_t^\mu$ and this vector field is related to the one-parameter diffeomorphism Φ_Δ that

* I have written the Killing vector in a coordinate based geometric notation and expanded in a coordinate basis. The $\partial_{\mathcal{T}}$ is the basis vector in the direction of the ‘time’ coordinate \mathcal{T} . For more details on the notation and Killing vectors see Carroll.⁴⁰

** This is also known as the Lie derivative with respect to Killing vector \mathbf{K} , expressed as $\mathcal{L}_K f_\omega = -i\omega f_\omega$

† A diffeomorphism is an invertible map (of all points) from a manifold to itself. One parameter diffeomorphisms are a family of diffeomorphisms and can be thought of as a smooth map $\mathbb{R} \times M \rightarrow M$. An example of this is a one-parameter diffeomorphism on the two-sphere with the coordinates (θ, ϕ) that transforms points like, $\Phi_t(\theta, \phi) = (\theta, \phi + t)$.

‡ The curve does not have to be a geodesic, they could be accelerating.

§ Of course, an observer can only travel in the direction of positive time, so this Killing vector must be future directed.

time translates a spacetime point, $\Phi_\Delta(t, \mathbf{x}) = (t + \Delta, \mathbf{x})$. This diffeomorphism forms geodesic curves that are inertial trajectories at every space point. This means that our time-like Killing vector is proportional to the tangent vector of an inertial observer at any \mathbf{x} .

We can now see that it would be advantageous to use a coordinate system adapted to the observer when finding modes that an observer would define.

The non-uniqueness of coordinate systems is often discussed only in the context of curved spacetime. In Minkowski spacetime, there is an obvious choice of flat coordinates (t, x, y, z) and Lorentz boosts to other coordinates (t', x', y', z') only changes the energy for a one particle state by a Lorentz transformation. However, depending on a detector's trajectory, even in Minkowski spacetime there are different⁴⁴ choices of coordinates or modes that may be more suitable for expanding the field in.

2.3 General formulation for modes

Through our analysis, we will often like to find the relation between different sets of modes. We will now present a general theory for this. Suppose we are in (1+1) dimensions and that we have a set of mode operators $\{a_k\}$ labelled* by momentum k , and mode functions $\{U_k\}$ that is a basis of solutions to the Klein-Gordon equation. The set of modes must be complete, in the sense that the field can be written as

$$\Phi(x) = \int dk \left\{ a_k U_k(x) + a_k^\dagger U_k^*(x) \right\}. \quad (2.16)$$

The mode operators are usually chosen to have normalised commutation relations

$$\left[a_k, a_{k'}^\dagger \right] = \delta(k - k'), \quad (2.17)$$

with all other commutators zero, while the mode functions are usually chosen** to be normalised under the Klein-Gordon inner product so that

$$(U_k, U_{k'}) = \delta(k - k'), \quad (2.18a)$$

$$(U_k, U_{k'}^*) = 0. \quad (2.18b)$$

Note that because of our definitions, we can write the mode operators as a Klein-Gordon inner product with the field,

$$a_k = (U_k, \Phi(x)). \quad (2.19)$$

The mode functions can be written in terms of the commutator between the mode operator and the field,

$$U_k(x) = - \left[a_k^\dagger, \Phi(x) \right] \quad (2.20)$$

* The generalisation to higher dimensions would involve labels for the momentum in different directions and integration over these labels. For discrete labels such as spin or angular momentum, that would involve adding sums over discrete indices to the field expansion.

** If we want to generalise to discrete labels, we would include Kronecker deltas in our expressions for the commutation relations and the Klein-Gordon inner products.

Similarly, if we had a different basis of mode operators $\{b_k\}$ and mode functions $\{u_k\}$ that obey

$$\left[b_k, b_{k'}^\dagger \right] = \delta(k - k') \quad (2.21a)$$

$$(u_k, u_{k'}) = \delta(k - k'), \quad (2.21b)$$

$$(u_k, u_{k'}^*) = 0, \quad (2.21c)$$

then we could expand the field in terms of

$$\Phi(x) = \int dk \left\{ b_k u_k(x) + b_k^\dagger u_k^*(x) \right\}, \quad (2.22)$$

we also have similar expressions for the mode operators and functions,

$$b_k = (u_k, \Phi(x)) \quad (2.23)$$

$$u_k(x) = - \left[b_k^\dagger, \Phi(x) \right]. \quad (2.24)$$

2.3.1 Bogolyubov transformations between sets of modes

Because both bases of modes are complete we can write,

$$b_k = (u_k, \Phi(x)) = \int dk' (u_k, U_{k'}) a_{k'} + (u_k, U_k^*) a_{k'}^\dagger. \quad (2.25)$$

This is called a Bogolyubov transformation. The inner products $\alpha_{kk'} \equiv (u_k, U_{k'})$ and $\beta_{kk'} \equiv (u_k, U_k^*)^* = (U_k^*, u_k)$ are called Bogolyubov coefficients.* Note that as there are no common conventions for the labelling of the coefficients, they will be defined differently in other references. These transformations tell us how one set of mode operators is related to the another set of modes. There also exists Bogolyubov transformation for the mode functions by taking the commutator,

$$u_k(x) = - \left[b_k^\dagger, \Phi(x) \right] = - \int dk' U_{k'} \left[b_k^\dagger, a_{k'} \right] + U_k^* \left[b_k^\dagger, a_{k'}^\dagger \right]. \quad (2.26)$$

2.4 The Unruh effect

The Unruh effect was first discovered by Davies¹⁹ and Unruh²² as a way to understand Hawking radiation with an eternal black hole. Its physical and mathematical underpinnings were elucidated by Fulling,¹⁸ who showed the non-uniqueness of canonical field quantisation in pseudo-riemannian (curved) spacetime.

The Unruh effect says that accelerating observers in flat spacetime detect a thermal distribution of particles. It shows how positive frequency modes (and therefore particles) are not observer independent. The Unruh effect still serves as a didactic calculational tool** and as an analogy for when we derive the QFT around a Schwarzschild black hole. We will review the derivation of the Unruh effect here for the massless, real scalar field in (1+1) spacetime.

* The second equality in definition of $\beta_{kk'}$ comes from the definition of the scalar product.

** Near the horizon of a black hole, the Schwarzschild metric can be approximated⁴⁹ by the Rindler metric/coordinates which are adapted to uniformly accelerating observers. This approximation will be used in the next chapter.

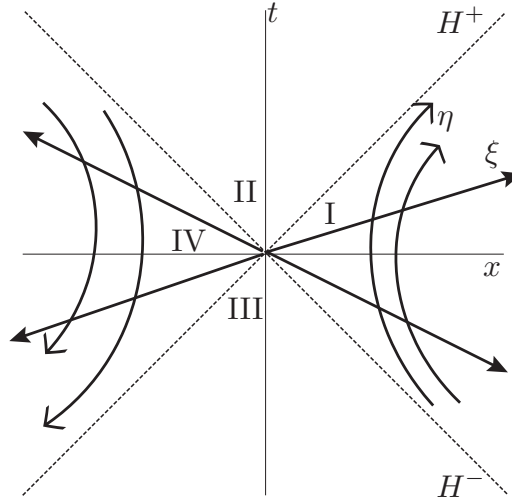


Figure 2.1: Minkowski spacetime with Minkowski and Rindler coordinates drawn. H^+ and H^- are the Rindler horizons seen by accelerating observers. These horizons are also Killing horizons which are null hyper-surfaces where a Killing vector is also null.

Since we will be considering accelerated trajectories, it will be useful to introduced Rindler coordinates which are defined by the following equations,

$$t = \frac{e^{a\xi}}{a} \sinh(a\eta), \quad x = \frac{e^{a\xi}}{a} \cosh(a\eta) \quad x > |t| \quad (2.27a)$$

$$t = -\frac{e^{a\xi}}{a} \sinh(a\eta), \quad x = -\frac{e^{a\xi}}{a} \cosh(a\eta) \quad x < |t|. \quad (2.27b)$$

The Rindler time coordinate is η and its spatial coordinate is ξ , both range from $(-\infty, \infty)$. The Minkowski metric is $ds^2 = -dt^2 + dx^2 = e^{2a\xi} (-d\eta^2 + d\xi^2)$. An observer at constant ξ measures the proper time according to $d\tau^2 = e^{2a\xi} d\eta^2 \implies d\tau = e^{a\xi} d\eta$. So we see that the proper time τ for an observer at constant ξ , is proportional to the Rindler time. In the case of $x > |t|$, henceforth denoted as the right Rindler wedge or Region I (see Fig. 2.1), the future directed (positive t) Killing vector is ∂_η while in $x < |t|$ (The left Rindler wedge or Region IV), the future directed Killing vector is $\partial_{-\eta} = -\partial_\eta$.^{*} An observer travelling on curves of constant ξ is in constant acceleration, which we can see if we calculate the magnitude of the 4-acceleration. The 4-acceleration is defined as the directional covariant derivative of the velocity vector $V^\mu = \frac{dx^\mu}{d\tau}$. That is,

$$A^\mu = \frac{dx^\nu}{d\tau} \nabla_\nu V^\mu. \quad (2.28)$$

If we calculate in Minkowski coordinates, we can ignore the Christoffel symbols in the covariant derivative. The components of the velocity and the acceleration are,

$$\begin{aligned} V^t &= \cosh(a\eta), & A^t &= ae^{-a\xi} \sinh(a\eta), \\ V^x &= \sinh(a\eta), & A^x &= ae^{-a\xi} \cosh(a\eta). \end{aligned}$$

The magnitude of the 4-acceleration, $\sqrt{-A_\mu A^\mu} = ae^{-a\xi}$, is constant for constant ξ . For constant ξ , $x^2 - t^2 = e^{2a\xi}/a$ displays the classic hyperbolic trajectory of a uniformly accelerating object. As

^{*} This is because in IV, there is a minus sign in Eq. (2.27b).

discussed in Section 2.2, this means that Rindler coordinates* are appropriate for uniformly accelerating observers. Using the same arguments from Section 2.2, we can also conclude that Minkowski coordinates are appropriate for observers on inertial trajectories. Thus, we should consider two different sets of modes, one with respect to Minkowski coordinates, and one with respect to Rindler coordinates.

The quantisation procedure proceeds—in the case of (1+1) spacetime—similarly to quantisation in Minkowski.** This is because the Rindler metric is conformally related to the Minkowski metric. This means $e^{-2a\xi} ds_{\text{Rindler}}^2 = d\eta^2 - d\xi^2$ is equivalent to the Minkowski metric after a relabelling of coordinates. From Eq. (2.2), we have $g^{\mu\nu} \nabla_\mu \nabla_\nu \Phi = 0$. The Klein-Gordon equation in Rindler coordinates is,

$$e^{-2a\xi} \left(\partial_\eta^2 - \partial_\xi^2 \right) \Phi = 0.$$

This equation of motion looks almost exactly the same as the equation of motion in Minkowski coordinates,

$$\left(\partial_t^2 - \partial_x^2 \right) \Phi = 0, \quad (2.29)$$

whose solution is given^{7,40} by the Minkowski plane wave expansion of the field,

$$\Phi(x) = \int_{-\infty}^{\infty} dp \frac{1}{\sqrt{4\pi\omega_p}} \left(a_p e^{-i(\omega_p t - px)} + a_p^\dagger e^{i(\omega_p t - px)} \right), \quad (2.30)$$

with $\omega_p = |p|$ and the commutator $[a_p, a_{p'}^\dagger] = \delta(p - p')$. In (1+1) we can further separate the field into right (left) moving modes where $p > 0$ ($p < 0$).

The challenge is getting a field expansion for Rindler coordinates. Fortunately, the field equation is exactly the same as in Minkowski, all we need to do is relabel the coordinates. There is a little complication related to the different positive frequency modes in I and IV. Remember that positive frequency modes that accompany the annihilation operator must be defined in terms of the future directed Killing vector. This Killing vector is different in I (∂_η) and IV ($-\partial_\eta$) so we must introduce two sets of modes that are positive frequency with respect to the future directed Killing vector in each region. These modes are

$$g_k^R = \begin{cases} \frac{1}{\sqrt{4\pi\omega_k}} e^{-i(\omega_k \eta - k\xi)}, & \text{I} \\ 0, & \text{IV} \end{cases} \quad (2.31a)$$

$$g_k^L = \begin{cases} 0, & \text{I} \\ \frac{1}{\sqrt{4\pi\omega_k}} e^{i(\omega_k \eta + k\xi)}, & \text{IV}, \end{cases} \quad (2.31b)$$

* The map from Rindler to Minkowski coordinates is bijective on the two wedges $x > |t|$ and $x < |t|$, consequently, one may say that the metrics $ds^2 = dt^2 - dx^2$ and $ds^2 = e^{2a\xi} (d\eta^2 - d\xi^2)$ are equivalent (isometric) on the two wedges.⁵⁰ ‘Rindler metric’ is an often used shorthand for Rindler coordinates, but it is actually a misnomer, it is equivalent to the Minkowski metric, but only on patches of spacetime. Strictly speaking, what we have are two Rindler charts (coordinate system) that cover the left and right wedge. One could define a Rindler *atlas* that covers the whole of spacetime if we also include *charts* that also cover the Rindler horizons and future and past wedge in such a way that the charts can be smoothly ‘sewn’ together.^{40,48}

** For those less familiar with QFT on flat spacetime, the curved theory presented above contains the flat space theory as a special case. Instead of a curved metric $g_{\mu\nu}$, we use the Minkowski metric $\eta_{\mu\nu}$ and covariant derivatives ∇_μ become partial derivatives ∂_μ . The natural choice of space-like hyper-surfaces are constant-time—Rindler or Minkowski time—spatial slices in Minkowski spacetime.

where $\omega_k = |k|$. Associated with these mode functions are the mode operators b_k^R and b_k^L which are defined to have the commutation relation,

$$\left[b_k^\sigma, b_{k'}^{\sigma'} \right] = \delta_{\sigma\sigma'} \delta(k - k'), \quad (2.32)$$

where $\sigma \in R, L$. When we write the field operator in these modes, the positive frequency modes (negative frequency modes) are accompanied by annihilation (creation) operators. For example, we will find a term $b_k^{R\dagger} g_k^{R*}$ in the field operator. The field operator in these modes, henceforth called Rindler modes, are

$$\Phi = \int_{-\infty}^{\infty} dk \left(b_k^R g_k^R + b_k^{R\dagger} g_k^{R*} + b_k^L g_k^L + b_k^{L\dagger} g_k^{L*} \right). \quad (2.33)$$

These operators define a vacuum state known as the Rindler vacuum, $|0_R\rangle$, which is annihilated by all the Rindler mode operators, $b_k |0_R\rangle = 0, \forall k$. Similar to the Minkowski expansion, we can also separate this into right (left) moving modes where $k > 0 (k < 0)$. We may also define Unruh mode functions from the Rindler modes functions by the Bogolyubov transformations,

$$h_k^R = \frac{1}{\sqrt{2 \sinh\left(\frac{\pi\omega_k}{a}\right)}} \left(e^{\frac{\pi\omega_k}{2a}} g_k^R + e^{-\frac{\pi\omega_k}{2a}} g_{-k}^{L*} \right), \quad (2.34a)$$

$$h_k^L = \frac{1}{\sqrt{2 \sinh\left(\frac{\pi\omega_k}{a}\right)}} \left(e^{\frac{\pi\omega_k}{2a}} g_k^L + e^{-\frac{\pi\omega_k}{2a}} g_{-k}^{R*} \right). \quad (2.34b)$$

Unlike the Rindler modes, these are well defined in all regions of Minkowski spacetime.* Associated with these Unruh modes are Unruh operators d_k^R, d_k^L , such that the field can be written as,

$$\Phi = \int_{-\infty}^{\infty} dk \left(d_k^R h_k^R + d_k^{R\dagger} h_k^{R*} + d_k^L h_k^L + d_k^{L\dagger} h_k^{L*} \right). \quad (2.35)$$

Using Eq. (2.24), we can find the Bogolyubov transforms between the mode operators

$$b_k^R = \frac{1}{\sqrt{2 \sinh\left(\frac{\pi\omega_k}{a}\right)}} \left(e^{\frac{\pi\omega_k}{2a}} d_k^R + e^{-\frac{\pi\omega_k}{2a}} d_{-k}^{L\dagger} \right), \quad (2.36a)$$

$$b_k^L = \frac{1}{\sqrt{2 \sinh\left(\frac{\pi\omega_k}{a}\right)}} \left(e^{\frac{\pi\omega_k}{2a}} d_k^L + e^{-\frac{\pi\omega_k}{2a}} d_{-k}^{R\dagger} \right). \quad (2.36b)$$

We could now go ahead and calculate the Bogolyubov transformations between Unruh modes and Minkowski modes, but the result is rather messy. In fact, we only need the general form³⁹ of the transformation, which can be written as

$$d_k^\sigma = \int dk p_{kp}^\sigma a_p, \quad (2.37)$$

* If we use Eqs. (2.27) and (2.31) and analytically extend $g_k^{R(L)}$ to all regions except IV (I), then we find that $h_k^R = \frac{e^{-\frac{\pi\omega_k}{2a}}}{\sqrt{4\pi\omega_k} \sqrt{2 \sinh\left(\frac{\pi\omega_k}{a}\right)}} e^{i\frac{\omega_k}{a}(-t+x)} i^{\frac{\omega_k}{a}}$ and $h_k^L = \frac{e^{\frac{\pi\omega_k}{2a}}}{\sqrt{4\pi\omega_k} \sqrt{2 \sinh\left(\frac{\pi\omega_k}{a}\right)}} e^{-i\frac{\omega_k}{a}(-t-x)} -i^{\frac{\omega_k}{a}}$.

where $\sigma \in \{R, L\}$ and $p_{kp}^\sigma = \left(h_k^\sigma, \frac{e^{-i(\omega p t - p x)}}{\sqrt{4\pi\omega p}} \right)$ is the Bogolyubov coefficient given by a Klein-Gordon inner product between the Unruh mode function and the Minkowski mode function. What this result tells us is that the Minkowski vacuum, defined as $a_k |0_M\rangle = 0, \forall k$, is also a vacuum for the Unruh mode operator d_k^σ , i.e.,

$$d_k^\sigma |0_M\rangle = 0. \quad (2.38)$$

2.4.1 Derivation of the Unruh effect

As noted earlier, the modes that an accelerating observer would use are the Rindler modes. This detector would generally sample a wave packet formed out of the Rindler modes. Therefore, we form a new mode out of the Rindler modes that represents what a detector might measure,

$$b(f) = \sum_\sigma \int dk f^\sigma(k) b_k^\sigma, \quad (2.39)$$

where $f^\sigma(k)$ is a wave packet* that obeys the normalisation condition $\sum_\sigma \int dk |f^\sigma(k)|^2 = 1$. This normalisation means that $[b(f), b(f)^\dagger] = 1$. If the observer is in the right wedge, we should expect that the mode is constructed only out of the b_k^R , but we will keep this more general form.

Suppose now that the state of the field is the Minkowski vacuum.** A detector that measures the wave packet $f^\sigma(k)$ sees a particle number $\langle 0_M | b(f)^\dagger b(f) | 0_M \rangle$. We will first evaluate,

$$\begin{aligned} b(f) |0_M\rangle &= \sum_\sigma \int dk f^\sigma(k) b_k^\sigma |0_M\rangle \\ &= \sum_\sigma \int dk f^\sigma(k) \frac{e^{-\frac{\pi\omega_k}{2a}}}{\sqrt{2 \sinh\left(\frac{\pi\omega_k}{a}\right)}} d_k^{\sigma\dagger} |0_M\rangle. \end{aligned}$$

Using the commutation relation $[d_k^\sigma, d_{k'}^{\sigma'}] = \delta_{\sigma\sigma'} \delta(k - k')$, which follows from Eqs. (2.32) and (2.78), we get the number expectation,

$$\begin{aligned} \langle 0_M | b(f)^\dagger b(f) | 0_M \rangle &= \sum_\sigma \int dk |f^\sigma(k)|^2 \frac{e^{-\frac{\pi\omega_k}{a}}}{2 \sinh\left(\frac{\pi\omega_k}{a}\right)} \\ &= \sum_\sigma \int dk \frac{|f^\sigma(k)|^2}{e^{2\pi\frac{\omega_k}{a}} - 1}. \end{aligned} \quad (2.40)$$

We immediately see that the number expectation value is given by the Bose-Einstein distribution $\frac{1}{e^{2\pi\frac{\omega}{a}} - 1}$. Thus, we can ascribe a temperature to the expectation value of Rindler modes that is dependent on the acceleration. Restoring units will help us see this. $\frac{1}{e^{2\pi\frac{\omega c}{a}} - 1} = \frac{1}{e^{2\pi\frac{(\hbar\omega = E)c}{\hbar a}} - 1} = \frac{1}{e^{\frac{E}{k_B T}} - 1}$ so we get the Unruh temperature,

$$T_{\text{Unruh}} = \frac{\hbar a}{2\pi k_B c}. \quad (2.41)$$

So we see that an accelerated observer in the Minkowski vacuum sees a thermal bath with a temperature that is proportional to the acceleration.

* This wave packet is not strictly necessary for a derivation, but it does prevent an ugly $\delta(0)$ that comes from commuting an annihilation and creation operator with the same index k .

** This could be argued from Poincaré symmetry or the observation that inertial observers don't see particles.

2.4.2 Correlations in the Minkowski vacuum

Let us examine the origin of the Unruh effect. Finding the inverse of Eq. (2.36b) and annihilating the Minkowski vacuum with an Unruh mode, we get

$$d_k^R |0_M\rangle = \frac{1}{\sqrt{2 \sinh\left(\frac{\pi\omega_k}{a}\right)}} \left(e^{\frac{\pi\omega_k}{2a}} b_k^R - e^{-\frac{\pi\omega_k}{2a}} b_{-k}^{L\dagger} \right) |0_M\rangle = 0 \quad (2.42)$$

$$\implies b_k^R |0_M\rangle = e^{-\frac{\pi\omega_k}{a}} b_{-k}^{L\dagger} |0_M\rangle \quad (2.43)$$

Similarly we can show that

$$d_k^L |0_M\rangle = \frac{1}{\sqrt{2 \sinh\left(\frac{\pi\omega_k}{a}\right)}} \left(e^{\frac{\pi\omega_k}{2a}} b_k^L - e^{-\frac{\pi\omega_k}{2a}} b_{-k}^{R\dagger} \right) |0_M\rangle = 0 \quad (2.44)$$

$$\implies b_k^L |0_M\rangle = e^{-\frac{\pi\omega_k}{a}} b_{-k}^{R\dagger} |0_M\rangle \quad (2.45)$$

Given these two equations let us propose that we can write the Minkowski vacuum in terms of the Rindler vacuum as

$$|0_M\rangle = F(b, b^\dagger) |0_R\rangle, \quad (2.46)$$

where b stands generally for all operators b_k^σ . Given that $[b_k^\sigma, b_{k'}^{\sigma'\dagger}] = \delta_{\sigma\sigma'}\delta(k - k')$, this means that

$$b_k^\sigma F |0_R\rangle = [b_k^\sigma, F] |0_R\rangle = \frac{\partial F}{\partial b_k^{\sigma\dagger}} |0_R\rangle. \quad (2.47)$$

We can then rewrite our two equations as,

$$\frac{\partial F}{\partial b_k^R} = e^{-\frac{\pi\omega_k}{a}} b_{-k}^{L\dagger} F \quad (2.48)$$

$$\frac{\partial F}{\partial b_k^L} = e^{-\frac{\pi\omega_k}{a}} b_{-k}^{R\dagger} F \quad (2.49)$$

which is solved by

$$F = \prod_k \exp \left\{ e^{-\frac{\pi\omega_k}{a}} b_k^{R\dagger} b_{-k}^{L\dagger} \right\}. \quad (2.50)$$

The Minkowski state is therefore

$$|0_M\rangle = Z \prod_k \exp \left\{ e^{-\frac{\pi\omega_k}{a}} b_k^{R\dagger} b_{-k}^{L\dagger} \right\} |0_R\rangle, \quad (2.51)$$

where Z is a normalisation constant. If we temporarily go to a big box normalisation we can rewrite the equation as a more common form seen in the literature,^{39,51}

$$|0_M\rangle = \prod_i \left(\sqrt{1 - e^{-\frac{2\pi\omega_i}{a}}} \sum_{n_i=0}^{\infty} e^{-\frac{\pi n_i \omega_i}{a}} |n_i, R\rangle \otimes |n_i, L\rangle \right) \quad (2.52)$$

where, $|n_i, R\rangle \otimes |n_i, L\rangle = \frac{1}{n_i!} \left(b_{k_i}^{R\dagger} b_{-k_i}^{L\dagger} \right)^{n_i} |0_R\rangle$. Big box normalisation discretises the frequencies allowed so i is an index for the frequencies. $b_{k_i}^{R\dagger}$ and $b_{-k_i}^{L\dagger}$ are Rindler creation operators in the right &

the left wedge, moving right ($k_i > 0$) & moving left ($k_i < 0$), respectively. What this equation tells us is that the Minkowski vacuum is actually a product of Rindler number states with perfect number correlation for every frequency/mode between the left and the right wedges.* For simplicity if consider a single mode only so we can write

$$|0_M\rangle = \left(\sqrt{1 - e^{-\frac{2\pi\omega}{a}}} \sum_{n=0}^{\infty} e^{-\frac{\pi n\omega}{a}} |n, R\rangle \otimes |n, L\rangle \right). \quad (2.53)$$

Suppose an accelerating observer is in the right wedge. Any local observable O^R they construct can only be made out of the right Rindler mode operators and so,

$$\begin{aligned} \langle 0_M | O^R | 0_M \rangle &= \left(1 - e^{-\frac{2\pi\omega}{a}} \right) \sum_{n, n'} e^{-\frac{\pi\omega(n+n')}{a}} \langle n', R | \otimes \langle n', L | O^R | n, R \rangle \otimes |n, L\rangle \\ &= \left(1 - e^{-\frac{2\pi\omega}{a}} \right) \sum_n e^{-\frac{2\pi\omega n}{a}} \langle n, R | O^R | n, R \rangle. \end{aligned}$$

If we recognise that,

$$\left(1 - e^{-\frac{2\pi\omega}{a}} \right)^{-1} = \text{Tr} \left(e^{-\frac{2\pi\omega}{a} b^{R\dagger} b^R} \right), \quad (2.54)$$

then the expectation of an operator/observable restricted to the right wedge is,

$$\langle 0_M | O^R | 0_M \rangle = \text{Tr} \left(\rho^R O^R \right), \quad (2.55)$$

if we define

$$\rho^R = \frac{e^{-\frac{2\pi\omega}{a} b^{R\dagger} b^R}}{\text{Tr} \left(e^{-\frac{2\pi\omega}{a} b^{R\dagger} b^R} \right)}. \quad (2.56)$$

This is the form of a thermal state if we interpret $e^{-\frac{2\pi\omega}{a} b^{R\dagger} b^R}$ as a Boltzmann factor $e^{-\frac{E}{T}}$ with $E = \omega b^{R\dagger} b^R$ and $T = \frac{a}{2\pi}$, the Unruh temperature. So we can interpret the thermal response of a detector as due to the tracing out of the left wedge.

2.5 Quantum field theory around a Schwarzschild black hole

Hawking radiation was discovered by Stephen Hawking²⁰ after analysing a scalar field theory on the curved spacetime of a Schwarzschild black hole. The assumptions that go into its derivation will be discussed in Chapter 3. Hawking found that under those assumptions, a black hole of mass M would thermally radiate with a temperature $T = \frac{1}{8\pi M}$. Hawking's derivation used a ray-tracing argument on a collapsing shell of matter. This calculation was improved by Bill Unruh²² and extended to eternal black holes.

Let us now review scalar field theory around an eternal Schwarzschild black hole and derive Unruh's result. We will follow the notation of Hodgkinson *et al.*⁵² The Schwarzschild metric in the Schwarzschild coordinates is,

$$ds^2 = -f(r)dt^2 + \frac{1}{f(r)}dr^2 + r^2 \left(d\theta^2 + \sin^2 \theta d\phi^2 \right), \quad (2.57)$$

* Those familiar with Quantum Optics will note in Eq. (2.51) that the Minkowski vacuum looks like a multi-mode squeezed state of the Rindler vacuum.

where $f(r) = 1 - 2M/r$ and M is the mass of the Schwarzschild black hole. Notice that as $r \rightarrow \infty$ the metric asymptotically approaches flat spacetime. This means that an inertial observer far away will measure time with respect to Schwarzschild time. Under this metric, the equation of motion for the scalar field (2.2) is,

$$\frac{1}{\sqrt{-g}} \partial_\mu (\sqrt{-g} g^{\mu\nu} \partial_\nu \Phi) = 0 \quad (2.58)$$

which is solved by the Schwarzschild modes,

$$\phi_{\omega lm}(x) = \phi_{\omega lm}(t, r, \theta, \phi) = \frac{1}{\sqrt{4\pi\omega}} e^{-i\omega t} Y_{lm}(\theta, \phi) R_{\omega l}(r)/r \quad (2.59)$$

where $\omega > 0$ is the frequency of the mode and $Y_{lm}(\theta, \phi)$ is a spherical harmonic of degree l and order m .^{*} The radial function $R_{\omega l}(r)$ satisfies

$$-\frac{d^2 R_{\omega l}}{dr_*^2} + V_l(r) R_{\omega l} = \omega^2 R_{\omega l}, \quad (2.60)$$

where $V_l(r)$ is the effective potential

$$V_l(r) = f(r) \left(\frac{l(l+1)}{r^2} + \frac{2M}{r^3} \right). \quad (2.61)$$

Here r_* is the tortoise coordinate

$$dr_* = dr/f(r), \quad r_* = r + 2M \ln(r/2M - 1), \quad (2.62)$$

where $r_* \rightarrow -\infty$ corresponds to the event horizon of the Schwarzschild black hole.

Let us first consider the field outside the event horizon, where there exist two sets of orthonormal modes that can completely represent the field. Note that Schwarzschild time is measured by observers at constant r, θ and ϕ . An observer must accelerate to stay at constant r, θ and ϕ , so these modes and this region of spacetime are analogous to the right Rindler wedge. The two sets of orthonormal modes are the upgoing and ingoing modes, denoted as $\phi_{\omega lm}^{\text{up}}(x)$ and $\phi_{\omega lm}^{\text{in}}(x)$, respectively. The asymptotic behaviour for the radial part of the upgoing mode (which is analogous to a right moving Rindler mode $k > 0$), $R_{\omega l}^{\text{up}}$, is

$$R_{\omega l}^{\text{up}} \sim \begin{cases} B_{\omega l}^{\text{up}} e^{i\omega r_*}, & r_* \rightarrow +\infty; \\ e^{i\omega r_*} + A_{\omega l}^{\text{up}} e^{-i\omega r_*}, & r_* \rightarrow -\infty, \end{cases} \quad (2.63)$$

and for the radial part of the ingoing mode (which is analogous to a left moving Rindler mode $k < 0$), $R_{\omega l}^{\text{in}}$, is

$$R_{\omega l}^{\text{in}} \sim \begin{cases} e^{-i\omega r_*} + A_{\omega l}^{\text{in}} e^{i\omega r_*}, & r_* \rightarrow +\infty; \\ B_{\omega l}^{\text{in}} e^{-i\omega r_*}, & r_* \rightarrow -\infty. \end{cases} \quad (2.64)$$

^{*} Note that ϕ is doing double duty here. $\phi_{\omega lm}$ are the Schwarzschild modes while ϕ is a spherical coordinate.

Here $A_{\omega l}^{\text{up}}$ ($A_{\omega l}^{\text{in}}$) and $B_{\omega l}^{\text{up}}$ ($B_{\omega l}^{\text{in}}$) are the reflection and transmission amplitudes* of the upgoing (ingoing) modes, respectively. They satisfy the following Wronskian relations⁵²,

$$|A_{\omega l}^{\text{up}}|^2 = 1 - |B_{\omega l}^{\text{up}}|^2, \quad (2.65)$$

$$|A_{\omega l}^{\text{in}}|^2 = 1 - |B_{\omega l}^{\text{in}}|^2, \quad (2.66)$$

$$|A_{\omega l}^{\text{up}}| = |A_{\omega l}^{\text{in}}|, \quad B_{\omega l}^{\text{up}} = B_{\omega l}^{\text{in}}. \quad (2.67)$$

The upgoing modes $\phi_{\omega l m}^{\text{up}}$ and ingoing modes $\phi_{\omega l m}^{\text{in}}$ are chosen to satisfy the orthonormality relations,

$$\left(\phi_{\omega l m}^{\text{up}}, \phi_{\omega' l' m'}^{\text{up}} \right) = \delta(\omega - \omega') \delta_{ll'} \delta_{mm'}, \quad (2.68a)$$

$$\left(\phi_{\omega l m}^{\text{in}}, \phi_{\omega' l' m'}^{\text{in}} \right) = \delta(\omega - \omega') \delta_{ll'} \delta_{mm'}, \quad (2.68b)$$

$$\left(\phi_{\omega l m}^{\text{up}}, \phi_{\omega' l' m'}^{\text{in}} \right) = 0, \quad (2.68c)$$

Here $(,)$ represents the Klein-Gordon inner product¹¹ in Eq. (2.3), which is defined on a space-like hyper-surface of constant Schwarzschild time is written as

$$(\varphi, \chi) = i \int_{2M}^{\infty} dr \frac{r^2}{f(r)} \int_{4\pi} d\Omega (\varphi^* \partial_t \chi - \chi \partial_t \varphi^*) \quad (2.69)$$

for any two solutions φ and χ of the Klein-Gordon equation in Eq. (2.58).

In the canonical quantization procedure, the scalar field Φ is regarded as an operator, satisfying the equal-time commutation relations, and is expanded as

$$\Phi(x) = \sum_{l=0}^{\infty} \sum_{m=-l}^l \int_0^{\infty} d\omega \left(b_{\omega l m}^{\text{up}} \phi_{\omega l m}^{\text{up}}(x) + b_{\omega l m}^{\text{in}} \phi_{\omega l m}^{\text{in}}(x) + \text{h.c.} \right) \quad (2.70)$$

where h.c. represents the Hermitian conjugate. The operators $b_{\omega l m}^{\text{up}}$ and $b_{\omega l m}^{\text{in}}$ represent upgoing and ingoing modes, respectively. They satisfy the commutation relations

$$[b_{\omega l m}^{\text{up}}, b_{\omega' l' m'}^{\text{up} \dagger}] = \delta(\omega - \omega') \delta_{ll'} \delta_{mm'}, \quad (2.71a)$$

$$[b_{\omega l m}^{\text{in}}, b_{\omega' l' m'}^{\text{in} \dagger}] = \delta(\omega - \omega') \delta_{ll'} \delta_{mm'}, \quad (2.71b)$$

with all other commutators zero, i.e. the up and in operators commute with each other. As an observer far away ($r \approx \infty$, $\phi = \theta \approx \text{const.}$) measures time with respect to proper time, the modes $\phi_{\omega l m}^{\text{up/in}}(x)$ have positive frequency for them. This means that an observer far away would define particles by $\phi_{\omega l m}^{\text{up/in}}(x)$ and the associated operator $b_{\omega l m}^{\text{up/in}}$.

2.5.1 An analogy to Unruh modes

There is an alternative coordinate system known as Kruskal-Szekeres coordinates^{40,53} in which the Schwarzschild metric, following Misner, Thorne and Wheeler's⁵³ notation can be written as,

$$ds^2 = -\frac{32M^3}{r} e^{-\frac{r}{2M}} d\tilde{v}d\tilde{u} + r^2 \left(d\theta^2 + \sin^2 \theta d\phi^2 \right) \quad (2.72)$$

* Reflection and transmission in the sense of considering Eq. (2.61) as a scattering potential

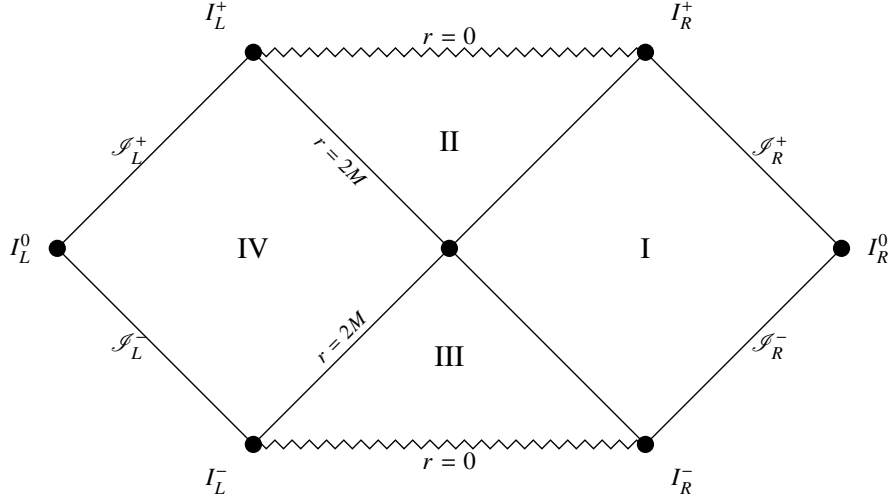


Figure 2.2: Penrose diagram of the maximally extended, eternal black hole. The individual regions of spacetime are denoted by the roman numerals in a similar scheme and in analogy to Minkowski spacetime in Fig. 2.1. The singularity is denoted by the sawtooth lines and the horizons are labelled. The region outside the black hole is denoted I. Note that the maximal extension includes a separate ‘universe’ IV as well as a ‘white’ hole in III. I (IV) will also be referred to as the right (left) exterior region. Angular coordinates are suppressed in the compactification of spacetime.

where the Kruskal-Szekeres lightcone coordinates \tilde{v} and \tilde{u} are related to the Schwarzschild coordinates outside of the black hole by,

$$\tilde{u} = -e^{-\frac{\mu}{4M}} = -\left(\frac{r}{2M} - 1\right)^{\frac{1}{2}} e^{\frac{r}{4M}} e^{-\frac{t}{4M}}, \quad (2.73a)$$

$$\tilde{v} = e^{\frac{\nu}{4M}} = \left(\frac{r}{2M} - 1\right)^{\frac{1}{2}} e^{\frac{r}{4M}} e^{\frac{t}{4M}} \quad (2.73b)$$

where $\mu = t - r_*$ and $\nu = t + r_*$ which are related to Eddington-Finkelstein coordinates. The usual Kruskal-Szekeres coordinates are $u \equiv \frac{1}{2}(\tilde{v} - \tilde{u})$ and $v \equiv \frac{1}{2}(\tilde{v} + \tilde{u})$. In these coordinates, there is a time-like killing vector $\tilde{\mathbf{K}} \equiv \frac{\partial}{\partial \tilde{u}}$. A radially falling observer measures time with respect to this time coordinate \tilde{u} .⁵³ An important fact that the Kruskal-Szekeres coordinates reveal is that the Schwarzschild coordinates only cover part of the Schwarzschild spacetime, namely Region I in Fig. 2.2. The Schwarzschild coordinates are like the Rindler coordinates for an accelerated observer who doesn’t know about Region IV in Fig. 2.1. If we extend the Schwarzschild coordinates to Region IV in a similar way to Eq. (2.27b) by introducing appropriate minus signs, we find that Schwarzschild time also runs ‘backward’ in Region IV just like Rindler time. This means that our original field theory was incomplete, and we need to expand it according to new functions, which we define in direct analogy to Eq. (2.31),

$$\phi_{\omega lm}^i(x) = \begin{cases} \phi_{\omega lm}^i(x), & \text{I} \\ 0, & \text{IV} \end{cases} \quad (2.74a)$$

$$\bar{\phi}_{\omega lm}^i(x) = \begin{cases} 0, & \text{I} \\ \phi_{\omega lm}^i(-t, r, \theta, \phi), & \text{IV}, \end{cases} \quad (2.74b)$$

where $i \in cbracketin, up$. Note that the unbarred $\phi_{\omega lm}$ now refers to a function without support in Region IV, while $\bar{\phi}_{\omega lm}$ has no support in Region I. This leads us to define a field expansion that has support in the extended spacetime,

$$\Phi(x) = \sum_{l=0}^{\infty} \sum_{m=-l}^l \int_0^{\infty} d\omega \left(b_{\omega lm}^{\text{up}} \phi_{\omega lm}^{\text{up}}(x) + \bar{b}_{\omega lm}^{\text{up}} \bar{\phi}_{\omega lm}^{\text{up}}(x) + b_{\omega lm}^{\text{in}} \phi_{\omega lm}^{\text{in}}(x) + \bar{b}_{\omega lm}^{\text{in}} \bar{\phi}_{\omega lm}^{\text{in}}(x) + \text{h.c.} \right), \quad (2.75)$$

where the new Schwarzschild operators \bar{b} have analogous commutation relations and commute with the unbarred b operators. This extended Schwarzschild expansion defines the Boulware vacuum $|0_B\rangle$ that is annihilated by the $\{d^i, \bar{d}^i\}$ operators. This leads us to define a new set of Unruh modes in analogy to the Unruh modes in Eq. (2.34),

$$w_{\omega lm}^i = \frac{1}{\sqrt{2 \sinh(4\pi M\omega)}} \left(e^{2\pi M\omega} \phi_{\omega lm}^i + e^{-2\pi M\omega} \bar{\phi}_{\omega lm}^{i*} \right), \quad (2.76a)$$

$$\bar{w}_{\omega lm}^i = \frac{1}{\sqrt{2 \sinh(4\pi M\omega)}} \left(e^{2\pi M\omega} \bar{\phi}_{\omega lm}^i + e^{-2\pi M\omega} \phi_{\omega lm}^{i*} \right). \quad (2.76b)$$

We could define a superposition (similar to the inverse of Eq. (2.37)) of these Unruh modes to get Kruskal-Szekeres modes (analogous to Minkowski modes) that are positive frequency with respect to the coordinate ν , but we will not proceed as we will not need it for our purposes. However, it is important to note that just as in the Minkowski case, these Unruh modes share the same vacuum as the Kruskal-Szekeres modes. These modes are associated with Unruh mode operators, $d_{\omega, l, m}^i, \bar{d}_{\omega, l, m}^i$ which obey the commutation relations,

$$\left[d_{\omega, l, m}^i, d_{\omega', l', m'}^{i'} \right] = \delta(\omega - \omega') \delta_{ii'} \delta_{ll'} \delta_{mm'}, \quad (2.77a)$$

$$\left[\bar{d}_{\omega, l, m}^i, \bar{d}_{\omega', l', m'}^{i'} \right] = \delta(\omega - \omega') \delta_{ii'} \delta_{ll'} \delta_{mm'}. \quad (2.77b)$$

The unbarred and overbarred operators commute with each other. All other commutators are zero. Note the similarity with Eq. (2.36b). They are related to the b modes by the Bogolyubov transformations

$$b_{\omega lm}^i = \frac{1}{\sqrt{2 \sinh(4\pi M\omega)}} \left(e^{2\pi M\omega} d_{\omega lm}^i + e^{-2\pi M\omega} \bar{d}_{\omega lm}^{i\dagger} \right) \quad (2.78a)$$

$$\bar{b}_{\omega lm}^i = \frac{1}{\sqrt{2 \sinh(4\pi M\omega)}} \left(e^{2\pi M\omega} \bar{d}_{\omega lm}^i + e^{-2\pi M\omega} d_{\omega lm}^{i\dagger} \right) \quad (2.78b)$$

and their corresponding inverse transformations given by

$$d_{\omega lm}^i = \frac{1}{\sqrt{2 \sinh(4\pi M\omega)}} \left(e^{2\pi M\omega} b_{\omega lm}^i - e^{-2\pi M\omega} \bar{b}_{\omega lm}^{i\dagger} \right) \quad (2.79a)$$

$$\bar{d}_{\omega lm}^i = \frac{1}{\sqrt{2 \sinh(4\pi M\omega)}} \left(e^{2\pi M\omega} \bar{b}_{\omega lm}^i - e^{-2\pi M\omega} b_{\omega lm}^{i\dagger} \right) \quad (2.79b)$$

With these Unruh modes we can define two more expansions of the field operator. The first is the Hartle-Hawking expansion,

$$\Phi(x) = \sum_{l=0}^{\infty} \sum_{m=-l}^l \int_0^{\infty} d\omega \left(d_{\omega lm}^{\text{up}} w_{\omega lm}^{\text{up}}(x) + \bar{d}_{\omega lm}^{\text{up}} \bar{w}_{\omega lm}^{\text{up}}(x) + d_{\omega lm}^{\text{in}} w_{\omega lm}^{\text{in}}(x) + \bar{d}_{\omega lm}^{\text{in}} \bar{w}_{\omega lm}^{\text{in}}(x) + \text{h.c.} \right). \quad (2.80)$$

The Hartle-Hawking expansion defines the Hartle-Hawking vacuum $|0_{HH}\rangle$ which is annihilated by all the Unruh mode operators, $\{d_{\omega lm}^i, \bar{d}_{\omega lm}^i\}$. It is important to note that these operators are not positive frequency for a far away observer in Region I. In fact as we will see later, the far away observer sees a thermal state for particles going out and into the black hole. The second expansion is the Unruh expansion,

$$\Phi(x) = \sum_{l=0}^{\infty} \sum_{m=-l}^l \int_0^{\infty} d\omega \left(d_{\omega lm}^{\text{up}} w_{\omega lm}^{\text{up}}(x) + \bar{d}_{\omega lm}^{\text{up}} \bar{w}_{\omega lm}^{\text{up}}(x) + b_{\omega lm}^{\text{in}} \phi_{\omega lm}^{\text{in}}(x) + \text{h.c.} \right). \quad (2.81)$$

The Unruh expansion defines the Unruh vacuum, $|0_U\rangle$ which is annihilated by $d_{\omega lm}^{\text{up}}, \bar{d}_{\omega lm}^{\text{up}}$ and $b_{\omega lm}^{\text{in}}$. The barred modes and operators create particles in Region IV either coming up (from the white hole) or going in the black hole. Note that while our Hartle-Hawking is defined for the maximally extended black hole, the Schwarzschild expansion is defined only in Region I and the Unruh expansion is a strange mix where the modes coming out are defined for the extended spacetime while ingoing modes are defined only for Region I. As ingoing modes from Region IV will only matter to a person in Region II and IV, it is left unspecified. The different definitions can be understood as different initial conditions of the field that are specified on spacetime hyper-surfaces of constant time coordinate.

2.5.2 Hawking radiation

As we noted before, people far from the black hole (where $r \rightarrow \infty$, labelled by \mathcal{S}_R^+ in Fig. 2.2) measure time according to Schwarzschild time t . Hence, positive frequency modes and particles are defined by $b_{\omega lm}^{\text{up}}$. Since we know that the Unruh vacuum is annihilated by $d_{\omega lm}^{\text{up}}$ we use this fact as well as Eq. (2.79) to express the formally Unruh vacuum as a function of the Boulware vacuum,

$$d_{\omega lm}^{\text{up}} |0_U\rangle = \frac{1}{\sqrt{2 \sinh(4\pi M\omega)}} \left(e^{2\pi M\omega} b_{\omega lm}^{\text{up}} - e^{-2\pi M\omega} \bar{b}_{\omega lm}^{\text{up} \dagger} \right) |0_U\rangle = 0 \quad (2.82)$$

$$\Rightarrow |0_U\rangle = Z \prod_{\omega, l, m} \exp \left\{ e^{-4\pi M\omega} b_{\omega lm}^{\text{up} \dagger} \bar{b}_{\omega lm}^{\text{up} \dagger} \right\} |0_B\rangle, \quad (2.83)$$

where Z is a normalisation constant. Note the similarity of Eq. (2.83) with Eq. (2.51). In the Minkowski vacuum, Rindler modes moving right (left) in the right wedge are in a two mode squeezed state* with Rindler modes moving left (right) in the left wedge. In comparison, in the Unruh vacuum, an upgoing mode in Region I is in a two mode squeezed state with an upgoing mode in Region IV.

Equation (2.83) implies that an observer at $r = \infty$ sees particle number,

$$\langle 0_U | b_{\omega lm}^{\text{up} \dagger} b_{\omega lm}^{\text{up}} | 0_U \rangle \propto \frac{1}{e^{8\pi M\omega} - 1} \quad (2.84)$$

which, compared to the Bose-Einstein distribution $\langle n(\omega) \rangle = \frac{1}{e^{\omega/T} - 1}$ yields the Hawking temperature

$$T_{\text{Hawking}} = \frac{1}{8\pi M} \quad (2.85)$$

* Note that this squeezing structure comes about because of the Bogolyubov transformations between modes. Because the general transform between modes $\{a_i\}$ and $\{b_j\}$ are of the form, $a_i = \sum_j \alpha_{ij} b_j + \beta_{ij} b_j^\dagger$. Where the Bogolyubov coefficients α_{ij} and β_{ij} come from the scalar product between the two sets of mode functions.

Note the difference between Hartle-Hawking and Unruh vacua. Through the same process we can show that

$$\langle 0_U | b_{\omega lm}^{\text{up} \dagger} b_{\omega lm}^{\text{up}} | 0_U \rangle = \langle 0_{HH} | b_{\omega lm}^{\text{up} \dagger} b_{\omega lm}^{\text{up}} | 0_{HH} \rangle = \langle 0_{HH} | b_{\omega lm}^{\text{in} \dagger} b_{\omega lm}^{\text{in}} | 0_{HH} \rangle, \quad (2.86)$$

which means there is a thermal state for the observer far away for outgoing Schwarzschild modes in the Unruh vacuum and for both outgoing and ingoing modes for the Hartle-Hawking vacuum. However, ingoing modes Schwarzschild in the Unruh vacuum are

$$\langle 0_U | b_{\omega lm}^{\text{in} \dagger} b_{\omega lm}^{\text{in}} | 0_U \rangle = 0. \quad (2.87)$$

We will explore the different definitions of vacuum states as well as the interpretation of the vacuum state of Eq. (2.83) in Chapter 3.

2.6 Unitary inequivalence

In QFT, an n-particle state of mode operators a_p is defined by,

$$|p_1, p_2, \dots, p_n\rangle = a_{p_1}^\dagger a_{p_2}^\dagger \dots a_{p_n}^\dagger |0_a\rangle. \quad (2.88)$$

The full Hilbert space is spanned by all possible combinations of n-particle states, also known as Fock space. Mathematically, if \mathcal{H} is the Hilbert space of states for one particle and the Hilbert space of 0-particle states is \mathbb{C} , the full Fock space is⁴⁸

$$\mathcal{F}(\mathcal{H}) \equiv \mathbb{C} \oplus \left[\bigoplus_{n=1}^{\infty} (\otimes_S^n \mathcal{H}) \right]. \quad (2.89)$$

\oplus is the direct sum and \otimes_S is the symmetrised tensor products as we are only considering bosons. Let us consider our derivation of the Unruh effect. We have Minkowski operators a_k and a_k^\dagger which can be considered a map from Minkowski Fock space to itself $\mathcal{F}_M \rightarrow \mathcal{F}_M$. Let us call the set of operators that map within the Fock space as $\mathcal{O}_M : \mathcal{F}_M \rightarrow \mathcal{F}_M$. The Minkowski vacuum is a vector in this Fock space, $|0_M\rangle \in \mathcal{F}_M$. Similarly, we have the Rindler operators $b_k \in \mathcal{O}_R$ that act on the Rindler Fock space \mathcal{O}_R . The Minkowski formulation and the Rindler formulation can be said to furnish a representation of the canonical commutation relations of the algebra of operators.^{54,55} One might ask then, whether these two representations are unitarily equivalent? That is, whether there exists a unitary map from the Minkowski Fock space to the Rindler Fock space $U : \mathcal{F}_M \rightarrow \mathcal{F}_R$, such that,

$$U \mathcal{O}_M U^{-1} = \mathcal{O}_R. \quad (2.90)$$

Equation (2.52) certainly seems to suggest that it is possible. But note the normalisation term $\sqrt{1 - e^{-\frac{2\pi\omega_i}{a}}}$ is less than 1. That means if there are an infinite number of modes (and there are), the equation is formally equal to 0. Thus, no such unitary operator exists. A sufficient condition^{45,54} for unitary inequivalence between two representations A and B with vacuums $|0_A\rangle$ and $|0_B\rangle$ and annihilation operators a and b is,

$$\sum_i \langle 0_B | a_i^\dagger a_i | 0_B \rangle = \infty \quad \text{or} \quad \sum_j \langle 0_A | b_j^\dagger b_j | 0_A \rangle = \infty \quad (2.91)$$

With this condition, we can show that Minkowski & Rindler are unitarily inequivalent, as is Unruh & Boulware. In QFT, there are unlimited degrees of freedom. For a scalar field in free space in a given representation, between a given ω_1 and ω_2 there are an uncountable infinite number of frequencies that the field can take. This form of infinity gives rise to ‘infra-red’ inequivalence. We could mitigate this inequivalence by putting the field in a box. Now there are only discrete frequencies, but there are still a countably infinite number of them which also leads to inequivalence with other representations. This is known as ultra-violet inequivalence. If we were to impose a frequency cutoff which is equivalent to a length scale cutoff, then we no longer have any unitary inequivalence. Mostly, we are comfortable with ultra-violet cutoffs, in fact, the renormalisation procedure means that our QFTs are really low energy ‘effective’ theories; we don’t expect our QFT to be correct to all length scales. How then, do we understand the field in a box procedure? Even if QFT were valid throughout the universe, we can only say that in some small region (that we have access to) we know the state of the field. Infra-red inequivalence can also be seen in quantum mechanics. A good example^{55,56} is the case of an infinitely long line of spin 1/2 particles. Through a similar argument, it can be shown that there is no unitary operator that can rotate a state of all spin up to a state with all spin down. States can only be transformed to other states that are finitely different. Thus, the state of all spin up belongs to a separate and inequivalent representation as compared to that of the state of all spin down. In fact, there are infinitely many of these representations, for example, the state with alternating spin up and spin down and so on. The existence of infra-red inequivalence is because of considering the theory from a global perspective while any observer is only localised to a small region. So while a low-energy & high-energy cutoff would solve the unitary inequivalence it remains to be seen how we might impose covariant cutoffs. Even with such a cutoff there may still be ambiguity as to which is the physically appropriate representation.

Nonetheless, this raises questions about the importance of vacuum states and particles in the minds of physicists. Algebraic Quantum Field Theory^{45,55,57} attempts to do away with non-local, flat spacetime concepts such as vacuums, particles, S-matrix, path integrals and Euclidean space.

2.7 Conclusion

The topic of Quantum Field Theory in Curved Spacetime is a rather rich and varied topic. While by construction it cannot affect the spacetime geometry, physicists hope that this theory can characterise some of the lower curvature interactions between gravity and quantum theory. This generalisation of Quantum Field Theory has had profound impact on the search for a unified theory and even now has a great capacity to surprise with its rich structure and surprising conceptual difference to its flat space cousin. In the following chapters I will expand on the concepts in this chapter and discuss their implications.

Chapter 3

Black hole field theory with a firewall

This chapter is based on the paper¹ “Black hole field theory with a firewall in two spacetime dimensions” which I wrote with Daiqin Su, Robert B. Mann and Timothy C. Ralph. All figures and calculations were made by me with analysis and interpretation shared amongst co-authors. The bulk of the text was written and edited by me.

The black hole information paradox, unresolved since its proposal by Hawking,⁵⁸ stems from the thermality of Hawking radiation. Assuming that Hawking radiation continues until the black hole is completely evaporated, the process of black hole evaporation could change a pure state into a mixed state, which is forbidden under unitary evolution.^{58–60} This means if the black hole was initially formed from systems that were pure states, then Hawking radiation cannot carry out the information contained within the pure state because the radiation is thermal. So what happens to the information? If the black hole completely evaporates then is the information lost? Maybe it does not completely evaporate and leaves a remnant?

These are questions that cannot be answered with certainty because the theory of Hawking radiation is dependent on the assumption of a very heavy (massive) black hole.⁶¹ This assumption is necessary for the ‘semi-classical’ analysis of quantum field theory on curved spacetime (QFTCS) because for massive black holes, the curvature at the horizon where we apply QFTCS is small. We expect general relativistic effects at large curvature, so for a massive black hole horizon, we expect that at least locally we do not require a true synthesis of GR and QFT. However, this is a problem as the assumption breaks down once the black hole loses enough mass from evaporation. Of course, given the lack of a consonant theory of gravity and quantum mechanics, almost all aspects of black hole evolution can be questioned.⁶² There are modified theories/suggestions where there is no black hole information paradox to resolve – such as remnants^{25,63} and information loss⁵⁸ – but these generate further difficulties and do not satisfactorily resolve the problem.⁶⁴ Black hole complementarity⁶¹ was one attempt to resolve the information paradox. Whilst problems with complementarity had been raised earlier,⁶⁵ the discord within complementarity was recently thrown into sharp focus by Almheiri *et al.*⁶⁶ who found that the postulates of black hole complementarity: unitarity, the equivalence principle, and field-theory locality are mutually inconsistent. Almheiri *et al.* suggested that the most conservative solution was to

forgo the equivalence principle leading to a free falling observer observing particles and burning up in a ‘firewall’ at the horizon. In a related and supporting development,⁶⁷ Braunstein, Pirandola and Życzkowski considered entanglement across the horizon which is ‘disentangled’ near the end of life of a black hole in order to resolve the information paradox. They found that this resulted in a firewall-like ‘energetic curtain’. There were a number of other arguments in favour of the firewall, noting that it arises from standard quantum field theory in curved spacetime.^{68–71} The paradox also provoked scepticism, with rebuttals* such as the fuzzball proposal,^{72–74} missing quantum gravity degrees of freedom,^{75,76} the ER=EPR proposal⁷⁷ and ‘non-violent’ non-locality.^{78,79} However, in this chapter we investigate the conservative solution to the firewall paradox of Almheiri *et al.*, offering a mechanism for the firewall.

3.1 Unitarity and Black hole complementarity

While it is expected that QFTCS breaks down near the singularity, Hawking proposed⁵⁸ that the breakdown occurs earlier during the process of gravitational collapse and unitarity is lost. Recently,⁸⁰ however, calculations using Euclidean quantum gravity²⁶ and loop quantum gravity^{81,82} suggest that black hole formation and evaporation is unitary. In addition, because of the unitarity⁸³ of Conformal Field Theories (CFT) and the AdS-CFT conjecture, string theory is also considered to support unitarity.²⁶ Black hole remnants are a proposed solution to the information paradox where there is incomplete evaporation of the black hole, resulting in a small massive object that no longer radiates. This proposal generates new problems⁸⁴ of its own—especially for black hole thermodynamics.**

Susskind *et al.*⁶¹ wanted to preserve unitary evolution without remnants so they proposed three postulates. The postulates from their paper⁶¹ are reproduced below.

Postulate 1:

The process of formation and evaporation of a black hole, as viewed by a distant observer, can be described entirely within the context of standard quantum theory. In particular, there exists a unitary S-matrix which describes the evolution from infalling matter to outgoing Hawking-like radiation.

Postulate 2:

Outside the stretched[†] horizon of a massive black hole, physics can be described to good approximation by a set of semi-classical field equations.

Postulate 3:

To a distant observer, a black hole appears to be a quantum system with discrete energy levels.

* For more in-depth discussion of alternative proposals please refer to [64] Mann, R. B. in *Black Holes: Thermodynamics, Information, and Firewalls* 1–95 (Springer International Publishing, 2015).

** The problem with remnants is that they appear to be able to carry an arbitrarily large amount of information. There exist alternative formulations²⁵ to remnants that do not have these problems.

† The concept of a stretched horizon was introduced by Susskind *et al.*⁶¹ For our purposes, we can substitute ‘horizon’ for ‘stretched horizon’.

The dimension of the subspace of states describing a black hole of mass M is the exponential of the Bekenstein entropy $S(M)$.

There is actually an additional postulate, although Susskind *et al.*⁶¹ do not call it a postulate; based on their understanding of the Einstein equivalence principle, they call it ‘certain’ and following Almheiri *et al.*⁶⁶, I will also call it the fourth postulate.

Postulate 4:

A freely falling observer experiences nothing out of the ordinary when crossing the horizon.

Susskind *et al.*⁶¹ showed that Postulate 1 implies that information would leak out of the black hole via correlations between early and late Hawking radiation which is required to ‘solve’ the information loss paradox if there is Hawking radiation. Postulate 2 ensures that we can use QFTCS to understand black hole physics. Postulate 3 is related to black hole thermodynamics and information theory. Finally, Postulate 4 defines the vacuum state of the field around a black hole.

It is worth discussing these postulates in detail because Hawking radiation and the black hole information paradox depends on accepting these postulates.

First, postulate 1. We mentioned that Hawking first suggested a breakdown of our theories. Some have suggested that QM must be generalised to allow for evolution to mixed states but Banks *et al.*²⁵ suggest that this could lead to violations of causality and energy-momentum conservation. Unruh & Wald⁶⁰ have suggested quantum gravity plays an important role in black hole formation and that quantum gravity could allow evolution from pure states into mixed states without violations of causality or energy-momentum conservation. This particular point has not been resolved entirely, although the prevailing viewpoint within string theory and loop quantum gravity is that non-unitary evolution do not contribute to quantum gravity processes.^{85,86}

Second, postulate 2. This is the assumption that QFTCS is applicable near the horizon. This assumption actually fails to hold as the black hole shrinks in mass from evaporation. In addition, the high curvature near the singularity means that semiclassical theory does not hold at any point in time. The scalar field equation Eq. (2.2) is an effective field equation and perhaps the high curvature near the singularity affects the theory in a fundamental way. Finally, QFTCS relies on certain global methods such as modes that extend through all of space, raising questions about its validity.

Third, postulate 3. Bekenstein first conjectured that black holes have an entropy proportional to their surface area.⁸⁷ It was observed by Bekenstein that if black holes did not have entropy, then the second law of thermodynamics could be violated by throwing mass into a black hole. The third postulate asserts that the statistical mechanics definition of entropy as the natural logarithm of the number of states holds for black holes, and that the entropy is given by the Bekenstein-Hawking entropy $S(M) = \frac{A}{4}$, where A is the area of the black hole’s event horizon. Indeed, the calculation of Bekenstein-Hawking entropy within string theory and loop quantum gravity⁸⁸ is highly suggestive of a unitary solution to the black hole information paradox.⁸⁹

3.2 Firewall

The idea of the firewall started with a paper by Almheiri *et al.*⁶⁶ that suggested that Postulates 1, 2 and 4 are not consistent. For information to leak out as suggested by postulate 1, the (scalar, Dirac, &c.) field could not be in a vacuum state for an inertial observer free falling through the horizon. The reason for this is due to the monogamy of entanglement. In the eternal black hole case (Eq. (2.83)) the Unruh vacuum means that the upgoing mode in our universe is maximally entangled with an upgoing mode in the other universe in Region IV in Fig. 2.2. In Hawking's²⁰ collapse calculation (where there is no other universe), from the point of view of the inertial observer, the vacuum state means that the upgoing modes of radiation are maximally entangled with the ingoing modes of radiation. A heuristic description is sometimes used: in a vacuum, pair creation occurs in which one of the pair falls into the black hole and the other escapes. The pair are called Hawking pairs. For information to leak

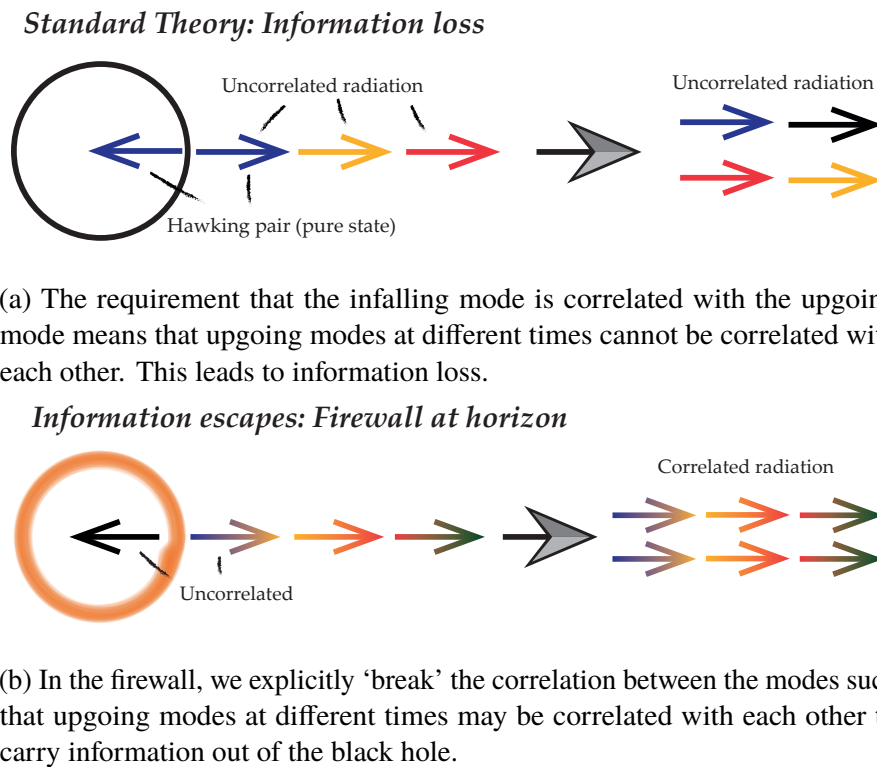


Figure 3.1: A cartoon of the two paradigms. The event horizon in (a) has no detectable feature for an infalling observer while the event horizon in (b) is characterised by a firewall indicated in orange. In both cases the black hole evaporates completely.

out, the present upgoing modes of radiation must be correlated with past upgoing modes of radiation. The maximal entanglement between the upgoing and the ingoing precludes any possible correlation between past and present upgoing radiation. To solve the inconsistency, they suggest that Postulate 4 should be rejected. This would lead to a non-zero particle state for the inertial observer and Almheiri *et al.*⁶⁶ argued that the inertial observer should see high energy modes. This is known as the firewall. Interestingly, this would suggest that semiclassical theory cannot account for all the physics near the horizon even for a massive black hole as some novel physics is involved that creates the correlation between different upgoing radiation at different time.

There is good reason for questioning the use of the equivalence principle in determining the state of the field. Singleton & Wilburn⁹⁰ noted that there appears to be a violation of the Einstein equivalence principle when considering Unruh and Hawking radiation. In their paper they showed that a detector experiencing a certain proper acceleration in Minkowski spacetime sees a thermal bath of particles with a different temperature to that of a detector hovering above a black hole at the same proper acceleration. In addition, crucial to the definition of a vacuum state is the construction of modes over a spatial hypersurface and the association of mode operators to these modes. Since modes that define the vacuum extend over all of space, the vacuum is also a nonlocal concept.⁵⁷ Observing the Unruh or the Hawking effect also requires peering outside of your spaceship laboratory. The observation (or lack) of Hawking radiation could be argued to be a non-local experiment where the equivalence principle is inapplicable. Perhaps the Einstein equivalence principle is inapplicable to determining the state of the field. We therefore have reasonable grounds to reject Postulate 4.

3.3 Boulware and Unruh vacua, and Black Holes

How shall we choose the vacuum state then? The standard choice for the vacuum state around an eternal black hole is the Unruh vacuum. However, as we discussed before in Section 2.5, it is well known^{45,91,92} that in addition to the Unruh vacuum, there are also the Hartle-Hawking and Boulware vacua. Indeed, a generic result of quantum field theory is that there is no unique vacuum state. There are many complete sets of modes and each set is associated with a vacuum state. These vacuum states are not all equivalent, so there are a large number of vacua that can be defined. This proliferation of vacua means that for each physical situation, we require additional constraints to determine a vacuum state.

Here we suggest that an appropriate alternative vacuum choice would be a modified Unruh vacuum, one that transitions from an Unruh vacuum at low frequency to a Boulware vacuum⁹³ at high frequency. By exploiting the correspondence^{49,94} between the Rindler and Schwarzschild spacetimes close to the horizon, we compute the response of a free falling detector across the horizon of a (1+1) dimensional Schwarzschild black hole. Given the choice of a modified Unruh vacuum we identify conditions for which the free-faller sees a firewall, whilst a stationary observer sees Hawking radiation—as proposed by Almheiri *et al.*⁶⁶

According to Israel⁹² and others,^{95,96} the Boulware vacuum state is, ‘...*the zero-temperature ground state appropriate to the space in and around a static star.*’ Although black holes (excluding primordials) form from collapsing stars,⁹⁷ the derivation of Hawking radiation using an eternal black hole^{22,64,66,98} asserts that the vacuum state around the black hole is the Unruh vacuum. A particularly subtle point is illustrated by comparing the different derivations of Hawking radiation. The first, which we shall call the collapse model, was pioneered by Hawking²⁰ and the second, which we shall call the eternal model, is exemplified by Unruh’s paper.²²

In the collapse model there is only one definition of vacuum:^{20,99} namely it is the state annihilated by asymptotic modes at past null infinity \mathcal{I}^- that are positive frequency with respect to Schwarzschild

time. This definition is also used in defining the Boulware and Unruh vacua in the eternal model. However in the collapse model this specification completely defines the vacuum, whereas in the eternal case additional initial conditions must be specified. Because of the unitary inequivalence between the Boulware and the Unruh vacua, we know that there cannot be any unitary time-evolution between them. Furthermore, we do not expect our low energy effective theory to be accurate to arbitrary length scales, so we impose a high frequency cutoff.* There is, however no easy way to do this covariantly. Even with a high frequency cutoff we still have infra-red inequivalence; however this is an artefact of the analysis. If we started the analysis with a star in a box and followed its collapse into a black hole, the field theory would not have infra-red inequivalence, as we discussed in Section 2.6. Therefore, a Boulware vacuum could unitarily evolve into an Unruh vacuum with a cutoff. We therefore posit that the vacuum state of the field may not be simply Boulware or Unruh, but something in between. We shall call this a modified Unruh vacuum.

In the eternal black hole case we have Eq. (2.83), the expression for an Unruh vacuum,

$$|0_U\rangle = Z \prod_{\omega, l, m} \exp \left\{ e^{-4\pi M \omega} b_{\omega l m}^{\text{up } \dagger} \bar{b}_{\omega l m}^{\text{up } \dagger} \right\} |0_B\rangle, \quad (3.1)$$

where $|0_U\rangle$ is the Unruh vacuum while $|0_B\rangle$ is the Boulware vacuum and Z is a normalisation constant. M is the mass of the Schwarzschild black hole, ω is the frequency measured with respect to Schwarzschild time, l and m are the degree and order in the spherical harmonic function Y_l^m . $b_{\omega l m}^{\text{up } \dagger} \left(\bar{b}_{\omega l m}^{\text{up } \dagger} \right)$ creates a positive frequency mode with respect to Schwarzschild time t in the right (left) exterior region of the maximally extended Schwarzschild solution that is asymptotically upgoing at spatial infinity. The overbar indicates the left exterior region. The right exterior region is identified with our universe and the left exterior upgoing mode is interpreted to be the ‘particle’ inside the horizon^{20,22} or the ‘ingoing’ mode, in the terminology of Almheiri *et al.*⁶⁶.

The modification to the Unruh vacuum in Eq. (3.1) that we propose is

$$|\tilde{\Psi}\rangle = Z \prod_{\omega < \tilde{\epsilon}, l, m} \exp \left\{ e^{-4\pi M \omega} b_{\omega l m}^{\text{up } \dagger} \bar{b}_{\omega l m}^{\text{up } \dagger} \right\} |0_B\rangle, \quad (3.2)$$

where $\tilde{\epsilon}$ is a cutoff frequency. This modification ensures Hawking radiation is retained for frequencies up to $\tilde{\epsilon}$, with higher frequencies available to carry out information via a modified theory. In what follows we shall explore the implications of this in Rindler space, modifying Eq. (3.2) accordingly.

3.4 Correspondence between Schwarzschild and Rindler metrics

We propose that the vacuum state after gravitational collapse is a modified Unruh vacuum state, and are particularly interested in the number of particles that a freely falling observer would detect near the horizon. To compute this we shall exploit the well known correspondence between Schwarzschild and Rindler metrics,⁹⁴ which has been useful in relativistic quantum information.⁴⁹ Specifically, near the event horizon

* While covariant cutoffs have begun to be considered¹⁰⁰, for simplicity we have chosen a non-covariant cutoff.

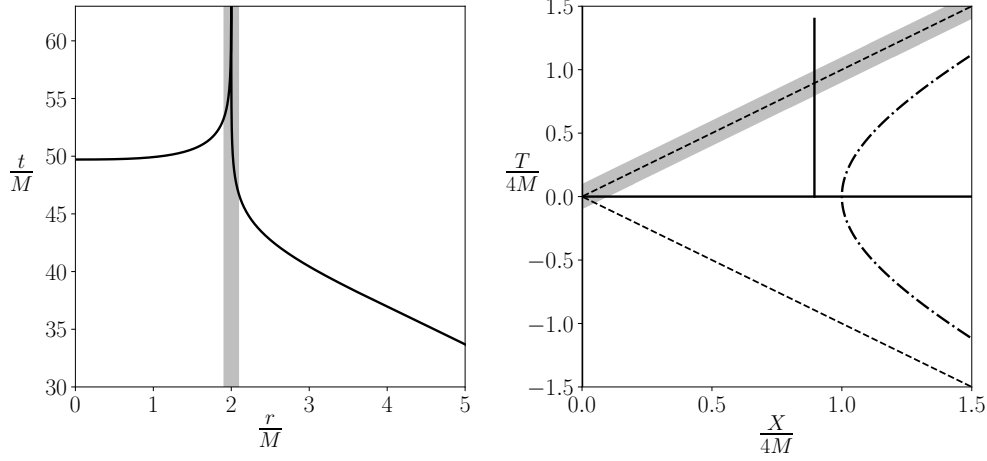


Figure 3.2: The left figure plots the geodesic initially stationary at $r = 10M$; note that the divergence at the horizon is an artifact of Schwarzschild coordinates and is absent in the free-faller's coordinates. The right figure shows the corresponding geodesic in flat space. The dot-dashed line is the $\xi = 0$ accelerating trajectory. The shaded region on both plots indicates the area where the flat space equivalence holds.

$$ds^2 = \left(1 - \frac{2M}{r}\right) dt^2 - \frac{1}{1 - \frac{2M}{r}} dr^2 \approx e^{2a\xi} (d\eta^2 - d\xi^2), \quad (3.3)$$

where t is Schwarzschild time, r is the Schwarzschild radial coordinate, η is Rindler time and ξ is the Rindler space coordinate. The approximate relation follows from setting $t = \eta$, $r = 2M(1 + e^{2a\xi})$ and expanding for $\xi \ll 0$, where $a = \frac{1}{4M}$. From Eq. (2.27), we have the relationship between Rindler and Minkowski coordinates (T, X) , which is

$$T = \frac{e^{a\xi}}{a} \sinh(a\eta), \quad X = \frac{e^{a\xi}}{a} \cosh(a\eta) \quad X > |T| \quad (3.4)$$

$$T = -\frac{e^{a\xi}}{a} \sinh(a\eta), \quad X = -\frac{e^{a\xi}}{a} \cosh(a\eta) \quad X < -|T|. \quad (3.5)$$

Henceforth we can always associate ξ with a radius r from a black hole. It must be noted that the correspondence is only approximate and holds with greater accuracy as ξ gets more negative. We see in Fig. 3.2 that as ξ gets more negative, we get closer to $r = 2M$, the event horizon which corresponds to $T = \pm X$.

3.5 Motion of the falling observer

For a freely falling (and initially stationary at r_0) observer their 4-velocity in Schwarzschild coordinates is

$$\frac{dx^\mu}{d\tau} = \left(\frac{\sqrt{1 - \frac{2M}{r_0}}}{1 - \frac{2M}{r}}, -\sqrt{\frac{2M}{r} - \frac{2M}{r_0}}, 0, 0 \right). \quad (3.6)$$

We shall now identify a Minkowski inertial trajectory with a the freely falling observer's trajectory in Schwarzschild. Consider a trajectory such that $X_0 = \text{const}$. From Eq. (3.4) we have $X_0^2 - T^2 = \frac{e^{2a\xi}}{a^2}$.

We rearrange this, make the approximation that $\frac{e^{2a\xi}}{X_0^2 a^2} \ll 1$ and use $r = 2M(1 + e^{2a\xi})$ to get,

$$T \approx X_0 \left(1 - \frac{1}{2X_0^2 a^2} \left(\frac{r}{2M} - 1 \right) \right). \quad (3.7)$$

We then integrate $\frac{dr}{d\tau} = -\sqrt{\frac{2M}{r} - \frac{2M}{r_0}}$ in Eq. (3.6) and then series expand around $r = 2M$ to get,

$$\tau \approx \text{const} - \frac{r - 2M}{\sqrt{1 - \frac{2M}{r_0}}}. \quad (3.8)$$

If we now identify Eq. (3.7) with Eq. (3.8), we may compare the coefficient of r to obtain,

$$X_0 = 4M \sqrt{\frac{r_0 - 2M}{r_0}}. \quad (3.9)$$

3.6 Number expectation for an observer coupling to Minkowski modes in the modified Minkowski vacuum

To calculate the response of a free falling detector we need to identify an appropriate vacuum state. The upgoing modes in the right exterior region in the Unruh vacuum of the standard approach map to the right moving modes of the Minkowski vacuum in the equivalent Rindler metric. Thus an inertial observer (free-faller) near the horizon sees no particles coming from the horizon, in accord with the equivalence principle. We note that such an observer does see non-zero particles from the sky (see discussion after Eq. (3.19) in Unruh²²) and an Unruh-Dewitt detector has been shown¹⁰¹ to respond non-trivially throughout its free fall in (1+1) Schwarzschild spacetime. Therefore, when we say a free faller sees a vacuum, what we mean is that they see no particles from the horizon. This can be seen in Eq. (3.1), where we see do not see any operators of the kind $b_{\omega lm}^{\text{in} \dagger} (\bar{b}_{\omega lm}^{\text{in} \dagger})$. On the other hand, a stationary observer in the Schwarzschild metric with the Boulware vacuum, sees no particles. The equivalent vacuum for the Rindler metric is the Rindler vacuum for which accelerated observers see no particles.

We now consider what an observer measuring in Minkowski modes will detect in a modified vacuum, focussing on a massless scalar field. The Minkowski vacuum can formally be written in terms of the Rindler vacuum,³⁹

$$|0_M\rangle \propto \exp \left\{ \int_0^\infty d\Omega e^{-\pi\Omega} \left(b_\Omega^{\text{RM}\dagger} \bar{b}_\Omega^{\text{RM}\dagger} + b_\Omega^{\text{LM}\dagger} \bar{b}_\Omega^{\text{LM}\dagger} \right) \right\} |0_R\rangle, \quad (3.10)$$

corresponding to Eq. (3.1), with Ω the Rindler frequency and unbarred (overbarred) operators signifying their operation on the right (left) Rindler wedge, where $b_\Omega^{\text{R/LM}}$ are Rindler modes. This is a slight recasting of Eq. (2.52) where the product over continuous frequency is replaced with an integral inside the exponential and we have separated the left moving and right moving modes explicitly to avoid confusion later. The Rindler wave-number k has been replaced with Ωa with $k > 0$ ($k < 0$)

represented by an RM (LM) superscript signifying right (left) moving modes. In this form, the Minkowski-Schwarzschild correspondence can be more easily seen.

To implement our proposed modified Unruh vacuum Eq. (3.2), we suppose that for Rindler frequencies below ϵ the state appears to be Minkowski vacuum and therefore define

$$|\Psi\rangle \propto \exp \left\{ \int_0^\epsilon d\Omega \sum_\sigma e^{-\pi\Omega} \left(b_\Omega^{\text{RM}\dagger} \bar{b}_\Omega^{\text{RM}\dagger} + b_\Omega^{\text{LM}\dagger} \bar{b}_\Omega^{\text{LM}\dagger} \right) \right\} |0_R\rangle, \quad (3.11)$$

which is a modified Minkowski vacuum. Note that we have suppressed an index distinguishing left and right movers in Eqs. (3.10) and (3.11).

One might expect based on the definition of the Unruh vacuum in Eq. (3.1) that the left movers in Eqs. (3.10) and (3.11) would be in the Rindler vacuum since they correspond to the ingoing modes outside the black hole which are in the Boulware vacuum. This is not the case in (3+1) dimensions. As was discussed in Crispino *et al.*¹⁰² and Singleton & Wilburn¹⁰³ and shown in Candelas⁹¹, in the (3+1) dimensional case an Unruh-Dewitt detector hovering above the horizon in the Unruh vacuum has a response function identical to that of a uniformly accelerated observer in the Minkowski vacuum. This is in contrast to the (1+1) dimensional case where the correspondence breaks down due to the decoupling of left and right movers. Physically, in the (3+1) case the response is due to the sum over all angular momentum modes. If we are near the horizon and are not looking directly radially away, most of the modes we see are upgoing modes that have been bent back towards the black hole. Indeed, it has been shown⁹¹ that ingoing modes can be neglected and an Unruh-Dewitt detector near the horizon sees a response only due to the upgoing modes. Because of the bending of the upgoing modes, the detector hovering at the horizon sees isotropic radiation as in the Unruh effect. This suggests that for a (1+1) theory to model what a detector in an Unruh vacuum near the horizon of a (3+1) black hole sees, the state of the field should be in the Minkowski vacuum Eq. (3.10) for both left and right movers. Likewise, for the modified Unruh vacuum (3.2) the flat space analogue is the modified Minkowski vacuum state (3.11) for both left and right movers. In this way, in the limit of $\epsilon \rightarrow \infty$ we regain the standard correspondence.

We see that for Rindler operators with $\Omega < \epsilon$, Eq. (3.11) behaves like a Minkowski vacuum while for $\Omega > \epsilon$ it behaves like a Rindler vacuum. This is the equivalent of our modified Unruh vacuum, valid in (1+1) when we are close to the horizon.

Note that Ω is the Rindler frequency scaled with respect to a , therefore $\Omega = \frac{\omega}{a}$ where ω is the Rindler frequency measured with respect to the Rindler time η in Eq. (3.4).

If we now calculate the number expectation value for a Minkowski mode a_k , with $|\Psi\rangle$ instead of $|0_R\rangle$ we find that

$$\begin{aligned} & \langle \Psi | a_k^\dagger a_k | \Psi \rangle \\ &= \frac{1}{2\pi\omega_k} \int_\epsilon^\infty d\Omega \frac{2}{e^{2\pi\Omega} - 1} \\ &= \frac{1}{\pi\omega_k} \left[\epsilon - \frac{1}{2\pi} \ln \left(e^{2\pi\epsilon} - 1 \right) \right], \end{aligned} \quad (3.12)$$

where $\omega_k = |k|$.

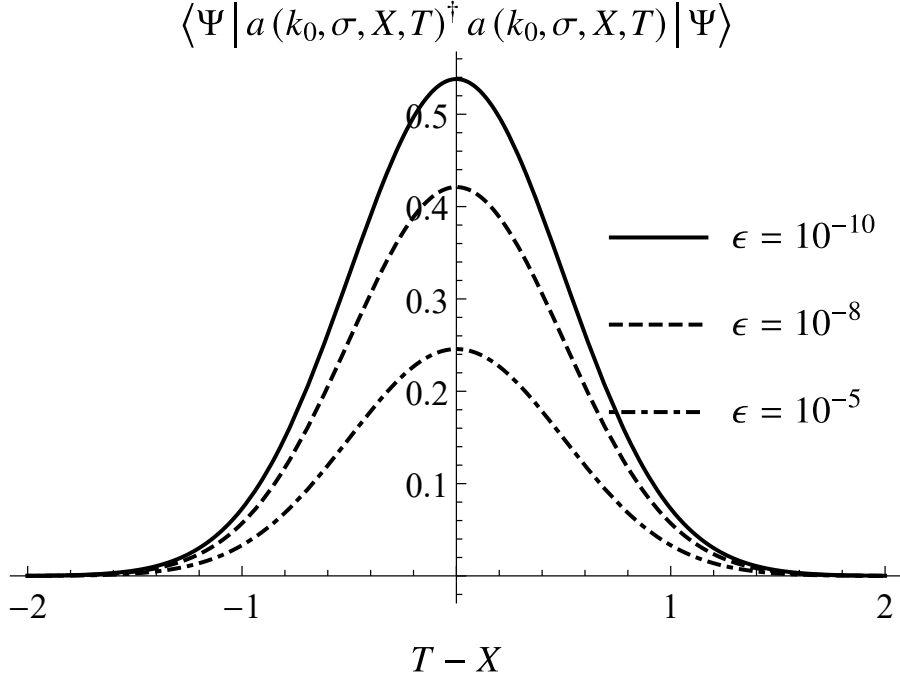


Figure 3.3: Numerical integration of Eq. (3.14) with $\sigma = 1$ and $k_0 = 10$ plotted with respect to $T - X$. We see that as we approach the horizon at $T - X = 0$, we encounter a finite response due to the firewall. Notice our approximations above Eq. (3.7) mean that this figure is valid only for $T - X \ll 2M$.

3.7 Position dependent response to the firewall

Consider the superposition of Minkowski modes a_k

$$a(k_0, \sigma, X, T) = \int_{-\infty}^{\infty} dk f(k, k_0, \sigma, X, T) a_k \quad (3.13)$$

with $f(k, k_0, \sigma, X, T) = \left(\frac{1}{2\pi\sigma^2}\right)^{\frac{1}{4}} e^{-\frac{(k-k_0)^2}{4\sigma^2}} e^{-i(\omega_k T - kX)}$. This wave-packet models a detector of finite size measuring with respect to a Gaussian wave-packet of Minkowski modes centred at k_0 with a width of σ . Assuming $|k_0| \gg \sigma$ we find

$$\begin{aligned} & \langle \Psi | a(k_0, \sigma, X, T)^\dagger a(k_0, \sigma, X, T) | \Psi \rangle \\ &= \int_{\epsilon}^{\infty} d\Omega \frac{2\sigma}{|k_0| \sqrt{2\pi}} \frac{1}{e^{2\pi\Omega} - 1} \\ & \quad \times \left[e^{-2\frac{\sigma^2[\Omega - (|k_0|T - k_0X)]^2}{k_0^2}} + e^{-2\frac{\sigma^2[\Omega + (|k_0|T - k_0X)]^2}{k_0^2}} \right] \end{aligned} \quad (3.14)$$

for the approximate position-dependent expectation value of the number operator in the modified Rindler vacuum. We plot this quantity in Fig. 3.3 for parameters $k_0 = 10$, $\sigma = 1$ and for three different values of ϵ . This result is a generalisation of Louko & Satz¹⁰⁴ where they calculate the response of an inertial Unruh-Dewitt detector in the Rindler vacuum. With our detector model, this corresponds to setting $\epsilon = 0$ and $X = \text{constant}$.

If we now consider a free falling observer dropped from r_0 , their inertial trajectory is given by Eq. (3.9) with $X = X_0$. To satisfy the semi-classical assumption,⁶⁶ M must be large, so we assume that $M \gg 0$. The response of such an observer, coupling to Minkowski modes can be seen in Fig. 3.3. If

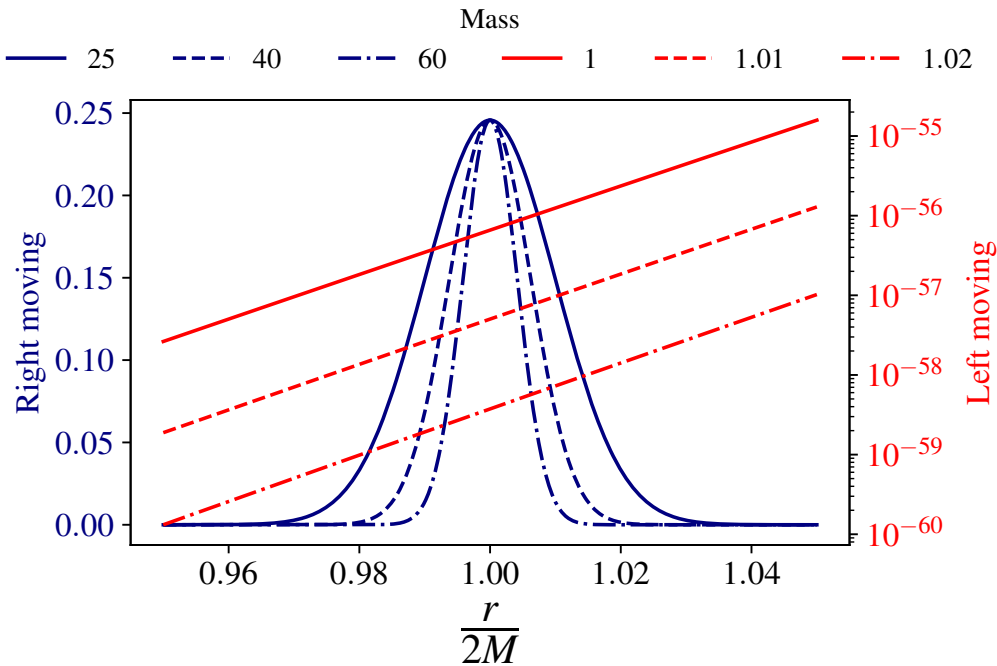


Figure 3.4: Numerical integration of Eq. (3.14) with $\sigma = 1$ and right movers ($k_0 = 10$) in blue and left movers ($k_0 = -10$) in red plotted with respect to $\frac{r}{2M}$ using Eq. (3.7) and Eq. (3.9) with $\epsilon = 10^{-5}$ and for several values of black hole mass M . Notice the large differences in the particle flux coming from the horizon (right movers) versus that coming from the sky (left movers) for the free-faller.

the detector measures right-moving modes ($k_0 > 0$), then as they approach the horizon at $T = X$ they encounter a finite number of particles. X is very large for $M \gg 0$ so $T + X$ is very large, therefore, detectors measuring left-moving modes ($k_0 < 0$) see very few particles as compared to right movers. Furthermore the number of particles they see from behind (i.e. left movers) is much smaller for larger mass black holes (See Fig. 3.4). This means that the freely falling observer runs into a ‘firewall’ at the horizon with negligible particles from behind as is expected. Interestingly, this firewall is not thermal. This can be seen in Eq. (3.12) and Eq. (3.14). The dependence on frequency at the horizon is $\frac{1}{|k_0|}$.

The particle number is larger for smaller ϵ which can be seen in Eq. (3.12). However, even for large ϵ , the inverse dependence on k_0 means that the total number of particles above any frequency is unbounded at the horizon in the absence of an UV cutoff. For example, suppose we consider a hydrogen atom in the ground state. There are an unbounded number of photons at and above the ionization energy 13.6 eV and so any hydrogen atom falling into the black hole will be ionized. This will be true for all atoms and molecules.

3.8 Cutoff

The correlations between the two modes, b_Ω and \bar{b}_Ω in Eq. (3.10) is both the cause of Hawking radiation and the origin of the problem raised by the firewall argument. In Eq. (3.11) we have excised the correlations between the two modes for $\Omega > \epsilon$. This allows the higher frequency modes to be correlated (via some modification of the standard theory) with other modes—as is required for information leakage—but has the unfortunate effect of eliminating Hawking radiation at these frequencies. However,

from the standpoint of renormalisation, we do not expect our effective field theory to be accurate for extremely high frequencies. Thus we should consider the cutoff to be a crude, but ultimately necessary admission of our ignorance of high energy physics. Above the cutoff we would expect novel physics—perhaps quantum gravity—to determine the exact structure of the firewall.

The problem is how to determine the cutoff ϵ . We note that via Wien's displacement law, the frequency spectral radiance of black body radiation peaks at $\omega_{\text{peak}} \approx 2\pi \times 2.82144T$. The cutoff frequency must therefore be $\omega_{\text{cutoff}} = \epsilon a \gg \omega_{\text{peak}}$. Using the Hawking temperature, this imposes the lower bound $\epsilon \gg 2.82144$, ensuring that most of the energy is given out via Hawking radiation for all but the highest frequencies. The specification of the cutoff at $\Omega_{\text{cutoff}} = \epsilon$ is independent of a .

3.9 Squeezing

An interesting property of the modified Minkowski vacuum is that Minkowski modes are squeezed. We define the X quadrature as $X = a + a^\dagger$ and the P quadrature as $P = -i(a - a^\dagger)$, where a is given by Eq. (3.13) with $T = X = 0$. $(\Delta X)^2$ is defined as $(\Delta X)^2 = \langle \Psi | X^2 | \Psi \rangle - (\langle \Psi | X | \Psi \rangle)^2$. ΔP is defined similarly. To simplify calculations, we can apply the approximation $|k| \gg 0$ and $|k| \gg \sigma$. With these approximations we find the variances

$$(\Delta X)^2 = 1 + \frac{2^{\frac{5}{2}}\sigma}{\pi^{\frac{1}{2}}|k_0|} \left(\epsilon - \frac{\ln(e^{\pi\epsilon} + 1)}{\pi} \right), \quad (3.15)$$

$$(\Delta P)^2 = 1 + \frac{2^{\frac{5}{2}}\sigma}{\pi^{\frac{1}{2}}|k_0|} \left(\epsilon - \frac{\ln(e^{\pi\epsilon} - 1)}{\pi} \right), \quad (3.16)$$

yielding

$$\lim_{\epsilon \rightarrow 0} (\Delta X)^2 = 1 - \frac{2^{\frac{5}{2}}\sigma \ln 2}{\pi^{\frac{3}{2}}|k_0|}, \quad (3.17)$$

$$\lim_{\epsilon \rightarrow 0} (\Delta P)^2 \rightarrow \frac{2^{\frac{5}{2}}\sigma}{\pi^{\frac{3}{2}}|k_0|} \ln(\epsilon) \rightarrow \infty \quad (3.18)$$

for $\epsilon \rightarrow 0$, in the limit of the Rindler vacuum. We see in Eqs. (3.15) and (3.17), $(\Delta X)^2$ is always less than 1, indicating single-mode squeezing (though not purely single-mode). We also see that squeezing disappears for $|k_0| \rightarrow \infty$ or for $\epsilon \rightarrow \infty$.

The origin of the squeezing comes from the Rindler aspects of the vacuum state. While the Minkowski vacuum is not a squeezed state of Minkowski modes, the Rindler vacuum is a two mode squeezed state of Unruh modes,

$$|0_R\rangle \propto \exp \left\{ - \int d\Omega \sum_{\sigma} e^{-\pi\Omega} \left(d_{\Omega}^{\text{RM}\dagger} \bar{d}_{\Omega}^{\text{RM}\dagger} + d_{\Omega}^{\text{LM}\dagger} \bar{d}_{\Omega}^{\text{LM}\dagger} \right) \right\} |0_M\rangle. \quad (3.19)$$

Unruh modes can be written in terms of Minkowski modes

$$d_{\Omega}^{\text{RM}} = \int_0^{\infty} dk p_{\Omega}(k) a_k \quad d_{\Omega}^{\text{LM}} = \int_0^{\infty} dk p_{\Omega}(-k) a_{-k}, \quad (3.20a)$$

$$\bar{d}_{\Omega}^{\text{RM}} = \int_0^{\infty} dk \bar{p}_{\Omega}(k) a_k \quad \bar{d}_{\Omega}^{\text{LM}} = \int_0^{\infty} dk \bar{p}_{\Omega}(-k) a_{-k}. \quad (3.20b)$$

Upon insertion of Eq. (3.20) into Eq. (3.19), we see that the Rindler vacuum is multi-mode squeezed in terms of Minkowski modes. Part of the multi-mode squeezing contains single-mode squeezing and it is this that contributes to the squeezing we see.

3.10 Correlations and leaking information

Central to the firewall argument of Almheiri *et al.* is the entanglement—in the standard picture—between upgoing and ingoing modes of radiation due to the free falling observer seeing a vacuum. This is the entanglement between $b_{\omega lm}^{\text{up } \dagger}$ and $\bar{b}_{\omega lm}^{\text{up } \dagger}$ in the Unruh vacuum. The entanglement precludes the leaking of information out of the black hole, which requires that the upgoing early and late radiation form a pure state. In our proposed modified Unruh vacuum, a free faller does not see a vacuum; entanglement between any two high frequency modes is absent, thus allowing the possibility that these modes can be correlated in a more complicated theory such that information may be carried out.

3.11 Conclusion

We have proposed a modified Unruh vacuum state to replace the Unruh vacuum state around a black hole. Using the correspondence between Schwarzschild and Rindler spacetimes close to the horizon, we constructed in (1+1) dimensions a modified Minkowski vacuum to model our modified Unruh state. Minkowski modes exhibit single-mode squeezing in this modified Minkowski vacuum state.

We found that this vacuum state led to a firewall as predicted by Almheiri *et al.*⁶⁶ The firewall is strikingly non-thermal: the particle number for a Gaussian detector is inversely proportional to the frequency. In the absence of a UV cutoff, any atom or molecule will immediately be ionized by the firewall due to the unbounded numbers of high energy photons. Thus any entanglement carried by atoms will be destroyed. This is in contrast to the situation that imposes a breaking of correlations across the horizon.^{105,106} The physical mechanism responsible for this remains to be found and it is not clear if it can satisfy unitarity requirements.

Our (1+1) dimensional calculation with the modified Minkowski vacuum state (3.11) is expected to be a very good approximation to the (3+1) dimensional case when a free falling observer detects very localised modes pointing in the radial direction. This provides us with confidence in our flat space calculation and the possibility that the standard theory with a modified vacuum choice could be enough to maintain Hawking radiation (with small deviations) and do the job of carrying out information. To better understand the implications of our proposal in more realistic settings will require a calculation of the behaviour of a detector in our modified Unruh vacuum (3.2) around an actual black hole.

Chapter 4

Particle creation by gravitational waves

Section 4.6 is based on the paper² “Black hole squeezers” which I wrote with Daiqin Su, Robert B Mann and Timothy C. Ralph. The bulk of the text and figures were prepared by Daiqin Su. The analysis and interpretation was shared amongst co-authors.

A major consequence of Quantum Field Theory on Curved spacetime is particle creation.^{11,41,45} From inflation^{107,108} and expanding spacetime⁴¹ to the Hawking effect²⁰ and superradiance^{109–111} in black holes, the lack of an invariant concept of a particle means that particle creation can be found everywhere.

One question of particular interest is whether gravitational waves (ripples of spacetime) can create quantum particles. Since the detection of gravitational waves,¹¹² this question is of renewed interest. Although a dynamical spacetime characteristically generates particles, it has been shown that particle creation by plane gravitational waves is forbidden.^{113–116} A similar statement applies to electromagnetic waves: electron-positron pairs cannot be produced by plane electromagnetic waves, no matter how strong we make the electromagnetic field;¹¹⁷ otherwise momentum conservation would be violated. These results were shown using an input-output formalism which obscures the origin of the (lack of) particle creation. In this chapter we will highlighting the precise reasons why—using Feynman diagrams—linear plane gravitational waves cannot create particle. Furthermore, I will show how higher order diagrams and gravitational waves also do not produce gravitational waves. Finally I will summarise the results in my paper² where we found the creation of particles for gravitational waves around a black hole.

Throughout this chapter we will consider a spacetime where we can write the metric as a background part and a perturbation,

$$g_{\mu\nu} = g_{B\mu\nu} + h_{\mu\nu}. \quad (4.1)$$

4.1 Linear gravitational waves in Minkowski spacetime

We will first consider the case where the background is Minkowski spacetime $g_{B\mu\nu} = \eta_{\mu\nu}$ with a weak perturbation also known as the weak field limit, where $h_{\mu\nu}$ is such that $h^{\mu\nu} = \eta^{\mu\alpha}\eta^{\nu\beta}h_{\alpha\beta}$ and

$$h^{\mu\nu} h_{\mu\nu} \approx 0,$$

$$g_{\mu\nu} = \eta_{\mu\nu} + h_{\mu\nu} \quad g^{\mu\nu} = \eta^{\mu\nu} - h^{\mu\nu}, \quad (4.2)$$

where $\eta_{\mu\nu}$ is the Minkowski metric and $h^{\mu\nu} h_{\nu\rho} = \delta_\rho^\mu$. With this linearisation, Einstein's field equation becomes,

$$R_{\mu\nu} = -\frac{1}{2} \left(\partial^2 h_{\mu\nu} - \partial_\mu \partial_\lambda h^\lambda{}_\nu - \partial_\nu \partial_\lambda h^\lambda{}_\mu + \partial_\mu \partial_\nu h^\lambda{}_\lambda \right) + O(h^2). \quad (4.3)$$

We still have all the freedom of coordinate transforms with which we can simplify the field equation further. Let us make the transformation $x^\mu \rightarrow x'^\mu = x^\mu + \epsilon^\mu(x)$. We require that $\partial_\mu \epsilon_\nu$ is small which leads us to

$$h'_{\mu\nu} = h_{\mu\nu} - \partial_\mu \epsilon_\nu - \partial_\nu \epsilon_\mu. \quad (4.4)$$

With this we can calculate that, $\partial'_\mu h'^\mu{}_\nu - \frac{1}{2} \partial'_\nu h' \approx \partial_\mu h^\mu{}_\nu - \frac{1}{2} \partial_\nu h - \partial^2 \epsilon_\nu$ where $\partial^2 = \partial_\mu \partial^\mu$, h is the trace $h = \eta^{\mu\nu} h_{\mu\nu}$ and $\partial'_\mu = \partial_\mu - (\partial_\mu \epsilon^\lambda) \partial_\lambda$. This means we can always pick an ϵ such that we impose four conditions known as the harmonic gauge condition,

$$\partial_\mu h^\mu{}_\nu = \frac{1}{2} \partial_\nu h, \quad (4.5)$$

is always true. In this harmonic gauge, the Einstein Field equation in vacuum ($T_{\mu\nu} = 0$)

$$R_{\mu\nu} = -\frac{1}{2} \partial_\alpha \partial^\alpha h_{\mu\nu} = 0. \quad (4.6)$$

We see that this reduces the dynamics of the perturbation to a relativistic wave equation. We have some residual freedom to simplify further. Note that $\partial_\mu h'^\mu{}_\nu - \frac{1}{2} \partial_\nu h' = \partial_\mu h^\mu{}_\nu - \frac{1}{2} \partial_\nu h - \partial^2 \epsilon_\nu$. This means that we can make one final change of coordinates such that $\partial^2 \epsilon_\nu = 0$ (which corresponds to four conditions) and still maintain the harmonic gauge condition. Originally the symmetric tensor $h_{\mu\nu}$ has 10 components. The harmonic gauge condition imposes 4 conditions, reducing the degree of freedom to 6. Finally, our residual transformation allows us to reduce it to $6-4 = 2$. But which final 4 conditions should we impose? The natural choice suggested by analogy with electromagnetic waves is something like the Coulomb gauge. First note that the solution to Eq. (4.6) is given by a superposition of linear plane waves,

$$h_{\mu\nu}(x) = \int d^4k C_{\mu\nu}(k) e^{ik \cdot x}. \quad (4.7)$$

The wave equation means that $k^2 = 0$ and the harmonic gauge condition means $k_\mu C^\mu{}_\nu(k) = \frac{1}{2} k_\nu C(k)$ where $C_{\mu\nu}(k)$ is a polarization tensor and $C(k) = C^\mu{}_\mu(k)$. We choose the final 4 conditions $C_{0,i} = 0$ for $i = 1, 2, 3$ and $C = 0$ as the transverse-traceless gauge. Suppose the gravitational wave is a cosine wave in the z -direction with frequency k_0 . Then $C_{\mu\nu}(k) = \tilde{C}_{\mu\nu}/2 \left(\delta^{(4)}(k - k_0) + \delta^{(4)}(k + k_0) \right) \implies h_{\mu\nu}(x) = \tilde{C}_{\mu\nu}(k_0) \cos(k_0 \cdot x)$ where $k_0^\mu = k_0(1, 0, 0, 1)$. Our conditions means that the polarization tensor must be of the form,

$$\tilde{C}_{\mu\nu}(k_0) = \begin{pmatrix} 0 & 0 & 0 & 0 \\ 0 & \tilde{C}_+ & \tilde{C}_\times & 0 \\ 0 & \tilde{C}_\times & -\tilde{C}_+ & 0 \\ 0 & 0 & 0 & 0 \end{pmatrix}, \quad (4.8)$$

which is characterised by two polarisations, \tilde{C}_+ and \tilde{C}_\times representing the two degrees of freedom.

4.2 Path integral formalism

For most of this chapter we will work with Feynman diagrams with rules derived from the path integral formalism. Before we apply the path integral formalism to fields, let us first review the formalism for quantum mechanics. Suppose we have a single particle with an initial state $|q_I\rangle$ and we want to find the amplitude for it to evolve to $|q_F\rangle$ after a time T . The dynamics of the particle are governed by a Hamiltonian (temporarily restoring operator hats) of the form,

$$\hat{H} = \frac{\hat{p}^2}{2m} + V(\hat{q}). \quad (4.9)$$

To find the amplitude we have to calculate

$$\langle q_F | e^{-i\hat{H}T} | q_I \rangle. \quad (4.10)$$

Let us discretise time into N segments such that $\delta t = T/N$. The amplitude becomes

$$\langle q_F | e^{-i\hat{H}T} | q_I \rangle = \langle q_F | e^{-i\hat{H}\delta t} e^{-i\hat{H}\delta t} \dots e^{-i\hat{H}\delta t} | q_I \rangle. \quad (4.11)$$

The states q are normalised such that $\langle q' | q \rangle = \delta(q' - q)$. The position eigenstate $|q\rangle$ and the momentum eigenstates $|p\rangle$ both form a complete set of states so $\int dq |q\rangle \langle q| = \int dp |p\rangle \langle p| = 1$. With this normalisation, the overlap is $\langle q | p \rangle = \frac{e^{ipq}}{\sqrt{2\pi}}$. We will now use the completeness of the position eigenstates and insert factors of $1 = \int dq_j |q_j\rangle \langle q_j|$ in the amplitude.

$$\langle q_F | e^{-i\hat{H}T} | q_I \rangle = \left(\prod_{j=1}^{N-1} \int dq_j \right) \langle q_F | e^{-i\hat{H}\delta t} | q_{N-1} \rangle \langle q_{N-1} | e^{-i\hat{H}\delta t} | q_{N-2} \rangle \dots \langle q_1 | e^{-i\hat{H}\delta t} | q_I \rangle. \quad (4.12)$$

Consider one of the factors above, $\langle q_{j+1} | e^{-i\hat{H}\delta t} | q_j \rangle$. Because δt is small, the exponential is well approximated by $1 - i\hat{H}\delta t$. If we insert $\int dp |p\rangle \langle p| = 1$ we find that the factor becomes,

$$\langle q_{j+1} | e^{-i\hat{H}\delta t} | q_j \rangle = \langle q_{j+1} | \left[1 - i \left(\frac{\hat{p}^2}{2m} \int dp |p\rangle \langle p| + V(\hat{q}) \right) \delta t \right] | q_j \rangle \quad (4.13)$$

$$= e^{-i\delta t V(q_j)} \int dp e^{-i\delta t \frac{p^2}{2m}} \langle q_{j+1} | p \rangle \langle p | q_j \rangle \quad (4.14)$$

$$= e^{-i\delta t V(q_j)} \int \frac{dp}{2\pi} e^{-i\delta t \frac{p^2}{2m}} e^{ip(q_{j+1}-q_j)}. \quad (4.15)$$

The integral is a Gaussian which can be calculated by the completing the square,

$$\langle q_{j+1} | e^{-i\hat{H}\delta t} | q_j \rangle = \left(\frac{-im}{2\pi\delta t} \right)^{\frac{1}{2}} e^{i\delta t \frac{m}{2} \left(\frac{q_{j+1}-q_j}{\delta t} \right)^2 - i\delta t V(q_j)}. \quad (4.16)$$

Putting this into Eq. (4.12) and defining $q_0 = q_I$ and $q_N = q_F$, we get

$$\langle q_F | e^{-i\hat{H}T} | q_I \rangle = \left(\frac{-im}{2\pi\delta t} \right)^{\frac{N}{2}} \left(\prod_{k=1}^{N-1} \int dq_k \right) e^{i\delta t \sum_{j=0}^{N-1} \left[\frac{m}{2} \left(\frac{q_{j+1}-q_j}{\delta t} \right)^2 - V(q_j) \right]}. \quad (4.17)$$

If we take the limit that $\delta t \rightarrow 0$ then $\frac{m}{2} \left(\frac{q_{j+1} - q_j}{\delta t} \right)^2 \rightarrow \dot{q}^2$ and $\delta t \sum_{j=0}^{N-1} \rightarrow \int_0^T dt$ then the measure for the integral over paths is

$$\int \mathcal{D}q = \lim_{N \rightarrow \infty} \left(\frac{-im}{2\pi\delta t} \right)^{\frac{N}{2}} \left(\prod_{k=1}^{N-1} \int dq_k \right). \quad (4.18)$$

We thus define the path integral as

$$\begin{aligned} \langle q_F | e^{-i\hat{H}T} | q_I \rangle &= \int \mathcal{D}q e^{i \int_0^T dt \left(\frac{m\dot{q}^2}{2} - V(q) \right)} \\ &= \int \mathcal{D}q e^{i \int_0^T dt L}, \end{aligned} \quad (4.19)$$

with L the Lagrangian for the system. Note that the right hand side is composed of c-numbers, not operators. Finally we note what happens if we want to calculate expectations of operators. If we have the Schrödinger operator (indicated by a subscript S) for the position \hat{q}_S that we want to calculate at t_2 and t_1 such that $t_2 > t_1$, then we can show that the expectation of the Heisenberg operators (indicated by subscript H) is

$$\begin{aligned} &\langle q_F | \widehat{q}_H(t_2) \widehat{q}_H(t_1) | q_I \rangle \\ &= \langle q_F | e^{-i\hat{H}(T-t_2)} \widehat{q}_S e^{-i\hat{H}(t_2-t_1)} \widehat{q}_S e^{-i\hat{H}(t_1)} | q_I \rangle \\ &= \int \mathcal{D}q e^{i \int_0^T dt L} q(t_2) q(t_1), \end{aligned} \quad (4.20)$$

with $q(t_j) | q_j \rangle = \widehat{q}_S | q_j \rangle$ such that $j\delta t = t_j$.

4.2.1 Path integrals for fields

Now that we have defined the path integral for quantum mechanics, let us apply it to field theory. Because the field at a given time t_1 is a function of position, instead of being a simple integral in the quantum mechanical case $\left(\int dq |q\rangle \langle q| \right) = 1$, the completeness relation for fields is itself a functional integral overall field configurations at t_1

$$\int \mathcal{D} \Phi_1(\mathbf{x}) | \Phi_1(\mathbf{x}) \rangle \langle \Phi_1(\mathbf{x}) | = 1. \quad (4.21)$$

With this completeness relation, we can derive a path integral for fields in a similar way as before. However, as the form of the path integral is extremely similar to the quantum mechanical case, we will define it by analogy.

Suppose we have a scalar field with the Lagrangian density*

$$\mathcal{L}_0 = \frac{1}{2} \left(\eta^{\mu\nu} \partial_\mu \Phi \partial_\nu \Phi - m^2 \Phi^2 \right). \quad (4.24)$$

* For the rest of this chapter except for Section 4.6, we will use the (+ - - -) convention so as to comport with the usual convention of particle physics QFT. We will also define the Fourier transform as,

$$f(x) = \int \frac{d^4 k}{(2\pi)^4} e^{-ik \cdot x} \tilde{f}(k) \quad (4.22)$$

$$\tilde{f}(k) = \int d^4 x e^{ik \cdot x} f(x). \quad (4.23)$$

We need to generalise Eq. (4.19) for fields. Notice that instead of q as the dynamical variable, we have the field $\Phi(x) = \Phi(\mathbf{x}, t)$ and the time integral over the Lagrangian is promoted to a spacetime integral over the Lagrangian density. The path integral is then defined as

$$Z = \int \mathcal{D}\Phi e^{i \int d^4x \mathcal{L}_0}. \quad (4.25)$$

For convenience we will introduce a source term $J(x)$ to the exponential. With the addition of the source term and a partial integration over the derivative terms, the path integral becomes

$$Z(J) = \int \mathcal{D}\Phi e^{i \int d^4x -\frac{1}{2}\Phi(\partial^2+m^2)\Phi + J(x)\Phi(x)}. \quad (4.26)$$

This integral can actually be done directly if we discretise spacetime into N points with spacing a . Letting j label the spacetime points, the differential operator becomes $\partial\Phi \rightarrow \frac{1}{a}(\Phi_{j+1} - \Phi_j) \equiv \sum_j M_{jk}\Phi_k$. The path integral is then of the form

$$\int \int \cdots \int dq_1 dq_2 \cdots dq_N e^{\frac{i}{2}q \cdot A \cdot q + iJ \cdot q} \quad (4.27)$$

$$= \left(\frac{(2\pi i)^N}{\det A} \right)^{\frac{1}{2}} e^{-\frac{i}{2}J \cdot A^{-1} \cdot J}. \quad (4.28)$$

For the proof of this equality, see Zee.⁴⁴ The matrix A is the discretised form of $-(\partial^2 + m^2)$. In the continuum limit, the discretised equation $A_{ij}(A^{-1})_{jk} = \delta_{ik}$ becomes (with the addition of a factor of i)

$$-(\partial^2 + m^2) D(x - y) = i\delta^{(4)}(x - y). \quad (4.29)$$

The propagator is also called the two-point Green's function as it is the inverse of a differential operator. The continuum limit of the inverse matrix A^{-1} is $D(x - y)$ is defined by Eq. (4.29). Then our result is,

$$\frac{Z(J)}{Z(0)} = e^{-\frac{i}{2} \int \int d^4x d^4y J(x) D(x-y) J(y)}. \quad (4.30)$$

$D(x - y)$ is known as the propagator which is given by

$$D(x - y) = \int \frac{d^4p}{(2\pi)^4} \frac{ie^{-ip \cdot (x-y)}}{p^2 - m^2 + i\epsilon}. \quad (4.31)$$

Instead of the ϵ we can equivalently define it as a slight anti-clockwise rotation (or a deformation) of a complex contour integral to avoid the poles at $p^2 = m^2$. This is also known as the Feynman propagator.

4.2.2 Correlation/Green's functions

Suppose instead of the Lagrangian density \mathcal{L}_0 we now have an interacting term and a new Lagrangian/Hamiltonian density. With this we have a new Hamiltonian $H(t) = \int d^3x \mathcal{H}$ with which we can define a time-evolution operator using a Dyson series

$$\begin{aligned} \widehat{U}(t, t_0) = & 1 - i \int_{t_0}^t dt_1 \widehat{H}(t_1) + (-i)^2 \int_{t_0}^t dt_1 \int_{t_0}^{t_1} dt_2 \widehat{H}(t_1) \widehat{H}(t_2) \\ & + (-i)^3 \int_{t_0}^t dt_1 \int_{t_0}^{t_1} dt_2 \int_{t_0}^{t_2} dt_3 \widehat{H}(t_1) \widehat{H}(t_2) \widehat{H}(t_3) + \dots \end{aligned} \quad (4.32)$$

Note that the Hamiltonians are arranged in time-order. We also introduce the time-ordering operator \mathcal{T} which arranges the operands into the correct time order. Together with the identity,

$$\int_{t_0}^t dt_1 \int_{t_0}^{t_1} dt_2 \int_{t_0}^{t_{n-1}} \cdots dt_n \widehat{H}(t_1) \widehat{H}(t_2) \cdots \widehat{H}(t_n) = \frac{1}{n!} \int_{t_0}^t dt_1 \int_{t_0}^{t_1} dt_2 \int_{t_0}^{t_2} \cdots dt_n \mathcal{T} \left\{ \widehat{H}(t_1) \widehat{H}(t_2) \cdots \widehat{H}(t_n) \right\} \quad (4.33)$$

we can rewrite the time-evolution operator as

$$\begin{aligned} \widehat{U}(t, t_0) &= 1 - i \int_{t_0}^t dt_1 \widehat{H}(t_1) + \frac{(-i)^2}{2!} \int_{t_0}^t dt_1 dt_2 \mathcal{T} \widehat{H}(t_1) \widehat{H}(t_2) + \dots \\ &\equiv \mathcal{T} \left\{ \exp \left[-i \int_{t_0}^t dt' \widehat{H}(t') \right] \right\}. \end{aligned} \quad (4.34)$$

The original Lagrangian \mathcal{L}_0 has the (Minkowski) vacuum state $|0\rangle$ with a zero energy as $\widehat{H}_0 |0\rangle = 0$. The new Lagrangian has a vacuum state $|\Omega\rangle$ and energy $\widehat{H} |\Omega\rangle = E_0 |\Omega\rangle$. Suppose there are discrete eigenstates of the new Hamiltonian H indexed by n . Then, the time-evolution operator acting on the vacuum is

$$\widehat{U}(T, 0) |0\rangle = e^{-iE_0 T} |\Omega\rangle \langle \Omega | 0\rangle + \sum_{n \neq 0} e^{-iE_n T} |n\rangle \langle n | 0\rangle. \quad (4.35)$$

Since $E_n > E_0$ we can remove the second term by sending $T \rightarrow \infty(1 - i\epsilon)$ to a slightly imaginary direction. This gives us an expression

$$|\Omega\rangle = \lim_{T \rightarrow \infty(1-i\epsilon)} \frac{e^{-iHT} |0\rangle}{e^{-iE_0 T} \langle \Omega | 0\rangle}. \quad (4.36)$$

This lets us define the new interacting vacuum in terms of the free vacuum which we will use presently. As we saw in Chapter 2, the concept of particles in Quantum Field Theory is a rather nebulous one. Nonetheless, $\Phi(x) |\Omega\rangle$ can be thought of as a particle as it is a single perfectly localised excitation of the field. Thus, similar to the quantum mechanical example before, the amplitude for a ‘particle’ at x_1 to ‘propagate’ or evolve to another ‘particle’ at x_2 is given by

$$\langle \Omega | \mathcal{T} \left\{ \widehat{\Phi}_H(x_1) \widehat{\Phi}_H(x_2) \right\} | \Omega \rangle \equiv \lim_{T \rightarrow \infty(1-i\epsilon)} \frac{\langle 0 | \mathcal{T} \left\{ \widehat{U}(T, x_2^0) \widehat{\Phi}_S(x_2^0, \mathbf{x}_2) \widehat{U}(x_2^0, x_1^0) \widehat{\Phi}_S(x_1^0, \mathbf{x}_1) \widehat{U}(x_1^0, -T) \right\} | 0 \rangle}{\langle 0 | \widehat{U}(T, -T) | 0 \rangle} \quad (4.37)$$

$$= \frac{\int \mathcal{D}\Phi e^{i \int d^4x \mathcal{L}} \Phi(x_1) \Phi(x_2)}{\int \mathcal{D}\Phi e^{i \int d^4x \mathcal{L}}} \quad (4.38)$$

$$= \frac{1}{Z(0)} \left(-i \frac{\delta}{\delta J(x_1)} \right) \left(-i \frac{\delta}{\delta J(x_2)} \right) Z(J)|_{J=0}, \quad (4.39)$$

In the equation we have used $\frac{\delta}{\delta J}$, which is a functional derivative that ‘pulls down’ the appropriate $\Phi(x)$ from Eq. (4.26). The functional derivative is defined such that

$$\frac{\delta}{\delta J(x)} J(y) = \delta^{(4)}(x - y), \quad (4.40)$$

with all other calculus rules such as chain rule, product rule etc. also holding. Evaluating Eq. (4.39) by taking the derivatives of Eq. (4.30), we find the two-point Green's function (also known as the two-point correlation function)

$$\langle 0 | \mathcal{T} \{ \Phi(x_1) \Phi(x_2) \} | 0 \rangle = D(x_1 - x_2). \quad (4.41)$$

This term is associated with the Feynman diagram

$$x_1 \text{ --- } x_2 = \int \frac{d^4 p}{(2\pi)^4} \frac{ie^{-ip \cdot (x_1 - x_2)}}{p^2 - m^2 + i\epsilon}. \quad (4.42)$$

We will draw our diagrams such that they are read from left to right.

There also exist higher order correlation/Green's functions, for example, the four-point correlation function,

$$\langle \Omega | \mathcal{T} \{ \Phi_1 \Phi_2 \Phi_3 \Phi_4 \} | \Omega \rangle \quad (4.43)$$

$$= \begin{array}{c} x_1 \text{ --- } x_2 \\ x_3 \text{ --- } x_4 \end{array} + \begin{array}{c} x_1 \\ | \\ x_3 \end{array} \begin{array}{c} x_2 \\ | \\ x_4 \end{array} + \begin{array}{c} x_1 \quad x_2 \\ \quad \diagdown \quad \diagup \\ x_3 \quad x_4 \end{array} \quad (4.44)$$

$$= D(x_1 - x_2)D(x_3 - x_4) + D(x_1 - x_3)D(x_2 - x_4) + D(x_1 - x_4)D(x_2 - x_3). \quad (4.45)$$

These higher order Green's functions can be defined an expansion of Eq. (4.26) in a power series of J

$$Z(J) = \sum_j \frac{i^j}{j!} \int d^4 x_1 \cdots d^4 x_j J(x_1) \cdots J(x_j) \left\{ \int \mathcal{D}\Phi e^{i \int \mathcal{L} d^4 x} \Phi(x_1) \cdots \Phi(x_j) \right\}, \quad (4.46)$$

where the j^{th} Green's function is the expression in the curly braces divided by $Z(J=0)$.

4.2.3 Φ^4 Interactions

Suppose we have a new Lagrangian with a Φ^4 interaction term

$$\mathcal{L} = \frac{1}{2} \left(\eta^{\mu\nu} \partial_\mu \Phi \partial_\nu \Phi - m^2 \Phi^2 \right) - \frac{\lambda}{4!} \Phi^4. \quad (4.47)$$

Then the path integral becomes

$$Z(J, \lambda) = \int \mathcal{D}\Phi e^{i \int d^4 x \left[-\frac{1}{2} \Phi (\partial^2 + m^2) \Phi - \frac{\lambda}{4!} \Phi^4 + J(x) \Phi(x) \right]}, \quad (4.48)$$

which with the use of functional derivatives and the methods we used above, can be rewritten as

$$Z(J, \lambda) = Z(0, 0) e^{-(i\lambda/4!) \int d^4 w [-i\delta/\delta J(w)]^4} e^{-\frac{1}{2} \int d^4 x d^4 y J(x) D(x-y) J(y)}. \quad (4.49)$$

Meanwhile, the j^{th} Green's function is given by

$$\frac{1}{Z(0, \lambda)} \left\{ \int \mathcal{D}\Phi e^{i \int \mathcal{L} d^4 x} \Phi(x_1) \cdots \Phi(x_j) \right\} = \frac{1}{Z(0, \lambda)} \left(-i \frac{\delta}{\delta J(x_1)} \right) \left(-i \frac{\delta}{\delta J(x_2)} \right) \cdots \left(-i \frac{\delta}{\delta J(x_j)} \right) Z(J, \lambda) |_{J=0}. \quad (4.50)$$

While we could use this expression to calculate the Green's functions to arbitrary order in λ the calculus proves to be extremely tedious and it is much easier to introduce Wick contractions and Feynman rules. Let us consider again the four-point Green's function—expanded in a power series of λ —which comes from the path integral

$$\begin{aligned} & \frac{\int \mathcal{D}\Phi e^{i \int d^4x \mathcal{L}} \Phi(x_1)\Phi(x_2)\Phi(x_3)\Phi(x_4)}{Z(0, \lambda)} \\ &= \frac{1}{Z(0, \lambda)} \int \mathcal{D}\Phi e^{i \int d^4x \mathcal{L}_0} \left(\Phi(x_1)\Phi(x_2)\Phi(x_3)\Phi(x_4) - \frac{i\lambda}{4!} \int d^4w \Phi(x_1)\Phi(x_2)\Phi(x_3)\Phi(x_4)\Phi(w)^4 + \dots \right). \end{aligned} \quad (4.51)$$

The rule for calculating the path integral of each is to contract each Φ with another, replacing them with a propagator. You continue for each permutation. For example, the ways to contract the first term in the round brackets are

$$\overbrace{\Phi(x_1)\Phi(x_2)\Phi(x_3)\Phi(x_4)} \quad \overbrace{\Phi(x_1)\Phi(x_2)\Phi(x_3)\Phi(x_4)} \quad \overbrace{\Phi(x_1)\Phi(x_2)\Phi(x_3)\Phi(x_4)}. \quad (4.52)$$

This gives us the three terms of Eq. (4.45). The second term has multiple ways we can contract. We can contract x_1, x_2, x_3, x_4 in the three ways we just mentioned. This would leave 3 ways to contract the remaining $\Phi(w)$ with each other. This contributes a term

$$\frac{-3i\lambda}{4!} \int d^4w D(w-w)^2 (D(x_1-x_2)D(x_3-x_4) + D(x_1-x_3)D(x_2-x_4) + D(x_1-x_4))D(x_2-x_3), \quad (4.53)$$

which is represented by the Feynman diagram

$$\left(\text{bubble} \left(\begin{array}{ccc} x_1 \text{ --- } x_2 & x_1 & x_2 \\ & | & | \\ x_3 \text{ --- } x_4 & x_3 & x_4 \end{array} + \begin{array}{ccc} & & x_1 \\ & & | \\ & & x_4 \\ & & | \\ & & x_3 \\ & & | \\ & & x_2 \end{array} + \begin{array}{ccc} & & x_1 & & x_2 \\ & & & \diagdown & / \\ & & x_3 & & x_4 \end{array} \right) \right). \quad (4.54)$$

The bubble on the left is a 'vacuum bubble' which we will discuss shortly. There is also another way to contract, each of the x_i is contracted with a w which forms a *vertex*. There are $4!$ ways to do this and is given by the diagram with the value

$$\begin{array}{ccc} x_1 & & x_2 \\ & \diagdown & / \\ & \bullet & \\ & / & \diagdown \\ x_3 & & x_4 \end{array} = -i\lambda \int d^4w D(x_1-w)D(x_2-w)D(x_3-w)D(x_4-w). \quad (4.55)$$

Finally, there are 6 other diagrams which involve sticking an 'ear' on the diagrams of Eq. (4.44). For example there are 3×4 ways of sticking an ear on the first diagram

$$\begin{array}{ccc} & \text{loop} & \\ & \bullet & \\ x_1 \text{ --- } & & \text{--- } x_2 \\ & & \\ x_3 \text{ --- } & & \text{--- } x_4 \end{array} = \frac{-12i\lambda}{4!} \int d^4w D(x_1-w)D(w-w)D(x_2-w)D(x_3-x_4). \quad (4.56)$$

These are self-interaction diagrams, also known as self-energy diagrams and they are related to renormalisation of particle mass.

4.2.4 Vacuum bubbles

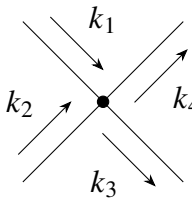
Notice how the vacuum bubble in Eq. (4.54) factorises out? In fact there is a general argument that shows that these vacuum bubbles exponentiate, factor and are cancelled by the $Z(0, \lambda)$ term⁷ in the definition of the Green's functions. While I will not show this, you can understand it heuristically by considering $Z(0, \lambda)$. By definition, it consists of the diagrams with no external source J . These diagrams in fact give us a formula for the vacuum energy of the interaction vacuum relative to the zero vacuum energy of the free vacuum. These diagrams form the quantum 'sea of roiling particles' where particle and antiparticle are created and quickly annihilate. There is a fascinating connection between the unitary inequivalence we saw in Chapter 2 and the unitary inequivalence between free and interacting theories. The lack of a unitary equivalence between the free and interacting operators and Hilbert spaces is known as Haag's theorem.

4.2.5 Momentum space Feynman diagrams

As we have seen, Feynman diagrams are calculational techniques for the probability amplitude for a physical process. The two-point Green's function gives the amplitude for a particle to propagate from x_1 to x_2 while the four-point Green's function gives the amplitude for two particles to propagate from x_1 and x_3 to x_2 and x_4 . With interactions there are additional contributions from the Φ^4 interaction. As we discussed, the vacuum bubble diagrams are factored out while the self-energy diagrams contributes only to the renormalisation of the particle mass, thus the important vertex we need to consider is Eq. (4.55). It is useful when comparing to experiments and customary to express Feynman diagrams in momentum space. This corresponds to taking the Fourier transform of the external points of the diagram. For example, the propagator which has two points, so we take the Fourier transform of the two external points,

$$\begin{aligned} & \int d^4x_1 e^{ik_1 \cdot x_1} \int d^4x_2 e^{ik_2 \cdot x_2} \text{---} x_1 \text{---} x_2 \\ &= \int d^4x_1 e^{ik_1 \cdot x_1} \int d^4x_2 e^{ik_2 \cdot x_2} \int \frac{d^4p}{(2\pi)^4} \frac{ie^{-ip \cdot (x_1 - x_2)}}{p^2 - m^2 + i\epsilon} \\ &= (2\pi)^4 \delta^{(4)}(k_2 - k_1) \frac{i}{k_1^2 - m^2 + i\epsilon}. \end{aligned} \tag{4.57}$$

Note how the exponential factor associated the the propagator imposes momentum conservation. Let us now look at the vertex, do the integral over w in Eq. (4.55) and then Fourier transform each point of the vertex. This leads to



$$= -i\lambda(2\pi)^4 \delta^{(4)}(k_4 + k_3 - k_2 - k_1) \frac{i}{k_1^2 - m^2 + i\epsilon} \frac{i}{k_2^2 - m^2 + i\epsilon} \frac{i}{k_3^2 - m^2 + i\epsilon} \frac{i}{k_4^2 - m^2 + i\epsilon}. \tag{4.58}$$

In general, for an n-point diagram with N_{in} lines going in and N_{out} lines going out, there is always an overall factor of $(2\pi)^4 \delta^{(4)}\left(\sum_i^{N_{out}} p_i - \sum_j^{N_{in}} k_j\right)$. Given that this is always the case, we will omit it from

the expression for the amplitude and take it as implied. Furthermore, while our Feynman diagrams represent amplitudes from the correlation functions, what we usually want is the S-matrix, which is the amplitude

$$\text{out} \langle \mathbf{p}_1 \cdots \mathbf{p}_{N_{\text{out}}} | \mathbf{k}_1 \cdots \mathbf{k}_{N_{\text{in}}} \rangle_{\text{in}} = \left\langle \Omega \left| a_{\mathbf{p}_1} \cdots a_{\mathbf{p}_{N_{\text{out}}}} \mathcal{T} \exp \left(-i \int_{-\infty}^{\infty} H_I(t') dt' \right) a_{\mathbf{k}_1}^\dagger \cdots a_{\mathbf{k}_{N_{\text{in}}}}^\dagger \right| \Omega \right\rangle, \quad (4.59)$$

where $a_{\mathbf{p}_i}$ are the Minkowski annihilation operators. The Lehmann, Symanzik and Zimmermann (LSZ) reduction formula gives a simple relation between correlation functions and S-matrix elements. To get the S-matrix elements, the external lines of a diagram are ‘amputated’. This means that the propagators for the external lines are not included in the S-matrix amplitude. With these patterns, we now enumerate the Feynman rules for finding the amplitude of a diagram. First, draw the diagrams of the process up to arbitrary order in λ . For example a process such as two particles scattering off each other is given by the four-point correlation function. Label each internal line with a momentum arrow and the momentum space propagator

$$\begin{array}{c} \xrightarrow{p} \\ \hline \end{array} = \frac{i}{p^2 - m^2 + i\epsilon}, \quad (4.60)$$

and each vertex is associated with the value

$$\begin{array}{c} \begin{array}{ccc} & k_1 & \\ & \searrow & \nearrow \\ k_2 & \bullet & k_4 \\ & \nearrow & \searrow \\ & k_3 & \end{array} = -i\lambda. \end{array} \quad (4.61)$$

Now restore the momentum conservation factors and integrate over the internal lines with the measure $\frac{d^4 p}{(2\pi)^4}$. Note that this rule does not apply to external lines and vertices. Finally, we must also include symmetry factors for the number of ways we could have drawn the diagram. These can be understood by thinking about the Wick contractions/functional derivatives that lead to each Feynman diagram.

4.3 Scalar field in gravitational waves

Let us now consider the scalar field with a gravitational wave. The full Lagrangian is

$$\mathcal{L} = \sqrt{|g|} \frac{1}{2} \left(g^{\mu\nu} \partial_\mu \Phi \partial_\nu \Phi - m^2 \Phi^2 \right). \quad (4.62)$$

From our linearisation of the metric before, $g_{\mu\nu} = \eta_{\mu\nu} + h_{\mu\nu}$ and $g^{\mu\nu} = \eta^{\mu\nu} - h^{\mu\nu}$ so the Lagrangian separates into a free part and an interacting part,

$$\mathcal{L} \approx \sqrt{1+h} \mathcal{L}_0 - \frac{1}{2} h^{\mu\nu} \partial_\mu \Phi \partial_\nu \Phi, \quad (4.63)$$

where

$$\mathcal{L}_0 = \frac{1}{2} \left(\eta^{\mu\nu} \partial_\mu \Phi \partial_\nu \Phi - m^2 \Phi^2 \right) \quad (4.64)$$

and

$$h = h_{\mu\nu}\eta^{\mu\nu}. \quad (4.65)$$

Because we can go to the transverse-traceless gauge in the first-order of h , we can ignore the trace and therefore we have,

$$\mathcal{L} \approx \mathcal{L}_0 - \frac{\lambda}{2} h^{\mu\nu} \partial_\mu \Phi \partial_\nu \Phi, \quad (4.66)$$

which for convenience we have added a λ term so we can ‘turn off’ the interacting term. We define the path integral,

$$Z(J, \lambda) = \int \mathcal{D}\Phi e^{i \int \mathcal{L}_0 + J\Phi - \frac{\lambda}{2} h^{\mu\nu} \partial_\mu \Phi \partial_\nu \Phi d^4x} \quad (4.67)$$

which can be integrated, simplified and rewritten using functional derivatives^{7,44} as

$$Z(J, \lambda) = Z(0, 0) e^{-i \frac{\lambda}{2} \int d^4z h^{\mu\nu}(z) \partial_\mu \left(\frac{\delta}{\delta J(z)} \right) \partial_\nu \left(\frac{\delta}{\delta J(z)} \right)} e^{-\frac{i}{2} \iint d^4x d^4y J(x) D(x-y) J(y)}. \quad (4.68)$$

Expanding Eq. (4.67) in a power series of J , we find that

$$Z(J, \lambda) = \sum_j \frac{i^j}{j!} \int d^4x_1 \cdots d^4x_j J(x_1) \cdots J(x_j) \left\{ \int \mathcal{D}\Phi e^{i \int \mathcal{L} d^4x} \Phi(x_1) \cdots \Phi(x_j) \right\}, \quad (4.69)$$

from which we define the j^{th} Green’s function as the expression in the curly braces divided by $Z(0, \lambda)$.

It follows that the two point Green’s function is

$$G(x_1, x_2) = \frac{1}{Z(0, \lambda)} \int \mathcal{D}\Phi e^{i \int \mathcal{L} d^4x} \Phi(x_1) \Phi(x_2), \quad (4.70)$$

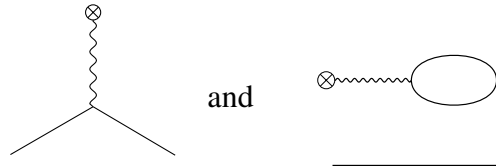
which can be rewritten by expressing the interaction Lagrangian as an infinite sum,

$$G(x_1, x_2) = \frac{1}{Z(0, \lambda)} \int \mathcal{D}\Phi e^{i \int \mathcal{L}_0 d^4x} \Phi(x_1) \Phi(x_2) \left(1 - i\lambda \int d^4x \frac{1}{2} h^{\mu\nu} \partial_\mu \Phi \partial_\nu \Phi + \dots \right). \quad (4.71)$$

The first term gives us the position space propagator in scalar field theory

$$x_1 \text{ --- } x_2 = D(x_1 - x_2) = \int \frac{d^4p}{(2\pi)^4} \frac{i}{p^2 - m^2 + i\epsilon} e^{-ip \cdot (x_1 - x_2)}. \quad (4.72)$$

The second term gives us two diagrams,



$$\text{and} \quad (4.73)$$

The second term is a disconnected diagram of a bubble diagram and the propagator. The bubble diagram is factored^{7,44} out by $1/Z(0, \lambda)$. We now need to find the value of the vertex. Setting $\lambda = 1$ from now on, we can evaluate the second term by the two ways we can Wick contract (or from the integrated functional derivative version in Eq. (4.69)) and ignoring the disconnected term, we find

$$\begin{aligned} & -i \frac{1}{Z} \int \mathcal{D}\Phi e^{i \int \mathcal{L}_0 d^4x} \Phi(x_1) \Phi(x_2) \int d^4x \frac{1}{2} h^{\mu\nu} \partial_\mu \Phi(x) \partial_\nu \Phi(x) \\ & = -i \int d^4x h^{\mu\nu} \partial_\mu D(x - x_1) \partial_\nu D(x - x_2) \\ & = i \int d^4x \frac{d^4p}{(2\pi)^4} \frac{d^4q}{(2\pi)^4} h^{\mu\nu} p_\mu \frac{i}{p^2 - m^2 + i\epsilon} e^{-ip \cdot (x - x_1)} q_\nu \frac{i}{q^2 - m^2 + i\epsilon} e^{-iq \cdot (x - x_2)}. \end{aligned}$$

If we Fourier transform this into momentum space, let $q \rightarrow -q$ and amputate the external scalar propagators, we find that the value of the diagram is

$$\begin{array}{c} \otimes \\ \text{wavy line} \\ \mu, \nu \\ \text{diagonal lines} \\ p \quad q \end{array} = -i \int d^4x h_{\mu\nu}(x) e^{i(q-p)\cdot x} p^\mu q^\nu = -\tilde{h}_{\mu\nu}(q-p) p^\mu q^\nu. \quad (4.74)$$

Because of the integration over x , the vertex already contains the momentum conservation requirement that $q - p = k$, the energy of the gravitation wave. This vertex is different from the earlier Φ^4 vertex as it couples the quantum scalar field with a classical field $h_{\mu\nu}(k)$ which is indicated by the crossed dot. Unlike before where all for lines of the vertex may be connected to a propagator or another vertex, there is no way to ‘connect’ with this crossed dot. The additional Feynman rule that we need is an integral over the internal momenta with measure $\frac{d^4k}{(2\pi)^4}$. With these vertices, we can only have two particle creation, with the diagrams formed from this vertex and the internal scalar propagators giving (LSZ reduction formula) the amplitude

$$\left\langle \Omega \left| a_p a_q \mathcal{T} \exp \left(-i \int_{-\infty}^{\infty} H_I(t') dt' \right) \right| \Omega \right\rangle. \quad (4.75)$$

The zeroeth order amplitude is obviously zero, while the first-order amplitude is given by the diagram

$$\begin{array}{c} q \\ \text{diagonal line} \\ \otimes \text{wavy line} \\ p \\ \text{diagonal line} \end{array} = \tilde{h}_{\mu\nu}(q+p) p^\mu q^\nu. \quad (4.76)$$

Because $\tilde{h}_{\mu\nu}(k)$ must obey the linearised equations of motions of the gravitational wave, so $k_\mu k^\mu = 0$. This means $(p+q)^2 = 0 = p^2 + q^2 + 2p \cdot q = 2m^2 + 2p \cdot q = 0$. Suppose we have $m = 0$. This implies that $p \cdot q = 0$. Let us rotate to the frame where the momentum of p is in the direction of z . In this coordinate frame, the dot product of $p \cdot q = 0$ is only possible if $q^\mu = \alpha(p^0, 0, 0, p^z)$ since in the coordinate frame, $p^\mu = (p^0, 0, 0, p^z)$. This means that if the dot product of two vectors is zero, they must be light-like vectors that are co-linear. Then $\tilde{h}_{\mu\nu}((1+\alpha)p)$ would be the frequency component in the direction of z but the transverse-traceless gauge says that $k^\mu \tilde{h}_{\mu\nu}(k) = 0$. So this diagram is zero. In fact, any diagram constructed from this is zero. Consider a diagram of the form

$$\begin{array}{c} \text{diagonal line } p \\ \otimes \text{wavy line} \\ \text{diagonal line } p' \\ \vdots \\ \otimes \text{wavy line} \\ \text{diagonal line } p' \\ \vdots \end{array} = \int \frac{d^4p'}{(2\pi)^4} \cdots \tilde{h}_{\mu\nu}(p'+p) p^\mu p'^\nu \cdots \quad (4.77)$$

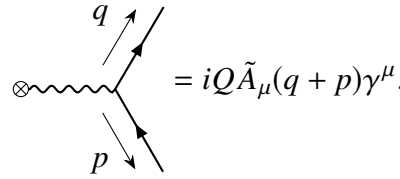
Note that before we do the integral over the internal momenta, they are not on-shell, ergo, $p'^2 \neq 0$. However, the gravitational wave still obeys the equation of motion. This means that $0 = (p' + p)^2 = p'^2 + 2p \cdot p' = p' \cdot (p' + 2p) \implies p' \propto p$. Once again, by the transverse-traceless gauge, this means that $\tilde{h}_{\mu\nu}(p' + p)p^\mu p'^\nu = 0$. This means that this diagram has an amplitude of zero. Note that a term where we have an external scalar always exists diagrams of this form, this leads us to conclude that linear plane gravitational waves to all orders of interaction cannot create particles.

4.4 Particle creation from classical electromagnetic field

We can draw a strong analogy to particle creation from classical electromagnetic fields. In a classic paper by Schwinger⁴³ he shows that plane electromagnetic fields cannot create particles. We will show this result and compare to the gravitational case. If we consider a Dirac field $(\psi, \bar{\psi})$ coupled to a classical electromagnetic field $F_{\mu\nu} = \partial_\mu A_\nu - \partial_\nu A_\mu$ then the Lagrangian is

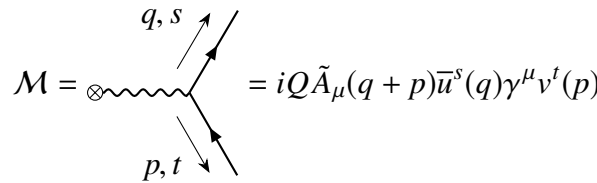
$$\mathcal{L} = \bar{\psi} [i\gamma^\mu (\partial_\mu - QA_\mu) - m] \psi - \frac{1}{4} F^{\mu\nu} F_{\mu\nu}, \quad (4.78)$$

where A^μ is the vector potential, γ^μ are the Dirac matrices, Q is the charge and m is the mass of the Dirac field. The primitive vertex for a classical electromagnetic field is



$$= iQ\tilde{A}_\mu(q+p)\gamma^\mu. \quad (4.79)$$

For external lines, the Feynman rules require that spinors $u^s(q)$ & $v^t(p)$ be associated with particles and antiparticles. The amplitude for the production of two particles is given by



$$\mathcal{M} = iQ\tilde{A}_\mu(q+p)\bar{u}^s(q)\gamma^\mu v^t(p). \quad (4.80)$$

If we take the square of this amplitude and sum over the spins (as we don't care about the orientation of the spins), we find that

$$\sum_{s,t} |\mathcal{M}|^2 = 4Q^2 \tilde{A}_\mu(q+p) \tilde{A}_\nu^*(q+p) \left(p^\mu q^\nu + p^\nu q^\mu - \eta^{\mu\nu} (q \cdot p + m^2) \right). \quad (4.81)$$

Once again supposing a linear plane wave we have $A_\mu(x) = \epsilon_\mu(k_0) e^{-ik_0 \cdot x} \implies \tilde{A}_\mu(k) = (2\pi)^4 \epsilon_\mu(k_0) \delta^{(4)}(k - k_0)$.

In the electromagnetic case, the analogous gauge to the gravitational transverse-traceless gauge is the Coulomb gauge which is also transverse (but not traceless as it is a vector field). This means that $k^\mu \tilde{A}_\mu(k) = 0$. We have two choices for external Dirac spinors, either $p^\mu = \alpha q^\mu$ or not. If p and q are co-linear the first two terms in the bracket vanishes due to the Coulomb gauge and we have

$$\sum_{s,t} |\mathcal{M}|^2 = -4Q^2 (\alpha + 1) m^2 \tilde{A}^\mu(q+p) \tilde{A}_\mu^*(q+p). \quad (4.82)$$

But because of the plane wave, we must also satisfy that $(q + p)^2 = 0 \implies 2m^2 + p \cdot q = 2m^2 + \alpha m^2 = 0 \implies m = 0$. So this amplitude is zero for co-linear particle creation. For the second case of non-collinear particle creation we have a problem where the momentum conservation condition $(q + p)^2 = 0$ cannot be satisfied either, because $p \cdot q > 0$ so this diagram is zero for all p and q . Thus we have shown, in concurrence with Schwinger finding that plane waves don't create particles.

The important point here is that we notice the vanishing amplitude for particle creation process in gravitational (electromagnetic) waves is due to a combination of the nature of plane gravitational (electromagnetic) waves having two degrees of freedom (encapsulated by the transverse-traceless gauge or Coulomb gauge) and the requirement that we have momentum conservation. Using the diagrammatic techniques we have developed we will now study the effect of second-order gravitational waves.

4.5 Diagrams and gravitational waves to second-order

In a similar way to Arcos *et al.*¹¹⁸ we will expand the metric to arbitrary order indicated by κ . However, we will keep the earlier notation by splitting the metric into a flat part and $h_{\mu\nu}$, which can itself be expanded order by order. Therefore we will write the metric as

$$g_{\mu\nu} = \eta_{\mu\nu} + \kappa h_{\mu\nu} \quad (4.83)$$

and from this we can get the inverse metric

$$g^{\mu\nu} = \eta^{\mu\nu} - \kappa h^{\mu\nu} + \kappa^2 h^\mu{}_\alpha h^{\alpha\nu} + \dots \quad (4.84)$$

and

$$\sqrt{|g|} = 1 + \frac{1}{2}\kappa h - \frac{1}{4}\kappa^2 h^\alpha{}_\beta h^\beta{}_\alpha + \kappa^2 \frac{h^2}{8} + \dots \quad (4.85)$$

with all indices raised and lowered with the Minkowski metric. From now on, we will only consider a massless scalar field. All of the terms in the Lagrangian up to 2nd order κ^2 are therefore

$$\mathcal{L} = \frac{1}{2} (\eta^{\mu\nu} \partial_\mu \Phi \partial_\nu \Phi) \quad (4.86)$$

$$+ \kappa \left(\frac{1}{4} h \eta^{\mu\nu} - \frac{1}{2} h^{\mu\nu} \right) \partial_\mu \Phi \partial_\nu \Phi \quad (4.87)$$

$$+ \kappa^2 \left[\left(\frac{1}{16} h^2 - \frac{1}{8} h^\alpha{}_\beta h^\beta{}_\alpha \right) \eta^{\mu\nu} - \frac{1}{4} h h^{\mu\nu} + \frac{1}{2} h^\mu{}_\alpha h^{\alpha\nu} \right] \partial_\mu \Phi \partial_\nu \Phi. \quad (4.88)$$

Let us group the Lagrangian by the metric, η or h that contracts with the field

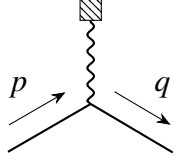
$$\mathcal{L} = \frac{1}{2} (\eta^{\mu\nu} \partial_\mu \Phi \partial_\nu \Phi) \quad (4.89)$$

$$+ \left[\frac{1}{4} \kappa h + \kappa^2 \left(\frac{1}{16} h^2 - \frac{1}{8} h^\alpha{}_\beta h^\beta{}_\alpha \right) \right] \eta^{\mu\nu} \partial_\mu \Phi \partial_\nu \Phi \quad (4.90)$$

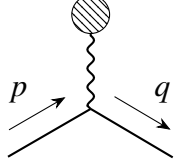
$$+ \left[-\frac{1}{2} \kappa - \frac{1}{4} \kappa^2 h \right] h^{\mu\nu} \partial_\mu \Phi \partial_\nu \Phi \quad (4.91)$$

$$+ \frac{1}{2} \kappa^2 h^\mu{}_\alpha h^{\alpha\nu} \partial_\mu \Phi \partial_\nu \Phi. \quad (4.92)$$

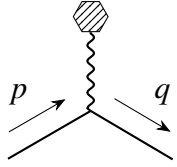
Because the derivatives on Φ are always contracted with an object that is symmetric and each interaction term is of the form $\frac{1}{2}F^{\mu\nu}\partial_\mu\Phi\partial_\nu\Phi$, if we follow the procedure in Section 4.3 the momentum space diagrams with external propagators removed are,



$$= i \int d^4x e^{i(q-p)\cdot x} \left[\frac{1}{2}\kappa h(x) + \kappa^2 \left(\frac{1}{8}h^2(x) - \frac{1}{4}h^\alpha{}_\beta(x)h^\beta{}_\alpha(x) \right) \right] \eta^{\mu\nu} p_\mu q_\nu, \quad (4.93)$$

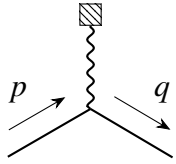


$$= i \int d^4x e^{i(q-p)\cdot x} \left[-\kappa - \frac{1}{2}\kappa^2 h(x) \right] h^{\mu\nu}(x) p_\mu q_\nu, \quad (4.94)$$

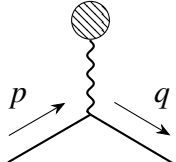


$$= i \int d^4x e^{i(q-p)\cdot x} \kappa^2 h^\mu{}_\alpha(x) h^{\alpha\nu}(x) p_\mu q_\nu. \quad (4.95)$$

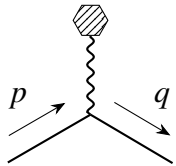
Using the convolution theorem for Fourier transforms, we find that we can rewrite the vertices as



$$= i \left[\frac{1}{2}\kappa \tilde{h}(q-p) + \kappa^2 \int \frac{d^4k}{(2\pi)^4} \left(\frac{1}{8}\tilde{h}(k)\tilde{h}(q-p-k) - \frac{1}{4}\tilde{h}^\alpha{}_\beta(k)\tilde{h}^\beta{}_\alpha(q-p-k) \right) \right] \eta^{\mu\nu} p_\mu q_\nu, \quad (4.96)$$



$$= i \left[-\kappa \tilde{h}^{\mu\nu}(q-p) - \frac{1}{2}\kappa^2 \int \frac{d^4k}{(2\pi)^4} \tilde{h}(k)\tilde{h}^{\mu\nu}(q-p-k) \right] p_\mu q_\nu, \quad (4.97)$$



$$= i \int \frac{d^4k}{(2\pi)^4} \kappa^2 \tilde{h}^\mu{}_\alpha(k)\tilde{h}^{\alpha\nu}(q-p-k) p_\mu q_\nu. \quad (4.98)$$

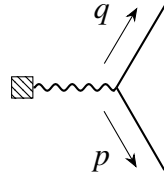
There is a slight subtlety here. These vertices are the second-order vertices for the Feynman perturbative sum. The $h_{\mu\nu}$ can itself contain a sum of higher order gravitational waves. Let us now expand $h_{\mu\nu}$ wave by orders of κ such that,

$$h_{\mu\nu} = {}^{(1)}h_{\mu\nu} + \kappa {}^{(2)}h_{\mu\nu} + \dots \quad (4.99)$$

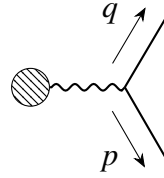
It should be noted that the different orders of the gravitational wave obey different equations of motions. Let us consider the second-order vertices with a first-order gravitational wave and see if any diagrams are non-zero,

$$h_{\mu\nu} = {}^{(1)}h_{\mu\nu}. \quad (4.100)$$

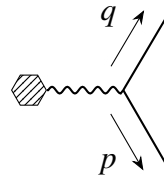
With first-order gravitational waves, we have the transverse-traceless gauge so the vertices simplify to,



$$= i \left[\kappa^2 \int \frac{d^4 k}{(2\pi)^4} \left(\frac{1}{4} \tilde{h}^\alpha{}_\beta(k) \tilde{h}^\beta{}_\alpha(q+p-k) \right) \right] \eta^{\mu\nu} p_\mu q_\nu, \quad (4.101)$$



$$= i \left[\kappa \tilde{h}^{\mu\nu}(q+p) \right] p_\mu q_\nu, \quad (4.102)$$



$$= -i \int \frac{d^4 k}{(2\pi)^4} \kappa^2 \tilde{h}^\mu{}_\alpha(k) \tilde{h}^{\alpha\nu}(q+p-k) p_\mu q_\nu. \quad (4.103)$$

Note that the second diagram is the same as before, so it's zero. In the first and third diagram, we have the momentum conserving conditions, $k^2 = 0$ and $(q+p-k)^2 = 0$. This implies that $q \cdot p = k \cdot (q+p)$. Note that the left side is independent of k this can only be the case if $k \cdot (q+p) = 0$ which would then mean p and q are co-linear, then both terms are zero. The first is zero because of the $p \cdot q$ term and the third is zero because $k \propto q+p$ and $q_\nu \tilde{h}^{\alpha\nu}(\beta q) = 0$ by the transverse-traceless gauge. Thus we have established that the second-order diagrams are zero for first-order gravitational waves. Despite the disappointing results, it should be noted that higher order gravitational waves can skirt all these issues. For example, the equation of motion for second-order gravitational waves is¹¹⁸

$$\partial_\rho \partial^{\rho(2)} h^\mu{}_\nu = N_{\mu\nu} \left({}^{(1)}h \right), \quad (4.104)$$

with $N_{\mu\nu} \left({}^{(1)}h \right)$ a function of the first-order gravitational waves. This is no longer a simple wave equation and is no longer transverse and traceless.¹¹⁹ While the analysis could proceed order by order, the procedure is difficult and tedious. One would normally choose to use exact gravitational waves and study the problem using input-output formalism. This was done by Yurtsever¹²⁰ and Dorca & Verdaguer¹²¹ where they find that collisions of exact non-linear plane waves can create particles. Both papers start with an asymptotically flat region, and end with a curved background which adds some further complications to the interpretation of whether the particle creation is due to the gravitational waves or the change in curvature. Of course the distinction between the background and gravitational waves is arbitrary but there is much greater didactic simplicity when the background spacetime starts and ends the same. With these motivating examples, we now turn to another situation where the gravitational waves are highly non-linear and propagate on a curved background: the coalescence of two black holes.

Why gravitational waves around black holes though? While we explicitly showed that particle creation is not allowed for a plane electromagnetic wave, pair production of electrons and positrons is possible if a nucleus is introduced to balance the momentum.¹²² In the gravitational wave case, one

might expect that an analogue to the nucleus, e.g., a black hole, has to be introduced to allow particle creation.

The first three gravitational wave events ever detected by Laser Interferometer Gravitational-Wave Observatory (LIGO) originated from the coalescence of two black holes.^{112,123,124} The observed gravitational wave signals reveals that the spacetime changes dramatically when two black holes merge into one, with a large amount of energy of order a few solar rest masses carried away by the emitted gravitational waves. If particles, e.g., photons, can be produced by gravitational perturbations they will travel along with the gravitational waves and could be detected if the particle creation efficiency is high enough. So far, the models studying gravitational waves do not include the possibility of particle creation. Thus if particle creation is possible, it would greatly change the models and our understanding of these merger events.

4.6 Particle creation by quasi-normal modes around a Schwarzschild black hole

The whole process of the coalescence of two black holes is a very complicated situation requiring numerical relativity,¹²⁵ so we will only study the final stage of merging: the ring-down stage. During the ring-down stage, gravitational oscillations of the black hole are dominant, which are known as the gravitational quasi-normal modes (QNMs). Because gravitational quasi-normal modes (QNMs) of a black hole have been extensively studied for decades,^{126–131} analytic techniques can be applied to them. We consider a minimally coupled massless real scalar field that propagates in the Schwarzschild background spacetime with quasi-normal perturbations. Using the tools in Section 2.5, where we studied the propagation of the scalar field in a background Schwarzschild spacetime, we will perturbatively study their coupling with the QNMs.

We derive the interaction Hamiltonian for the scalar field, which implies that the QNMs play the role of a multimode squeezer. We show that the QNMs ‘squeeze’ the initial state (vacuum or thermal state) of the scalar field and produce particles. In this sense black holes themselves can be quantum squeezers.

4.6.1 Coupling between QNMs and the scalar field

We consider a Hermitian massless scalar field Φ that minimally couples to the curved spacetime with metric $g_{\mu\nu}$. The Lagrangian for the scalar field is¹¹

$$\mathcal{L} = \frac{1}{2} \sqrt{-g} g^{\mu\nu} (\partial_\mu \Phi)(\partial_\nu \Phi), \quad (4.105)$$

where g is the determinant of $g_{\mu\nu}$. Note that the metric signature is now $(- + + +)$ and we define the Lagrangian as a scalar density where the action is $S = \int d^4x \mathcal{L}$. We assume that the metric $g_{\mu\nu}$ can be decomposed into a background part $g_{B\mu\nu}$ and a perturbation $h_{\mu\nu}$, namely, $g_{\mu\nu} = g_{B\mu\nu} + h_{\mu\nu}$. The background metric usually possesses some symmetries (time-translation invariance, rotational

invariance etc.) and the dynamics of the scalar field in the background spacetime has been reviewed in Section 2.5. The perturbation $h_{\mu\nu}$ is assumed to be small so that perturbation theory is applicable. Expanding the Lagrangian Eq. (4.105) with respect to $h_{\mu\nu}$ and keeping terms to first-order, we find

$$\mathcal{L} = \mathcal{L}_0 + \mathcal{L}_1, \quad (4.106)$$

where the background part \mathcal{L}_0 and perturbed part \mathcal{L}_1 are

$$\mathcal{L}_0 = \frac{1}{2} \sqrt{-g_B} g_B^{\mu\nu} (\partial_\mu \Phi)(\partial_\nu \Phi), \quad (4.107)$$

$$\mathcal{L}_1 = \frac{1}{4} \sqrt{-g_B} (h^\alpha{}_\alpha g_B^{\mu\nu} - 2h^{\mu\nu}) (\partial_\mu \Phi)(\partial_\nu \Phi), \quad (4.108)$$

with g_B the determinant of the background metric and $h^\alpha{}_\alpha \equiv g_{B\alpha\beta} h^{\alpha\beta}$ the trace of the metric perturbation. Note that indices are raised by the background metric: $h^{\mu\nu} \equiv g_B^{\mu\alpha} g_B^{\nu\beta} h_{\alpha\beta}$.

The canonically conjugate field of Φ is also decomposed into a background and perturbed part,

$$\Pi = \Pi_0 + \Pi_1, \quad (4.109)$$

where

$$\Pi_0 = \frac{\partial \mathcal{L}_0}{\partial(\partial_t \Phi)} = \sqrt{-g_B} g_B^{tt} (\partial_t \Phi), \quad (4.110)$$

$$\Pi_1 = \frac{\partial \mathcal{L}_1}{\partial(\partial_t \Phi)} = -\frac{1}{2} \sqrt{-g_B} [2h^{t\nu} (\partial_\nu \Phi) - h^\alpha{}_\alpha g_B^{tt} (\partial_t \Phi)]. \quad (4.111)$$

The Hamiltonian density is

$$\mathcal{H} = \mathcal{H}_0 + \mathcal{H}_1, \quad (4.112)$$

where

$$\begin{aligned} \mathcal{H}_0 &= \Pi_0 (\partial_t \Phi) - \mathcal{L}_0 \\ &= \frac{1}{2} \sqrt{-g_B} [g_B^{tt} (\partial_t \Phi)^2 - g_B^{ij} (\partial_i \Phi)(\partial_j \Phi)] \end{aligned} \quad (4.113)$$

is the unperturbed Hamiltonian density and

$$\begin{aligned} \mathcal{H}_1 &= \Pi_1 (\partial_t \Phi) - \mathcal{L}_1 \\ &= -\frac{1}{2} \sqrt{-g_B} [h^{tt} (\partial_t \Phi)^2 - h^{ij} (\partial_i \Phi)(\partial_j \Phi)] + \frac{1}{2} h^\alpha{}_\alpha \mathcal{H}_0 \end{aligned} \quad (4.114)$$

is the perturbed Hamiltonian density.

For the Schwarzschild background spacetime, $\sqrt{-g_B} = r^2 \sin \theta$, so the perturbed Hamiltonian is

$$\begin{aligned} H_1 &= \int d^3x \mathcal{H}_1 \\ &= \frac{1}{2} \int_{2M}^{\infty} dr \int_{4\pi} d\Omega r^2 \left\{ -h^{tt} (\partial_t \Phi)^2 + h^{ij} (\partial_i \Phi)(\partial_j \Phi) + \frac{1}{2} h^\alpha{}_\alpha [g_B^{tt} (\partial_t \Phi)^2 - g_B^{ij} (\partial_i \Phi)(\partial_j \Phi)] \right\} \end{aligned} \quad (4.115)$$

where $d\Omega = \sin\theta d\theta d\phi$. Recalling Eq. (2.57), the scalar field can be expanded as

$$\Phi(x) = \sum_{l=0}^{\infty} \sum_{m=-l}^l \int_0^{\infty} d\omega \left(b_{\omega lm}^{\text{up}} \phi_{\omega lm}^{\text{up}}(x) + b_{\omega lm}^{\text{in}} \phi_{\omega lm}^{\text{in}}(x) + \text{h.c.} \right) \quad (4.116)$$

As we are studying the exterior of the black hole we will not be using the maximally extended scalar field expansion in Eq. (2.75). We will also be using the Schwarzschild expansion as we are interested in what an observer far away sees.

4.6.2 Gravitational quasi-normal modes

Let us now consider the perturbation of spacetime around a Schwarzschild black hole. Taking $g_{B\mu\nu}$ to be Schwarzschild spacetime and $h_{\mu\nu}$ to be the perturbation, we can expand Einstein's field equations and get the equation of motion for $h_{\mu\nu}$ which we can then proceed to solve. In comparison with gravitational waves in flat spacetime, the process is rather involved so I'll sketch an overview. A more in depth summary can be found in Su *et al.*²

The perturbations (Quasi-normal modes) around a Schwarzschild black hole were first derived by Regge & Wheeler¹³² and Zerilli.¹³³ Because of the time translation and spherical symmetry of the background metric, they found that the perturbations could be decomposed into a set of modes characterised by parity, complex frequency $\omega = \omega_R - i\omega_I$ and spherical harmonic numbers l and m . This is almost directly analogous to Eq. (2.59). The form of QNMs in the Regge-Wheeler-Zerilli gauge is,

$$h_{\mu\nu}^{(p)} = \tilde{h}_{\mu\nu}^{(p)}(r) e^{-i\omega t} f_{\nu}^{(p)}[Y_{lm}(\theta, \phi)], \quad (4.117)$$

where p denotes either odd (o) or even (e) parity solutions, $\tilde{h}_{\mu\nu}^{(p)}(r)$ are solutions to various radial equations and $f_{\nu}^{(p)}[Y_{lm}(\theta, \phi)]$ are functions that depend on the parity p and μ, ν . The frequencies of QNMs are complex so the imaginary part of the frequency characterises the decay of the mode.

4.6.3 Time-evolution with quasi-normal modes

Now let us look at the time-evolution of a scalar field with the perturbation Eq. (4.115). In the interaction picture, the time-evolution operator is

$$U = T \exp \left\{ -i \int_0^{\infty} dt H_1(t) \right\}, \quad (4.118)$$

with the interacting Hamiltonian

$$H_1 = \frac{1}{2} \int_{2M}^{\infty} r^2 dr \iint \sin\theta d\theta d\phi \left[-h^{tt} (\partial_t \Phi)^2 + h^{rr} (\partial_r \Phi)^2 + 2h^{rA} (\partial_r \Phi) (\partial_A \Phi) + h^{AB} (\partial_A \Phi) (\partial_B \Phi) \right], \quad (4.119)$$

where A and B are dummy indices summed over angular variables. Note that we have changed to a gauge called the ingoing radiation gauge, which simplifies the form of the QNMs. If we substitute Eq. (4.117) and Eq. (4.116) into Eq. (4.119), we have integrals over r, θ & ϕ . The full details

are in the paper, but I will review some of the main points of the calculation. The integrals can be approximately evaluated if we make a few assumptions and approximations. We will ignore ingoing terms as no observer outside the black hole can observe them. To reduce the number of integrals, we will use the rotating wave approximation. In the integrand, we will have terms with $a_{\omega l m} a_{\omega' l' m'}$, $a_{\omega l m}^\dagger a_{\omega' l' m'}$, $a_{\omega l m} a_{\omega' l' m'}^\dagger$ & $a_{\omega l m}^\dagger a_{\omega' l' m'}^\dagger$ multiplied by $h_{\mu\nu}^{(p)}$ or $h_{\mu\nu}^{(p)*}$. Associated with each term are exponential factors,

$$\begin{aligned} e^{\pm i(\omega_R - \omega - \omega')t}, & e^{\pm i(\omega_R + \omega + \omega')t}, \\ e^{\pm i(\omega_R + \omega - \omega')t}, & e^{\pm i(\omega_R - \omega + \omega')t}. \end{aligned}$$

ω_R comes from the QNMs while ω and ω' are from scalar field mode creation or annihilation operators. The rotating wave approximation means we only keep terms with $e^{\pm i(\omega_R - \omega - \omega')t}$ as these terms dominate the other, faster oscillating terms.

With these simplifications, we can calculate the angular and radial integrals. The angular integrals over θ & ϕ can be analytically calculated using the properties of spherical harmonics to functions of Wigner 3 – j symbols and Γ functions.* The radial integral is much more difficult. We assume that the decay of the QNMs is slow, i.e. $2M\omega_l \ll 1$. The integrand diverges at $r = 2M$ and $r = \infty$ which require us to analytically extend the integral to the complex plane and perform a branch cut and a ‘keyhole’ contour integral.** We do not have analytic solutions of $\tilde{h}_{\mu\nu}^{(p)}(r)$ so we must use asymptotic solutions at the horizon $r = 2M$ and at infinity $r = \infty$. The divergence at $r = 2M$ and $r = \infty$ allows us to ‘patch’ the two regions together using their asymptotic solutions while ignoring the intermediate region as its contribution to the integral is comparatively small. With these assumptions and approximations, an analytic expression for the radial integral can be calculated. Finally, although nothing prevents us from doing otherwise, for simplicity of analysis, we will assume that the angular momentum in the z direction of QNMs is zero (QNMs with $m = 0$ in Eq. (4.117)). Now we can substitute the expression for the interacting Hamiltonian and do the integral over t —a simple integral over exponentials—we find that,

$$\begin{aligned} U(t_f, t_i) \approx T \exp \left\{ -i \int d\omega \int d\omega' \sum_{p \in \{e, o\}} \sum_{l=0}^{\infty} \sum_{l'=0}^{\infty} \sum_{m=-\min(l, l')}^{\min(l, l')} \mathcal{F}_{lml'}^{(p)}(\omega, \omega') b_{\omega l m}^{\text{up} \dagger} b_{\omega' l' -m}^{\text{up} \dagger} \right. \\ \left. + \mathcal{F}_{lml'}^{(p)*}(\omega, \omega') b_{\omega l m}^{\text{up}} b_{\omega' l' -m}^{\text{up}} \right\}. \end{aligned} \quad (4.120)$$

The function $\mathcal{F}_{lml'}^{(p)}(\omega, \omega')$ consists of angular and radial integrals of the QNM parts that are defined and numerically calculated in Su *et al.*²

The basic structure of the unitary tells us that the QNMs induce a squeezing type Hamiltonian between particles with m and $-m$ angular momentum in the z direction. While the unitary does couple particles with different total angular momenta $l \neq l'$, the pair production of particles with m and $-m$ means that angular momentum is conserved as we have explicitly assumed QNMs with zero angular

* See Appendix C & D in Su *et al.*² for more details.

** Further details are in Appendix A. Su *et al.*²

momentum in the z direction. Realistic quantitative predictions with this unitary is difficult. Although we calculated the functions $\mathcal{F}_{lm}^{(p)}(\omega, \omega')$ in the paper² by assuming a particular form of QNMs, realistic parameters used for the QNM are difficult to estimate. Finally, we have the same problem we discussed in Chapter 3, namely the choice of initial vacuum states. If we consider the LIGO events, the problem here is even more complex as a single black hole was initially formed from two black holes. The dynamics of a scalar field for two black holes is poorly understood and it is not known whether a vacuum state can even be defined for such a case. It is possible that the extreme gravitation of the in-spiral and merger cannot be understood under our current field theoretic paradigms.

4.7 Conclusion

We have seen how gravitational plane waves in Minkowski cannot create particles, even to second-order, due to a combination of the transverse-traceless gauge and momentum conservation. This led us to realise that higher order gravitational waves, or non-linear gravitational waves could create particles. Finally, we gave a summary of the results of our research in Su *et al.*² where we found non-zero particle creation by quasi-normal modes around a black hole. The discovery of this process could have important implications for our current models of black hole mergers. So far, localising gravitational events have been steadily improving¹³⁴ to the point that we have detected light and gravitational waves from a neutron star merger.¹³⁵ In the case of binary black hole mergers, the current models do not assume any particle creation. Any detection of the effect we discovered could change the estimate of the masses of the binary black holes and other parameters of the merging event.

Chapter 5

Violation of a causal inequality in a spacetime with definite causal order

This chapter is based on the paper³ “Violation of a causal inequality in a spacetime with definite causal order” which I wrote with Fabio Costa, Christina Giarmatzi and Timothy C. Ralph. All figures and calculations were made by me with analysis and interpretation shared equally amongst co-authors. The bulk of the text was written and edited by me.

It is customary to think of physical processes and phenomena as built from events with definite causal relations. Recently, there has been a great interest in whether more general causal structures are possible. A main motivation is the expectation that a fundamental theory combining the indeterminacy of quantum physics and the dynamical causal structure of general relativity should include *indefinite causal structures*.^{136,137} Processes with no definite causal structure have also been proposed as possible resources for a variety of tasks,^{138–143} with an ongoing effort towards their practical realisation.^{144–147}

The correlations between events in a definite causal structure satisfy *causal inequalities*,^{28,148–150} derived from the assumption that only one-way signalling is possible: if an event A is the cause of an event B , then B cannot be the cause of A . A violation of such inequalities would imply that no definite causal order between the events exists. It has been shown that it is possible to violate the causal inequalities within a framework that only assumes the local validity of quantum theory but makes no assumptions regarding a possible background causal structure.²⁸ The physical interpretation of such a framework is however still uncertain.

In practice, a causal inequality could be violated trivially simply by allowing parties to exchange information across an extended period of time; any probability distribution can be obtained in this way. Without conditions on the communication task, such a violation would not imply the existence of indefinite causal order. The interest in the subject derives from the possibility—so far only theoretically speculated—that the inequalities might be violated under stricter conditions, thus demonstrating genuinely new types of causal relations. In Oreshkov *et al.*²⁸ these conditions were proposed to be that of *closed laboratories*—each event is generated through a single operation on a physical system, which cannot interact with the outside world during the operation—and of *free choice*—an experimenter can

perform an arbitrary operation in the closed lab and the choice of operation is not caused by any other variable relevant to the system under investigation. To date no physical process has been proposed that can violate causal inequalities under such conditions.

Here, we propose a protocol in which two parties can violate a causal inequality by acting on Gaussian-localised field modes of photons in Minkowski spacetime. This is possible because operations on the modes are extended in time, so that each intersects the future light-cone of the other. From an operational point of view, freely chosen operations on the modes provide a realisation of closed laboratories, satisfying the conditions for a genuine violation of the inequalities. Such laboratories that perform the operations are strictly localised in space and their operations are temporally extended and centred around a spacetime event which is also used as a label for the operation. For example, a lab is a space of finite spatial extent Δx_{lab} much smaller than the distance to other labs that performs operations centred at $(t_{\text{lab}}, x_{\text{lab}})$ on certain specified modes. However, naively taking the spatio-temporal localisation of the operations as a definition of a *closed* laboratory would suggest that the violation is due to the failure of the closed lab condition. We comment how this latter perspective is problematic, since any finite-energy mode is necessarily temporally extended, and a small violation of the inequalities is always possible.

5.1 Causal inequalities

We consider two parties, A (Alice) and B (Bob), who receive classical inputs x, y and generate classical outputs a, b , respectively. For simplicity, we restrict to binary variables and assume that the inputs are uniformly distributed, $P(x, y) = \frac{1}{4}$ for any pair of values x, y .

The goal for the parties is to guess each other's input, i.e., to maximise the probability¹⁴⁹

$$P_{\text{succ}} = \frac{1}{2} [P(x = b) + P(y = a)]. \quad (5.1)$$

A definite causal order between the labs imposes constraints on the probability of success: if Alice can signal to Bob, Bob cannot signal to Alice and vice versa. Even if the causal order between the labs is unknown, or decided with some probability by some external variables, the probability of success is bounded by the *causal inequality*¹⁴⁹

$$P_{\text{succ}} \leq \frac{3}{4}. \quad (5.2)$$

This inequality (a simplified version of the original one²⁸) must be satisfied if the operations producing the correlations are each performed between two time instants, defined with respect to a background causal structure, and the system on which Alice (Bob) performs the operation is isolated from the outside world between those two instants. In a quantum setting, the times at which operations are performed can be subject to indeterminacy. This opens the possibility of violating a causal inequality with operations that still satisfy a reasonable 'closed laboratory' assumption. As sketched by Oreshkov *et al.*²⁸ a 'closed lab' can be defined operationally and without reference to a background causal structure in terms of the possible operations that can be performed in it. If a party is free to choose any operation that formally transforms an input Hilbert space to an output Hilbert space, and

each operation can in principle be verified through tomography by external parties feeding appropriate states and performing appropriate measurements, we say—by definition—that the party acts in a closed lab. Crucially, the input and output Hilbert spaces do not have to be identified with instants in time: even when a background spacetime structure is assumed, quantum labs can be delocalised in time.¹⁵¹

5.2 Gaussian field modes

We now present a scenario that, by exploiting temporally-delocalised field modes, enables the violation of the above inequality while satisfying the closed laboratory assumption.

Quantum particles are not and cannot be perfectly localised in spacetime. In non-relativistic QM, if one confines the wavefunction to vanish outside a finite region e.g. a rectangle function, the non-relativistic QM propagator ensures that sinc-like sinusoidal tails develop faster than the speed of light over all of space.^{152,153} Such a problem does not exist for classical particles. In QFT, particles are excitations of the field and localisation presents a unique problem here.^{154,155} A ‘localisation’ that avoids these problems is Gaussian localisation. In particular, we consider Gaussian-localised single-particle excitations of optical field modes in Minkowski spacetime,

$$|1, j\rangle = a_j^\dagger(t, x) |0\rangle, \quad (5.3)$$

where $j = h, v$ is a polarisation index and the mode is defined by a Gaussian superposition of plane wave modes with annihilation operators

$$a_j(t, x) = \int dk \frac{e^{-\frac{(k-k_0)^2}{4\sigma^2}}}{(2\pi\sigma^2)^{\frac{1}{4}}} e^{-i(\omega_k t - kx)} a_{k,j}, \quad (5.4)$$

where we use units for which $c = \hbar = 1$, $a_{k,j}$ are single frequency Minkowski operators with wavenumber k and frequency ω_k . $|0\rangle$ is the Minkowski vacuum which is annihilated ($a_k |0\rangle = 0$, $\forall k$) by the Minkowski operators. Note that Eq. (5.3) is a pure state and so contains all information about the particle. This Gaussian-localised particle has a central wave number of k_0 and is peaked along the trajectory $(\omega_{k_0} t - k_0 x) = 0$ with a spatio-temporal width of $1/\sigma$. More realistically we can also require a transverse Gaussian profile for the mode that localises the particle in the transverse directions as well. However, provided we assume that all operations are carried out close to the focus of the mode then the paraxial approximation implies that the 1 + 1 dimensional description of the mode in Eq. (5.4) is a good approximation to the full 3 + 1 dimensional description. Note that this Gaussian-localised single particle has finite energy. Given the Hamiltonian operator,

$$H = \sum_j \int dk \frac{|k|}{(2\pi)^{1/2}} a_{k,j}^\dagger a_{k,j}, \quad (5.5)$$

we find that the expectation,

$$\langle 1, j | H | 1, j \rangle = \int \frac{dk}{2\pi\sigma} |k| e^{-\frac{(k-k_0)^2}{2\sigma^2}} \quad (5.6)$$

$$\approx_{k_0 \gg \sigma} \frac{\sigma}{2\pi} \left(\sqrt{2\pi} \frac{k_0}{\sigma} + e^{-\frac{k_0^2}{\sigma^2}} \frac{2\sigma^2}{k_0^2} + \mathcal{O} \left[\left(\frac{\sigma}{k_0} \right)^3 \right] \right) \quad (5.7)$$

is finite in energy for $\sigma < \infty$. For the case the $\sigma = \infty$, we have a perfectly localised particle at a single spacetime point which has infinite energy and is therefore unphysical. In general, particles with perfect localisation spread over a sharply defined region of spacetime have been found to have infinite energy.^{156,157}

For such a physical and therefore delocalised particle, operationally defined events such as ‘particle enters lab’ is not a clear concept. Even if we define a physical lab as a sharply defined region of spacetime, a Gaussian-localised particle propagating towards the lab is in some sense inside the lab already because of its Gaussian tails. We cannot escape this except by perfect localisation which is unphysical. Furthermore, Hegerfeldt¹⁶² shows the impossibility of preparing a one-particle state in a finite space region (compact support) and Vázquez *et al.*⁵⁴ examines this by explicitly constructing such compact-supported modes, showing that if you split up space into separate finite regions, such modes are unitarily inequivalent (to global modes) representations of the canonical commutation relations and exist in a separate Hilbert space to the global modes.

This problem with localisation means that the concept of a closed lab as presented in Oreshkov *et al.* was not sufficiently general and must be reconceived. Given that these delocalised Gaussian modes are physical modes that a lab can act upon, it suggests that we should define our labs in terms of the modes they are allowed to act upon.

5.3 Definition of a closed lab

We will redefine a closed lab in this way: a party A (respectively, B) that can perform arbitrary operations on—and only on—the single-particle states of such a mode effectively defines a ‘closed lab’. To make this definition operationally meaningful, we assume that mode selective mirrors at the input I_A (I_B) and output O_A (O_B) allow only a single mode, a_A (a_B), to enter and leave Alice’s (Bob’s) lab (see Fig. 5.1). Note that the labs are finite in spatial extent with a size much smaller than the distance to each other, so the two do not intersect. Modes that are orthogonal to a_A (a_B) are completely reflected. In this way the operations in each lab are restricted to a single mode. The operations that act on the mode are centred around an event (t_X, x_X) , $X = A, B$. (We assume the mirrors are polarisation insensitive and so allow either polarisation mode to enter or leave.) Passive mirrors and lenses external to the labs are allowed to direct and focus fields into the labs and to direct fields away from the labs.

The closed lab assumption requires that each party can perform arbitrary operations on the respective single-particle space. Possible operations include unitaries, projective measurements of states $a_j^\dagger(t_X, x_X) |0\rangle$, and preparation of states in the same modes. More general operations could require interactions with a local ancilla, e.g., applying a controlled unitary on input and output system followed by a detection of control and input system, Fig. 5.1 a). Interactions with an ancilla do not violate the closed lab assumption as long as the ancilla is not correlated with any other system outside the lab. Crucially, the assumption can be verified operationally, separately for each lab, by an external party sending selected states to the input mirror and performing measurements at the output. The verifier would then be able to tomographically reconstruct the operations, certifying that each party is

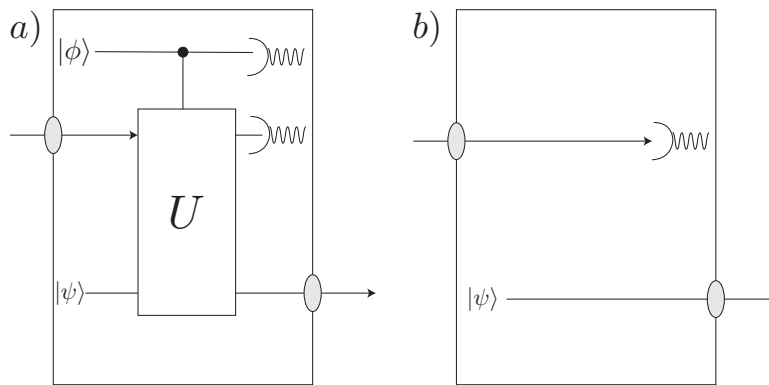


Figure 5.1: a) An illustration possible operations in a lab. b) The setup we use to violate the inequality has no control qubits and no interactions between input and output.

indeed free to perform an arbitrary operation on the respective mode.

The operations allowable in the lab are no different from any allowable operations one may do in a lab. The only difference is that these are delocalised modes so operations must be matched to these modes. Then any unitary operation such as quantum gates could be done on these modes provided we interpret the operators in the unitaries to be operators on the delocalised modes. In particular, as the physical unitaries doing the operations are localised in space while the mode itself is delocalised, then this means that the unitaries are delocalised in time. Such unitaries have a causal order in terms of their central time or spatial order, but their temporal spread—the same as the mode if it is properly mode matched—means that their operations overlap in time.

However, if all of the above conditions are fulfilled, we could perform any unitary within the lab. This would include measurement and preparing the output state. This is indicated in Fig. 5.1 a). In particular, the output state can be prepared conditional on the measurement outcome of the input state, thus justifying the view that—from the laboratory perspective—the measurement causally precedes the preparation. This would not be possible in a protocol where causal inequalities are violated thanks to “open laboratories”, where a party performs the preparation first and the measurement later, after the system has gone through the other party’s lab.

5.4 Physical setup and violation of inequality

We now consider the specific set-up of Fig. 5.1(b) and assume that Alice and Bob’s modes have the same width σ . In general, this need not be the case, but as we are trying to maximise the violation, this is the simplest choice. Also, for simplicity we assume all operations and detections have unit efficiency. The protocol proceeds in the following way. Alice measures the polarisation state of her incoming mode in the horizontal/vertical basis and records her guess a for Bob’s bit. Three results are possible: (i) a h -polarized photon is detected; (ii) a v -polarized photon is detected; (iii) no photon is detected. In case (i) Alice records $a = 0$, in case (ii) she records $a = 1$, and in case (iii) she randomly chooses to record a zero or a one. Simultaneously,* Alice prepares the single photon state: $a_j^\dagger(t_A, x_A)|0\rangle$, choosing

* While we could have Alice sending out a photon after she measures, sending a photon out simultaneously simplifies the problem by preventing the introduction of two separate times.

the polarisation to be $j = h$ or v according to the value $x = 0$ or $x = 1$ of the random bit she is trying to send Bob. As the mode of the photon matches the acceptance mode of the output mirror, it escapes from Alice's lab with no attenuation. Bob's protocol is identical except that he measures and prepares the single photon states $a_j^\dagger(t_B, x_B)|0\rangle$, matching the acceptance mode of his input and output mirrors respectively. Fig. 5.1 suggests that Alice and Bob's modes are right moving modes, i.e., localised on the trajectories $t_X - x_X$. We assume Bob is to the right of Alice (see Fig. 5.2) and allow a passive mirror outside Bob's station to reflect Bob's output from right-moving to left-moving. A similar mirror outside Alice's lab reflects left-moving modes back into right moving modes that impinge on Alice's mode selective input mirror. In the following we will ignore the slight asymmetry of this situation and assume the effective propagation distance between the labs is simply $|x_A - x_B|$.

Given our assumptions about the ideal operation of the components it is clear that if Alice (Bob) detects a photon in their polarisation detector they will successfully determine the bit value sent by Bob (Alice). Hence, in order to calculate the value of $P_{\text{succ,local}}$ (Eq. 5.1) we need to determine the probability for Alice (Bob) to detect the photon prepared by Bob (Alice). We can calculate the transmission probability for an excitation of Alice's mode to get through Bob's input mirror via the absolute square of the overlap between their modes:*

$$P_{\text{Bob's mirror}} = |\langle 0 | a(t_B, x_B) a^\dagger(t_A, x_A) | 0 \rangle|^2 \quad (5.8)$$

$$= \left| \int dk \frac{e^{-\frac{(k-k_0)^2}{2\sigma^2}}}{(2\pi\sigma^2)^{\frac{1}{2}}} e^{i[\omega_k(t_A-t_B)-k(x_A-x_B)]} \right|^2 \quad (5.9)$$

$$= e^{-(t_A-t_B+\tau)^2\sigma^2}. \quad (5.10)$$

where $\tau \equiv x_B - x_A$, with the assumption that $k_0 \gg \sigma$ and using the usual commutation rule $[a_k, a_{k'}^\dagger] = \delta(k - k')$. The above analysis can be repeated for a photon from Bob to Alice with $k_0 < 0$, travelling the opposite direction. We obtain the similar result:

$$P_{\text{Alice's mirror}} = |\langle 0 | a(t_A, x_A) a^\dagger(t_B, x_B) | 0 \rangle|^2 \quad (5.11)$$

$$= e^{-(t_B-t_A+\tau)^2\sigma^2}. \quad (5.12)$$

We can now specify the probability that Bob measures Alice's bit correctly as the probability that the photon is transmitted through Bob's mirror, after which he can definitely know the bit value, plus the probability that the photon is reflected multiplied by the probability he correctly guesses Alice's bit, i.e. $\frac{1}{2}$. Hence we obtain

$$P(y = a) = e^{-(t_A-t_B+\tau)^2\sigma^2} + \frac{1}{2} \left(1 - e^{-(t_A-t_B+\tau)^2\sigma^2} \right). \quad (5.13)$$

Similarly for Alice measuring Bob's qubit,

$$P(x = b) = e^{-(t_B-t_A+\tau)^2\sigma^2} + \frac{1}{2} \left(1 - e^{-(t_B-t_A+\tau)^2\sigma^2} \right). \quad (5.14)$$

* $\langle 0 | a(t_B, x_B) a^\dagger(t_A, x_A) | 0 \rangle$ can be thought of as the Feynman propagator $\langle 0 | \mathcal{T} [\phi(t', x'), \phi(t, x)] | 0 \rangle$ except our excitations are Gaussian-localised particles.

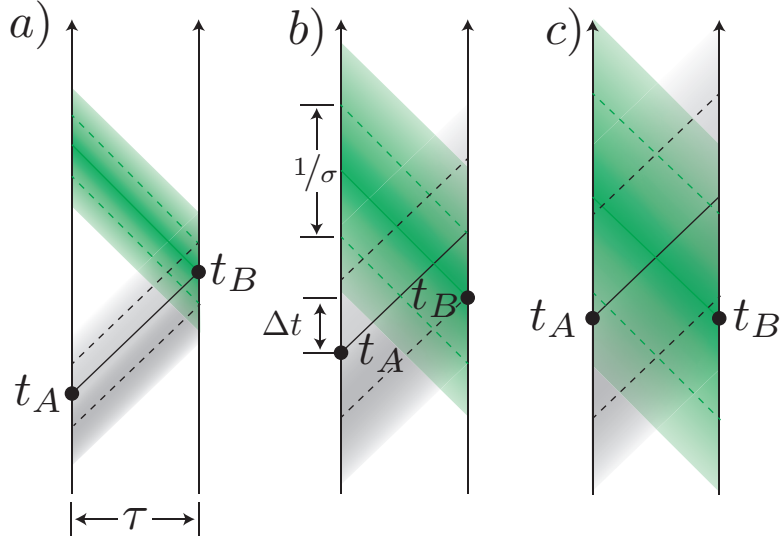


Figure 5.2: A sketch of three regimes. The vertical black lines represent the labs with negligible size on the scale of the diagram. The black dots represent the times t_A and t_B . The dotted lines and shaded areas represents the temporal width of the wavepacket $\frac{1}{\sigma}$. a) is the optimal choice for t_A and t_B when $\sigma \gtrsim \frac{1}{\tau}$ and $\Delta t = \pm\tau$ b) is the optimal choice when $\frac{1}{\sqrt{2}\tau} < \sigma \lesssim \frac{1}{\tau}$ and c) is the optimal choice when $\sigma \leq \frac{1}{\sqrt{2}\tau}$ and $\Delta t = 0$.

The probability of success is therefore,

$$P_{\text{succ}} = \frac{1}{4} \left(2 + e^{-(t_A - t_B + \tau)^2 \sigma^2} + e^{-(t_B - t_A + \tau)^2 \sigma^2} \right). \quad (5.15)$$

This is our main result—for any choice of a finite σ and τ , timings can be found for which $P_{\text{succ}} > \frac{3}{4}$ (Eq. 5.2).

We now investigate the optimal $\Delta t \equiv t_B - t_A$ that maximises this probability of success. From the perspective of perfectly localised particles this should be the case when $\Delta t = \pm\tau$ but here there is the competing effect of delocalisation. As a result, the best-case scenario depends on the parameters. For $\sigma \gtrsim \frac{1}{\tau}$, it is optimised by $\Delta t \approx \pm\tau$. When $\frac{1}{\sqrt{2}\tau} < \sigma \lesssim \frac{1}{\tau}$, the optimal Δt is $0 < |\Delta t| < \tau$. In this regime, the average send times of Alice and Bob are no longer light-like separated, instead t_A and t_B become increasing more symmetric as σ gets smaller. When $\sigma \leq \frac{1}{\sqrt{2}\tau}$, the optimum separation in time is $\Delta t = 0$ where $t_A = t_B$ and we have the symmetric case. In the asymmetric case where $\Delta t = \pm\tau$,

$$P_{\text{succ}} = \frac{1}{4} \left(3 + e^{-(2\tau)^2 \sigma^2} \right) \quad (5.16)$$

and we have a violation of the inequality for any $\sigma < \infty$. In the symmetric case, $\Delta t = 0$ and the probability of success is,

$$P_{\text{succ}} = \frac{1}{2} \left(1 + e^{-\tau^2 \sigma^2} \right) \quad (5.17)$$

for which $P_{\text{succ}} \geq \frac{3}{4}$ when $\sigma \leq \frac{\sqrt{\ln 2}}{\tau}$. In all cases, it is always possible for $P_{\text{succ}} > \frac{3}{4}$. In the limit of strong photon and lab delocalisation $\sigma \rightarrow 0$, the probability goes to 1, i.e. $P_{\text{succ}} \rightarrow 1$, approaching a maximal violation of the inequality. It may seem that in the limit $\sigma \rightarrow \infty$ we obtain perfect localisation, and we get back the causal inequality where $P_{\text{succ}} \leq \frac{3}{4}$. However, this is an unphysical limit. In order for our solutions to be valid we require $\sigma \ll k_0$ (this ensures that the mode function doesn't

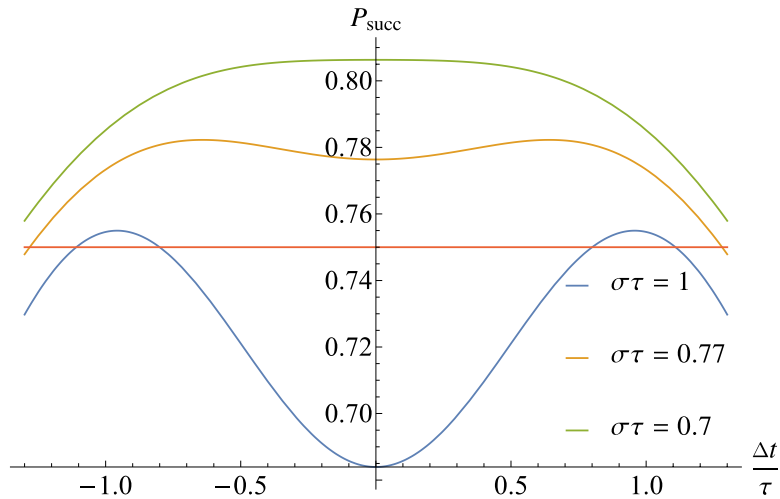


Figure 5.3: The probability of success for three values of $\sigma\tau$ are plotted showing the three regimes where the probability of success is maximised. The red line indicates a probability of success of 0.75 which can be exceeded for certain choices of $\frac{\Delta t}{\tau}$.

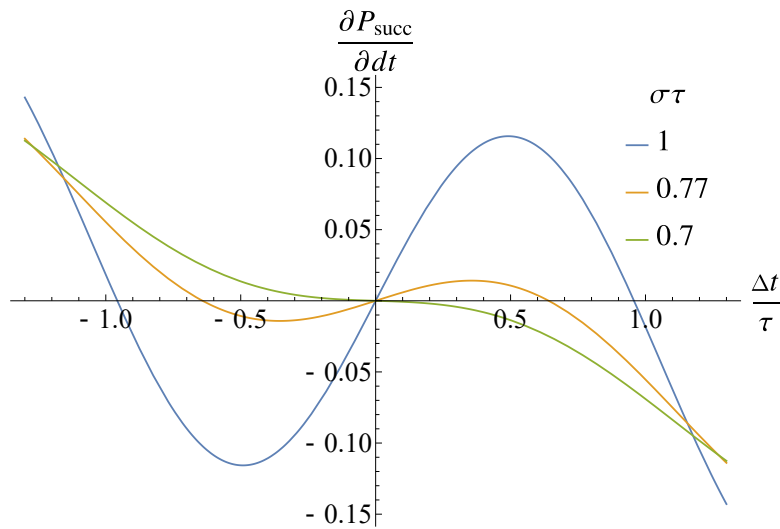


Figure 5.4: The derivative of the probability of success is plotted for three values of $\sigma\tau$ showing the value of Δt for which the probability of success is maximised. The zeros of the functions indicate the extrema of the probability of success.

bifurcate into both right *and* left moving components). As a result $\sigma \rightarrow \infty$ implies $k_0 \rightarrow \infty$ and hence infinite energy. The violation of the inequality is our main result. We now discuss in more detail the construction and properties of the local labs.

5.5 The mode selective mirror

Earlier we modelled the mode selective mirror as a projective measurement onto the lab mode. Here we present a more detailed model of the mirror. Let us consider Alice's lab. Fig.1 represents the mode selective mirror. A complete set of orthonormal modes, $\{a_i\}$, impinges from the outside. This basis set is chosen such that Alice's lab mode, a_0 , is a member of the set (this can always be done¹⁵⁸). A complementary and orthogonal set of modes $\{b_i\}$, impinges from the inside. An incoming mode, c_{in}

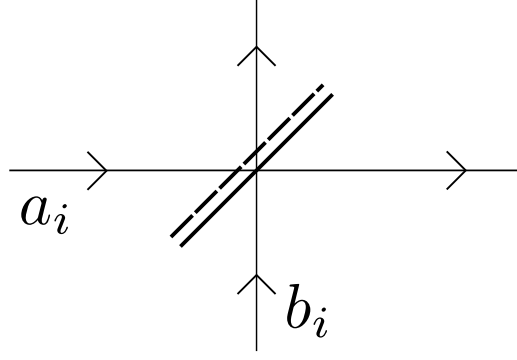


Figure 5.5: A setup of the mode selective mirror. The beamsplitter is given by the unitary in Eq. (5.19). The state from bob enters from the left and the lab is to the right of the beamsplitter.

from the outside can then be decomposed as

$$c_{\text{in}} = \sqrt{\eta} a_0 + \sum_{i \neq 0} f_i a_i, \quad (5.18)$$

where $\sqrt{\eta} = [c_{\text{in}}, a_0^\dagger]$ is given by the overlap of c_{in} and a_0 . Also note that $\eta + \sum_{i \neq 0} |f_i|^2 = 1$. Alice's mode selective mirror can then be modelled by the direct product of unitaries

$$U = \prod_{i \neq 0} e^{i \frac{\pi}{2} (a_i b_i^\dagger + a_i^\dagger b_i)}, \quad (5.19)$$

which reflects all a_i with $i \neq 0$, but transmit a_0 . So a single photon state from Bob, $(|\Psi\rangle = c_{\text{in}}^\dagger |0\rangle)$, going through the mirror becomes

$$U |\Psi\rangle = U c_{\text{in}}^\dagger U^\dagger U |0\rangle = \left(\sqrt{\eta} a_0^\dagger + i \sum_{i \neq 0} f_i b_i^\dagger \right) |0\rangle, \quad (5.20)$$

where we have used that $U^\dagger U$ is the identity and $U |0\rangle = |0\rangle$. If we trace over the reflected outside modes b_i , the reduced density operator of the state in mode a_0 inside the lab is,

$$\rho = \eta a_0^\dagger |0\rangle \langle 0| a_0 + (1 - \eta) |0\rangle \langle 0|. \quad (5.21)$$

All other modes are in the vacuum state. Any operation carried out in the lab will have the maximum probability (η) of interacting with the photon if it is carried out on the lab mode, a_0 . A physical implementation of the mode-selective mirror requires an active interaction such as the pulse gate introduced by Eckstein *et al.*¹⁵⁹

5.6 Measurements with different timing precision than the mode

Let us suppose that Alice sends out a mode with a width σ_A and Bob tries to measure a mode with a width σ_B , then we find that

$$P_{\text{Bob's mirror}} = \left| \langle 0 | a(t_B, x_B, \sigma_B) a^\dagger(t_A, x_A, \sigma_A) | 0 \rangle \right|^2 \quad (5.22)$$

$$= \frac{2\sigma_A \sigma_B e^{-\frac{2(\Delta t + \tau)^2 \sigma_A^2 \sigma_B^2}{\sigma_A^2 + \sigma_B^2}}}{\sigma_A^2 + \sigma_B^2}. \quad (5.23)$$

In the case of maximum probability, this gives

$$P_{\text{Bob's mirror, max}} = \frac{2\sigma_A\sigma_B}{\sigma_A^2 + \sigma_B^2} \quad (5.24)$$

$$= \frac{2\frac{\sigma_A}{\sigma_B}}{1 + \frac{\sigma_A^2}{\sigma_B^2}}. \quad (5.25)$$

Which is strictly < 1 for $\frac{\sigma_A}{\sigma_B} \neq 1$. The generalised probability of success is therefore

$$P_{\text{succ}} = \frac{1}{4} \left(2 + \frac{2\sigma_A\sigma_B e^{-\frac{2(\Delta t + \tau)^2 \sigma_A^2 \sigma_B^2}{\sigma_A^2 + \sigma_B^2}}}{\sigma_A^2 + \sigma_B^2} + \frac{2\sigma_A\sigma_B e^{-\frac{2(-\Delta t + \tau)^2 \sigma_A^2 \sigma_B^2}{\sigma_A^2 + \sigma_B^2}}}{\sigma_A^2 + \sigma_B^2} \right). \quad (5.26)$$

So we see that anything other than $\sigma_A = \sigma_B$ would cause a decrease in the violation of the causal inequality. In particular, the violation would be reduced if Bob tries to measure a mode with greater timing precision (i.e. $\sigma_B > \sigma_A$) than the mode that Alice actually sent.

5.7 Feedback loop for a CNOT gate

The violation of the causal inequality indicates that signals can be sent efficiently both from Alice to Bob and from Bob to Alice. As we have commented, preparations of outputs conditional on inputs is allowed by our formalism. One might then worry that this somehow leads to inconsistent behaviour such as Alice sending a message to her own input telling her not to send a message. Of course, our formalism is based on quantum field theory so we expect consistent solutions. The situation we have described is in fact a quantum feedback loop.¹⁶⁰ Whilst in general this problem is very difficult to solve there exists solutions for zero-time feedback loops.¹⁶¹ In the following we investigate a non-trivial loop in the limit of zero-time feedback, where $\tau\sigma \ll 1$ such that the time of travel is much smaller than the temporal spread in the wave packet (i.e. an extreme case of scenario c).

Let us consider a CNOT gate implemented with a cross Kerr non-linearity and dual rail encoding. The CNOT gate is depicted in Fig. 5.6.

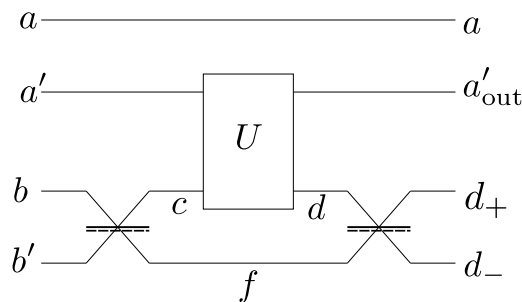


Figure 5.6: CNOT gate with a cross Kerr non-linearity. The beamsplitters are 50:50. A control qubit is encoded as $|0_c\rangle = a^\dagger |0\rangle$ and $|1_c\rangle = a'^\dagger |0\rangle$. The target qubit is encoded as $|0_t\rangle = b^\dagger |0\rangle$ and $|1_t\rangle = b'^\dagger |0\rangle$.

The cross Kerr non-linearity is given by a unitary,

$$U = e^{i\pi c^\dagger c a'^\dagger a'}. \quad (5.27)$$

The output of this circuit is,

$$a'_{\text{out}} = e^{-i\pi c^\dagger c} a' \quad (5.28)$$

$$d_{\pm} = \frac{1}{2} \left[\left(e^{-i\pi a'^{\dagger} a'} \pm 1 \right) b + \left(e^{-i\pi a'^{\dagger} a'} \mp 1 \right) b' \right]. \quad (5.29)$$

Now if we feed the output a & a' to the input b & b' , then we have the circuit in Fig. 5.7. Notice that nominally this assignment can be inconsistent. For example if we prepare the a modes in the state $|+\rangle = 1/\sqrt{2} (|01\rangle + |10\rangle)$ and the b modes in the state $|+\rangle$, then the a_{out} modes are in the state $|-\rangle = 1/\sqrt{2} (|01\rangle - |10\rangle)$, so the a_{out} and b modes seems inconsistent. If we try to fix this by making the b modes in the state $|-\rangle$ then the a_{out} modes switch to $|+\rangle$ —seemingly inconsistent again. However, we will see that the actual solution is consistent.

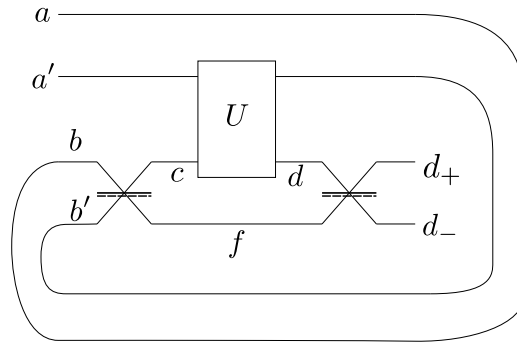


Figure 5.7: CNOT gate with zero-time feedback.

By equating $b = a$ and $b' = a'_{\text{out}}$ we are assuming the loop is short and the feedback is effectively instantaneous. Notice that we have reduced the Hilbert space of the problem down to 2 dimensions from the previous 4.

$$d_{\pm} = \frac{1}{2} \left[\left(e^{-i\pi a'^{\dagger} a'} \pm 1 \right) a + \left(e^{-i\pi a'^{\dagger} a'} \mp 1 \right) e^{-i\pi c^\dagger c} a' \right]. \quad (5.30)$$

While we have a self-recursive expression for $c = \frac{1}{\sqrt{2}} (a + e^{-i\pi c^\dagger c} a')$ we will see that we don't need an explicit expression. We can now calculate what this circuit does to logical 0s and 1s.

$$\begin{aligned} d_{\pm} a'^{\dagger} |0\rangle &= \frac{1}{2} (1 \pm 1) |0\rangle \\ \implies \langle 0 | a d_{\pm}^{\dagger} d_{\pm} a'^{\dagger} |0\rangle &= \begin{cases} 1 & \text{for } d_{+} \\ 0 & \text{for } d_{-} \end{cases} \\ d_{\pm} a'^{\dagger} |0\rangle &= \left(e^{-i\pi a'^{\dagger} a'} \mp 1 \right) e^{-i\pi c^\dagger c} a' a'^{\dagger} |0\rangle \\ &= \frac{1}{2} (1 \mp 1) |0\rangle \\ \implies \langle 0 | a' d_{\pm}^{\dagger} d_{\pm} a'^{\dagger} |0\rangle &= \begin{cases} 0 & \text{for } d_{+} \\ 1 & \text{for } d_{-} \end{cases} \end{aligned}$$

We see that although we do not know the expression for c , $e^{-i\pi c^\dagger c}$ acts on the vacuum. For arbitrary input states we find

$$\langle 0 | (\alpha^* a + \beta^* a') d_+^\dagger d_+ (\alpha a^\dagger + \beta a'^\dagger) | 0 \rangle = |\alpha|^2, \quad (5.31)$$

$$\langle 0 | (\alpha^* a + \beta^* a') d_-^\dagger d_- (\alpha a^\dagger + \beta a'^\dagger) | 0 \rangle = |\beta|^2. \quad (5.32)$$

So we see that the zero-time feedback for a CNOT gate (up to a phase rotation) is actually just the identity.

Let us now consider modes extended in time. For the case in Fig. 5.6, it is clear how to proceed, we simply specify that the unitary and mirrors are mode matched to modes a, a', b, b' . However, when there is a finite-time feedback loop, the modes reentering are shifted in time. If we continue using the mode matched unitary as before, then in the case of scenario a) where the temporal spread of the modes is small compared to the distance between labs, we expect that the unitary would not be matched to the mode by the time most of it propagates back. Therefore in scenario a), we expect that the unitary is also the identity.

5.8 Conclusion

Causal inequalities represent interesting constraints only if additional conditions are imposed on how the correlations are generated—with no restrictions, it is always possible to generate arbitrary correlations, without the need of quantum effects or exotic spacetime geometry. Although the inequalities are device and theory independent, the conditions on the protocols are model-dependent and have to rely on additional assumptions.

Crucial to the original formulation of Oreshkov *et al.*²⁸ is the assumption of closed laboratories, which prevents exploiting simple multi-round protocols. We have considered a possible natural background-independent formalisation of this assumption, namely the identification of closed laboratories with field modes. We have presented a protocol where operations matched to particular field modes enable a violation of a causal inequality.

However, when analysed from the perspective of a background causal structure, the same protocol may seem to violate the closed laboratory assumption: The two ‘laboratories’ act on delocalised modes and therefore sit in regions that are extended in time, both future and past light cone of each region have a large overlap with the other region, and information can freely travel between the two.

Nonetheless, it is questionable whether it is physically meaningful to take the existence of a background causal structure as a primitive notion. Spacetime points are sometimes a useful abstraction of physical events. In classical physics we often consider (point) particles that are perfectly localised, thus physical events such as ‘particle enters lab’ correspond to a spacetime point or a spacetime event. Such cannot be said for a quantum particle which is always delocalised. Spacetime events are therefore of limited use when we consider quantum physics. Thus, it is perhaps better to consider spacetime events/points as a useful mathematical tool rather than a primitive constituent of physical theory. With this view, events do not exist on their own: they make sense as relational properties

between physical degrees of freedom, quantum fields in our case. It is therefore more meaningful to adopt a background-independent notion of local degrees of freedom. Furthermore, sharply-localised modes are unphysical in quantum field theory as they would be associated with infinite energy.^{156,157} Thus, it would never be possible to strictly satisfy the closed lab assumption, as formulated from the background causal structure point of view. This is a manifestation of the well-known problem of localisation in QFT^{54,154,162} (tightly related with the entanglement in the quantum vacuum^{22,163–172}), namely the question of which quantum degrees of freedom should be associated with local spacetime regions.^{173–181} Here we have exposed yet another manifestation of this issue: The localisation problem challenges a meaningful, background-independent definition of causal relations in quantum field theory. A formulation of quantum mechanics with no background causal structure²⁸ that includes quantum fields will necessarily have to face this issue.

As the violation of a causal inequality is possible with measurements in a fixed basis, the ‘local operations’ cannot be embedded in the ‘process matrix formalism’ in which fixed-basis measurements in a bipartite scenario always lead to definite causal order.^{28,182} This leaves open the question of whether, in order to be compatible with field theory, the process matrix formalism needs to be extended to allow for non-linear probabilities or whether the basic structure and the assumption of closed laboratories need to be reformulated in order to exclude such possibilities.

Chapter 6

Optical levitation of a mirror

Levitation by light is an accessible stage where we can see the push and pull between gravity and quantum physics. Optomechanical systems such as pendula, in which gravity provides part of the restoring force, have proven to be extremely versatile, ranging from generating squeezed light^{183,184}, laser cooling of harmonic oscillators¹⁸⁵ to precision metrology^{186,187}, and finding applications from the nanoscale¹⁸⁸ to the kiloscale, most notably by LIGO^{189,190}. Such macroscopic optomechanical systems have opened up the possibility of testing quantum-gravity interaction models^{191,192}. The ultimate such system, often invoked as a gedanken experiment, is when a mirror is solely suspended by radiation pressure. Such levitating systems have been proposed as a way to reduce noise and decoherence from unwanted coupling^{193,194}. The levitating mirror is thus of interest as a low-dissipative *and* macroscopic optomechanical system. While the levitating mirror has been of renewed interest lately—a tripod¹⁹⁵ and a double Fabry-Pérot cavity¹⁹⁶ have been recently proposed as systems for levitating mirrors—there has not yet been a full quantum optomechanical analysis of a levitating mirror.

In addition to metrology, the floating mirror has relevance to relativistic quantum theory. As we have seen in Chapters 2 and 3, due to Einstein's equivalence principle, the Unruh effect is a useful device for understanding and exploring QFTCS. However, in current research, the acceleration of a detector (such as an Unruh-Dewitt detector) to probe relativistic quantum effects is mostly modelled using classically accelerated trajectories. As the laser levitating the mirror is a quantum source of acceleration, this chapter seeks to understand how a quantum source of acceleration might affect our current understanding. More speculatively, through the equivalence principle, the laser could be considered as a quantum source of *gravity*; this has relevance to the recent proposal of modelling black hole evaporation as a parametric down conversion with the black hole mass modelled as a quantum coherent state.^{197–199}

In this chapter, I set out the quantum theory for a one dimensional levitating mirror, compare its behaviour with common optomechanical systems and finally, examine its stability and dynamics in an experimentally accessible regime.

6.1 Quantum Optomechanics

In open quantum systems we have a system that is coupled to an environment which can comprise mechanisms for loss, damping and ways to probe the system. In this chapter we will assume for simplicity that the system is one dimensional and coupled to a ‘bath’ and this is the sense in which it is an open quantum system. The following discussion will follow the notation of Bowen & Milburn²⁰⁰ while the derivation will follow Gardiner & Collett.²⁰¹ The general form of the Hamiltonian is,

$$H = H_{\text{system}} + H_{\text{system-bath}}. \quad (6.1)$$

A simple model for the bath is to consider it as a collection of independent oscillators that are coupled to the system via position q , that is:

$$H_{\text{system-bath}} = \int d\omega \left[\frac{p_\omega^2}{2m_\omega} + k_\omega (q_\omega - q)^2 \right] \quad (6.2)$$

where $q_\omega = \sqrt{\frac{\hbar}{2m_\omega\omega}} (a_\omega + a_\omega^\dagger)$, $p_\omega = i\sqrt{\frac{\hbar m_\omega\omega}{2}} (a_\omega^\dagger - a_\omega)$ and a_ω is the annihilation operator of each bath oscillator. With these definitions, the canonical commutation relations $[q_\omega, p_\omega] = i\hbar$ means that the bath operators obey the commutation relation $[a_\omega, a_\omega^\dagger] = 1$. We will only consider cases where the system is also a harmonic oscillator with mass m and frequency Ω , so $q = \sqrt{\frac{\hbar}{2m\Omega}} (a + a^\dagger)$ and a are the annihilation operators for the system. Similar to the bath operators, the system operator obey the commutation relation $[a, a^\dagger] = 1$. The frequency of the system harmonic oscillator is often much faster than the damping rate due to the bath (related to k_ω). In the Hamiltonian there are terms of the form $a_\omega a$ and $a_\omega^\dagger a^\dagger$ which oscillate with frequency $\Omega + \omega$ while the terms $a_\omega a^\dagger$ and $a_\omega^\dagger a$ oscillate with frequency $\Omega - \omega$. In the rotating wave (RW) approximation we only keep terms oscillating with frequency $\Omega - \omega$ as these terms dominate the faster oscillating terms. This can be thought of as averaging the bath interaction over a period of the system’s oscillation.²⁰⁰ Substituting the expressions for q and q_ω in terms of the annihilation operator and applying the RW approximation, the Hamiltonian simplifies to,

$$H_{\text{system-bath, RWA}} = \int d\omega \left[\hbar\omega a_\omega^\dagger a_\omega + i\hbar\gamma_\omega (a_\omega a^\dagger - a_\omega^\dagger a) \right], \quad (6.3)$$

with $\gamma_\omega \equiv -i\frac{1}{2\sqrt{m_\omega\omega}\sqrt{m\Omega}}k_\omega$. The Heisenberg equation of motions give,

$$\dot{a}_\omega = -i\omega a_\omega - \gamma_\omega a, \quad (6.4)$$

$$\dot{O} = -\frac{i}{\hbar} [O, H_{\text{system}}] + \int d\omega \gamma_\omega \{ [O, a^\dagger] a_\omega - a_\omega^\dagger [O, a] \}, \quad (6.5)$$

where O is a system operator. We can solve Eq. (6.4) formally, to get,

$$a_\omega(t) = e^{-i\omega(t-t_0)} a_\omega(t_0) - \gamma_\omega \int_{t_0}^t e^{-i\omega(t-t')} a(t'), dt' \quad (6.6)$$

where $t_0 < t$ and $a_\omega(t_0)$ is the ‘initial value’ of the operator at some earlier time t_0 . We make the first Markov approximation where $\gamma_\omega = \sqrt{\gamma/2\pi}$ which means that the coupling to the bath is frequency

independent. We also note that $\int_{-\infty}^{\infty} d\omega e^{-i\omega(t-t')} = 2\pi\delta(t-t')$ and $\int_{t_0}^t c(t')\delta(t-t')dt' = \frac{1}{2}c(t)$.^{*} We also define an in field

$$a_{\text{in}}(t) = \frac{1}{\sqrt{2\pi}} \int d\omega e^{-i\omega(t-t_0)} a_{\omega}(t_0) \quad (6.7)$$

which satisfies the commutation relation $[a_{\text{in}}(t), a_{\text{in}}(t')] = \delta(t-t')$. With this, we substitute (6.6) into (6.5) to get,

$$\dot{O}(t) = -\frac{i}{\hbar} [O, H_{\text{system}}] + [O, a^{\dagger}(t)] \left(-\frac{\gamma}{2}a(t) + \sqrt{\gamma} a_{\text{in}}(t) \right) - \left(-\frac{\gamma}{2}a^{\dagger}(t) + \sqrt{\gamma} a_{\text{in}}^{\dagger}(t) \right) [O, a(t)] \quad (6.8)$$

Note that while $a(t)$ is unitless— $a^{\dagger}a$ being the number of excitations— $a_{\text{in}}^{\dagger}a_{\text{in}}$ has the units s^{-1} —a measure of the flux of quanta incident on the system.

We can also consider the output of the system, where $t_1 > t$, we get another form of (6.6),

$$a_{\omega}(t) = e^{-i\omega(t-t_1)} a_{\omega}(t_1) + \gamma_{\omega} \int_t^{t_1} e^{-i\omega(t-t')} a(t') dt' \quad (6.9)$$

where we define an analogous out field

$$a_{\text{out}}(t) = \frac{1}{\sqrt{2\pi}} \int d\omega e^{-i\omega(t-t_1)} a_{\omega}(t_1) \quad (6.10)$$

using an analogous equality, $\int_t^{t_1} c(t')\delta(t-t')dt' = \frac{1}{2}c(t)$ leads us to a time-reversed Langevin equation

$$\dot{O}(t) = -\frac{i}{\hbar} [O, H_{\text{system}}] + [O, a^{\dagger}(t)] \left(\frac{\gamma}{2}a(t) + \sqrt{\gamma} a_{\text{out}}(t) \right) - \left(\frac{\gamma}{2}a^{\dagger}(t) + \sqrt{\gamma} a_{\text{out}}^{\dagger}(t) \right) [O, a(t)]. \quad (6.11)$$

Comparing the two equations, we get

$$a_{\text{out}}(t) = a_{\text{in}}(t) - \sqrt{\gamma} a(t). \quad (6.12)$$

6.2 Hamiltonian of the system

Now that we have reviewed the basics of open systems, we will now set out the dynamics of the system. We start with a Fabry-Pérot cavity where the lower mirror is stationary and the upper mirror (henceforth, referred to as the mirror) is free to move along the cavity axis. We will couple a laser into the cavity which will support the mirror by radiation pressure alone. q and p are the position and momentum of the mirror with the usual commutation relation $[q, p] = i\hbar$, measured from a resting length L (see Fig. 6.1) and $\Omega_c(q) = \frac{j\pi c}{L-q}$ is the position dependent resonant frequency of the cavity, j is the j th mode in the cavity the laser couples to and L is the initial length of the cavity. a and a^{\dagger} are the annihilation and creation operators of the intracavity mode with the commutation relation $[a, a^{\dagger}] = 1$ and $[q, p] = i\hbar$. The Hamiltonian for the system is

$$H = \frac{p^2}{2m} - mgq + \hbar\Omega_c(q)a^{\dagger}a. \quad (6.13)$$

^{*} This result can be seen if we think of the Dirac delta function as the limit of a Gaussian, $\delta(t) = \lim_{w \rightarrow 0} \frac{1}{w\sqrt{\pi}} e^{-(\frac{t}{w})^2}$. Then for $\epsilon \neq 0$, $\int_{-\epsilon}^{\epsilon} \delta(t) dt = 1$. Because $\int_{-\epsilon}^0 \delta(t) dt = \int_0^{\epsilon} \delta(t) dt$ this implies that $\int_{-\epsilon}^0 \delta(t) dt = \frac{1}{2}$.

For convenience, we transform to rotating frame of the laser frequency Ω_L

$$H = \frac{p^2}{2m} - mgq + \hbar(\Omega_c(q) - \Omega_L) a^\dagger a. \quad (6.14)$$

As the mirror is supported by an external laser, we will need to use input-output theory so that we can probe the behaviour of the system.

6.3 Markov approximation for cavity and mirror coupled to separate baths

To model the coupling of the laser into the cavity and the input-output of the system, we will assume that the cavity and the mirror are individually coupled to Markovian baths. We will also use the rotating wave approximation. Implicit in our modelling is that the mirror has perfect reflectivity while the lower stationary mirror is the input-output port to which the laser is coupled. This leads to a Langevin equation^{200,201} which is the sum of two versions of Eq. (6.11), one for the cavity and one for the mirror. However, because we have not yet demonstrated how the mirror acts as a oscillator we will rewrite the Langevin equation with q and p as the dynamical variables instead of annihilation and creation operators. The combined Langevin equation for the cavity and the mirror is therefore

$$\begin{aligned} \dot{O} = & \frac{1}{i\hbar} [O, H] - [O, a^\dagger] \left(\frac{\kappa}{2} a - \sqrt{\kappa} a_{\text{in}}(t) \right) + \left(\frac{\kappa}{2} a^\dagger - \sqrt{\kappa} a_{\text{in}}^\dagger(t) \right) [O, a] \\ & + i \frac{\sqrt{\Gamma}}{\hbar} ([O, q] p_{\text{in}}(t) - [O, p] q_{\text{in}}(t)) + \frac{\Gamma}{i\hbar} ([O, q] p - [O, p] q) \end{aligned} \quad (6.15)$$

p_{in} is the input momentum, q_{in} is the input displacement and Γ is the damping due to the mirror's bath. a_{in} is the input due to the cavity's bath and the κ is the rate due to the cavity's bath.

6.3.1 The Langevin parameters and optical cavity

Let us now review the basic details of a Fabry-Pérot cavity with a single port (i.e. a perfectly reflective second mirror) characterised by several parameters and properties: T , the intensity transmission of the input-output (lower) mirror, α , a loss coefficient for internal absorption or scattering, p , the optical pathlength of one round trip and the detuning $\Delta = \Omega_c - \Omega_L$ which is the difference between the cavity frequency and the input laser frequency. *Finesse* (F), is often used as a measure for the quality of a cavity. This depends on the reflectivity R and internal scattering and absorption α , but for our system, it is,

$$F = \frac{\pi (R \exp(-\alpha p))^{1/4}}{1 - \sqrt{R \exp(-\alpha p)}}. \quad (6.16)$$

Meanwhile, the cavity damping rate is given by,

$$\kappa = \frac{c}{p} \left(1 - \sqrt{R \exp(-\alpha p)} \right) \quad (6.17)$$

For a high finesse cavity, with high reflectivity (where transmissivity $T = 1 - R \ll 1$) and low scattering and absorption $\alpha p \ll 1$, we can approximately say that,

$$\kappa \approx \frac{c}{2(L-q)} \frac{\pi}{F} \quad (6.18)$$

$$\approx \frac{c}{2L} \frac{\pi}{F} \quad (6.19)$$

while, strictly speaking the damping rate κ and Finesse F is dependent on the cavity length, we are specifically interested in the regime where $\frac{q}{L} \ll 1$. This means that in practice, κ and F is not dependent on the state of the system. For further details on cavity equations see Bachor & Ralph.²⁰²

Usually damping on the mirror is due to some armature or spring that physically damps the mirror. In our case, we have no such thing and the damping on the mirror seems to be slightly mysterious. We note, of course, that the mirror is also interacting with the outside field; although we do not know exactly how to model the damping due to this, we subsume it into Γ . The cavity damping κ can be controlled by changing the resting length of the cavity or the reflectivity of the lower mirror. We will propose a method to control Γ later.

6.4 Equations of motion

With the Langevin equation Eq. (6.15) we can derive,

$$\dot{a} = - \left[\frac{\kappa}{2} + i(\Omega_c(q) - \Omega_L) \right] a + \sqrt{\kappa} a_{\text{in}}, \quad (6.20)$$

$$\dot{q} = \frac{p}{m} - \frac{\Gamma}{2} q + \sqrt{\Gamma} q_{\text{in}}, \quad (6.21)$$

$$\dot{p} = mg - \frac{\hbar \Omega_c^2(q)}{j\pi c} a^\dagger a - \frac{\Gamma}{2} p + \sqrt{\Gamma} p_{\text{in}}. \quad (6.22)$$

We assume that these operators \mathcal{O} can be written as a steady state solution $\langle \mathcal{O} \rangle = \mathcal{O}_{\text{SS}}$ and a linearised component $\delta \mathcal{O}$ that is small $\langle \delta \mathcal{O} \delta \mathcal{O} \rangle \ll \mathcal{O}_{\text{SS}}^2$ and has zero expectation $\langle \delta \mathcal{O} \rangle = 0$. That is, $\mathcal{O} = \langle \mathcal{O} \rangle + \delta \mathcal{O}$ with $\frac{d}{dt} \langle \mathcal{O} \rangle = 0$. To derive steady state equations, we take the expectation value of the equations and set $\langle \dot{a} \rangle = \langle \dot{q} \rangle = \langle \dot{p} \rangle = 0$. We will also require that $q_{\text{in,SS}} = p_{\text{in,SS}} = 0$ which means that the mirror's bath applies no coherent force on the mirror. We will not make this assumption on $a_{\text{in,SS}}$ which is non-zero as the bath input is a coherent laser beam that provides the power to levitate the mirror. Defining the steady state cavity number* $N_c \equiv \langle a^\dagger a \rangle \approx \langle a^\dagger \rangle \langle a \rangle$ and the input photon rate $N_{\text{in}} = \langle a_{\text{in}}^\dagger a_{\text{in}} \rangle \approx \langle a_{\text{in}}^\dagger \rangle \langle a_{\text{in}} \rangle$, we find that the steady state equations are,

$$\left[\frac{\kappa^2}{4} + (\Omega_c(q_{\text{SS}}) - \Omega_L)^2 \right] N_c = \kappa N_{\text{in}}, \quad (6.23)$$

$$p_{\text{SS}} = 0, \quad (6.24)$$

$$0 = mg - \frac{\hbar \Omega_c^2(q_{\text{SS}})}{j\pi c} N_c. \quad (6.25)$$

* Due to the requirement that the linearised part is small, $\langle a^\dagger a \rangle = \langle a^\dagger \rangle \langle a \rangle + \langle \delta a^\dagger \delta a \rangle \approx \langle a^\dagger \rangle \langle a \rangle$.

The two steady state solutions are,

$$q_1 = \frac{gm \left[-4jc\pi\Omega_L + L(\kappa^2 + 4\Omega_L^2) \right] - 2\sqrt{\pi} \sqrt{cgmj \left[-cgmj\pi\kappa^2 + N_{\text{in}}\kappa\hbar(\kappa^2 + 4\Omega_L^2) \right]}}{gm(\kappa^2 + 4\Omega_L^2)}, \quad (6.26)$$

$$N_{c,1} = \frac{-4cgmj\pi(\kappa^2 - 4\Omega_L^2) + 4\kappa N_{\text{in}}\hbar(\kappa^2 + 4\Omega_L^2) + 16\sqrt{\pi}\Omega_L \sqrt{cgmj \left[-cgmj\pi\kappa^2 + N_{\text{in}}\kappa\hbar(\kappa^2 + 4\Omega_L^2) \right]}}{\hbar(\kappa^2 + 4\Omega_L^2)} \quad (6.27)$$

and

$$q_2 = \frac{gm \left[-4jc\pi\Omega_L + L(\kappa^2 + 4\Omega_L^2) \right] + 2\sqrt{\pi} \sqrt{cgmj \left[-cgmj\pi\kappa^2 + N_{\text{in}}\kappa\hbar(\kappa^2 + 4\Omega_L^2) \right]}}{gm(\kappa^2 + 4\Omega_L^2)}, \quad (6.28)$$

$$N_{c,2} = \frac{-4cgmj\pi(\kappa^2 - 4\Omega_L^2) + 4\kappa N_{\text{in}}\hbar(\kappa^2 + 4\Omega_L^2) - 16\sqrt{\pi}\Omega_L \sqrt{cgmj \left[-cgmj\pi\kappa^2 + N_{\text{in}}\kappa\hbar(\kappa^2 + 4\Omega_L^2) \right]}}{\hbar(\kappa^2 + 4\Omega_L^2)}. \quad (6.29)$$

Note these solutions do not necessarily fulfil our criteria $\frac{q}{L} \ll 1$ which must be checked explicitly. Furthermore, we can absorb mg into N_{in} and N_c by defining $N_{\text{in}} = mg\widetilde{N}_{\text{in}}$ and $N_c = mg\widetilde{N}_c$. We will use this fact to define a dimensionless laser power later. This means that the steady state parameters, q_1 and $\widetilde{N}_{c,1}$ can be written as $q_1 = q_1(\widetilde{N}_{\text{in}}, \Omega_L, j, L, \kappa)$ and $\widetilde{N}_{c,1} = \widetilde{N}_{c,1}(\widetilde{N}_{\text{in}}, \Omega_L, j, L, \kappa)$. We will simplify the parameter dependence later with some assumptions.

6.5 Conditions on parameters and Detuning

Let us first consider how we might set up this experiment. We support the mirror at a distance L from the lower stationary mirror and then start up the laser until the intracavity field is strong enough to hold the mirror without the support. This means that the laser would address the mode j with the smallest ‘detuning’ $\Delta \equiv \frac{j\pi c}{L-q} - \Omega_L$. We will thus approximate $j = \text{Round}\left(\frac{L\Omega_L}{\pi c}\right)$. This reduces the parameter dependence of our steady state solutions. In particular, to ensure that we are really only addressing one mode, we require that $\Delta \ll \frac{\pi c}{L-q}$, which means that the detuning is small with respect to the frequency spacing $\frac{\pi c}{L-q}$ between the modes in the cavity. Furthermore, the damping rate κ for a good cavity must be much smaller than the frequencies in play such as Ω_L and Ω_c , therefore, we also require that $\frac{\kappa}{\Omega_L} \ll 1$. Let us now consider a single laser photon with frequency Ω_L entering the cavity and becoming an excitation in the cavity with frequency Ω_c if $\Delta = \Omega_c - \Omega_L > 0$, this means that the photon must ‘gain’ energy to enter the cavity, and the only place it can get this energy from is from the mirror. This is an intuitive argument for why $\Delta > 0$ —also known as red detuning—‘cools’ the mirror, or more precisely, downward phonon (mirror excitons) number transitions are enhanced when you have red detuning while for blue detuning upward transitions are enhanced (See Fig. 6.2). See chapter 3 & 4 of Bowen and Milburn²⁰⁰ for further details. The cooling from red detuning is a problem for our floating mirror, as the ground state of the mirror is arbitrary, it can continue to keep losing energy by falling lower.

6.5.1 Detuning of the steady state solutions

Given the importance of the detuning, we need to determine the detuning of the two steady state solutions. We can express the detuning $\Delta = \Omega_c - \Omega_L$ in terms of the steady state solutions,

$$\Delta_1 = \frac{2N_{\text{in}}\kappa\Omega_L\hbar - \sqrt{\pi} \sqrt{cgmj [-cgm\pi\kappa^2 + N_{\text{in}}\kappa\hbar (\kappa^2 + 4\Omega_L^2)]}}{2cgmj\pi - 2N_{\text{in}}\kappa\hbar} \quad (6.30)$$

$$\Delta_2 = \frac{2N_{\text{in}}\kappa\Omega_L\hbar + \sqrt{\pi} \sqrt{cgmj [-cgm\pi\kappa^2 + N_{\text{in}}\kappa\hbar (\kappa^2 + 4\Omega_L^2)]}}{2cgmj\pi - 2N_{\text{in}}\kappa\hbar}. \quad (6.31)$$

To determine which solution is blue or red detuned we need reasonable estimates of the system parameters. Let us consider the simplest case of a black object that is levitated by a laser. In this case, the change in momentum is due to the absorption of a photon with frequency Ω_L is $\hbar\Omega_L/c$. Thus, a laser supporting the object must have an output power of $P = \hbar N_{\text{in}}\Omega_L = mgc$.^{*} This gives us a rough idea of how large N_{in} should be. This also suggests defining a dimensionless power $\tilde{P} = \frac{P}{mgc} = \frac{\hbar N_{\text{in}}\Omega_L}{c}$. With this definition and the previous definition of $j = \text{Round}\left(\frac{L\Omega_L}{\pi c}\right)$, the parameter dependence of the detuning is $\Delta = \Delta(\tilde{P}, \Omega_L, L, \kappa)$. Thus, the denominator is approximately $2cgm\left(j\pi - \frac{\kappa}{\Omega_L}\right)$; since we require that $\frac{\kappa}{\Omega_L} \ll 1$, we know for any good cavity, the denominator is always positive. This means that only the first solution can be blue detuned ($\Delta < 0$). Using the same argument that we must have a good cavity, we can approximate the numerator as

$$2N_{\text{in}}\kappa\Omega_L\hbar - \sqrt{\pi} \sqrt{cgmj [-cgm\pi\kappa^2 + N_{\text{in}}\kappa\hbar (\kappa^2 + 4\Omega_L^2)]} \quad (6.32)$$

$$\approx 2N_{\text{in}}\kappa\Omega_L\hbar - \sqrt{\pi} \sqrt{cgmjN_{\text{in}}\kappa\hbar 4\Omega_L^2}. \quad (6.33)$$

Substituting our rough estimate of N_{in} , we find that

$$2N_{\text{in}}\kappa\Omega_L\hbar - \sqrt{\pi} \sqrt{cgmjN_{\text{in}}\kappa\hbar 4\Omega_L^2} \quad (6.34)$$

$$= 2\kappa mgc - mgc\sqrt{\pi j\kappa\Omega_L} \quad (6.35)$$

and finally, we know that $j > 0, j \in \mathbb{N}$ so $\sqrt{\pi j} > 1$ and again, $\frac{\kappa}{\Omega_L} \ll 1$, so $\sqrt{\Omega_L\kappa} \gg \kappa$. This ensures that for a good cavity we must have $\Delta_1 < 0$.

We thus conclude that we have two steady state solutions, one above the resonance point (blue detuned where $\Delta < 0$) and one below (red detuned where $\Delta > 0$). The blue detuned solution is depicted in Fig. 6.1

^{*} Remember that N_{in} has dimensions of photons per second.

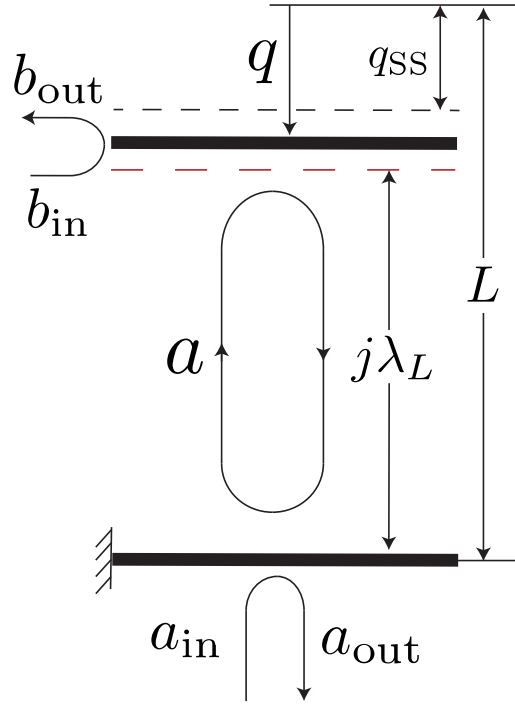


Figure 6.1: A visual representation of the system. The bottom mirror is fixed and forms a cavity with the free floating mirror above. We show the case of blue detuning where $\Delta < 0$. In the case of red detuning, the red line is above the q_{SS} line.

6.6 Standard optomechanical theory

Let us first review standard optomechanical theory as there are some important differences that need to be highlighted later. In a standard optomechanical system, the mirror is attached to a spring and therefore has a natural harmonic frequency of Ω_M so in terms of the mirror operator b and cavity operator a , the Hamiltonian can be written as

$$H = \hbar\Omega_M b^\dagger b + \hbar\Omega_c(q)a^\dagger a, \quad (6.36)$$

where $q = \sqrt{\frac{\hbar}{2m\Omega_M}} (b + b^\dagger)$ and Ω_c is defined in the same way as ours and the operators obey the same commutation relations. Linearisation of $\Omega_c(q) \approx \Omega_c(q_{SS}) \left(1 + \frac{q - q_{SS}}{L}\right)$ gives

$$H = \hbar\Omega_M b^\dagger b + \hbar\Omega_c a^\dagger a + \hbar g_0 a^\dagger a (b^\dagger + b). \quad (6.37)$$

We now assume that a and b have coherent amplitudes $\alpha = -\frac{\epsilon}{\Delta + 2\beta g_0}$ and $\beta = \frac{-g_0 \alpha^2}{\Omega_M}$ with an additional coherent driving term in the Hamiltonian $\hbar\epsilon(a^\dagger + a)$ we obtain,

$$H = \hbar \left(\Delta - \frac{2g_0^2 \alpha^2}{\Omega_M} \right) a^\dagger a + \hbar\Omega_M b^\dagger b + \hbar g_0 \left[\alpha (a + a^\dagger) + a^\dagger a \right] (b + b^\dagger). \quad (6.38)$$

We can arrive at the same place by using our Langevin equations and linearising around steady state solutions by $\alpha_{SS} = \sqrt{\kappa_{in}} \alpha_{in} \left[\frac{\kappa}{2} + i(\Delta + 2\beta_{SS} g_0) \right]^{-1}$ and $\beta_{SS} = \frac{-g_0 \alpha_{SS}^2}{\Omega_M}$. For consistency with Bowen and Milburn²⁰⁰ I have used their method of deriving the linearised optomechanical system in this section. Since we can control the detuning, we redefine by allowing $\Delta \rightarrow \Delta + \frac{2g_0^2 \alpha^2}{\Omega_M}$. Finally, we make the

linearisation approximation by neglecting the second term in the square brackets. This leads to the standard linearised optomechanical Hamiltonian,

$$H = \hbar\Delta a^\dagger a + \hbar\Omega_M b^\dagger b + \hbar g_0 \alpha (a + a^\dagger) (b + b^\dagger). \quad (6.39)$$

6.6.1 Strong coupling

In the standard optomechanical case, we are free to tune our parameters such that $\Delta = \Omega_M$. In this regime the mirror and the cavity act as a pair of coupled linear oscillators with degenerate frequencies. The Hamiltonian in Eq. (6.39) can be diagonalised by defining $c = \frac{1}{\sqrt{2}}(a + b)$, $d = \frac{1}{\sqrt{2}}(a - b)$ and using the rotating wave approximation to ignore cc , $c^\dagger c^\dagger$, dd and $d^\dagger d^\dagger$ terms. The Hamiltonian simplifies to

$$H = \hbar(\Omega_M + g_0\alpha) c^\dagger c + \hbar(\Omega_M - g_0\alpha) d^\dagger d, \quad (6.40)$$

where c and d are now independent harmonic oscillators. This can be easily solved in the Heisenberg picture to get

$$a(t) = [a(0) \cos(g_0\alpha t) - ib(0) \sin(g_0\alpha t)] e^{-i\Omega_M t}, \quad (6.41a)$$

$$b(t) = [b(0) \cos(g_0\alpha t) - ia(0) \sin(g_0\alpha t)] e^{-i\Omega_M t}. \quad (6.41b)$$

We see now that in this case the cavity (a) and the mirror (b) coherently interchange their quantum states. This assumes there is no coupling to the outside. Where there is coupling to the mirror and cavity bath, for strong coupling we also require that $g_0\alpha > \{(2\bar{n} + 1)\Gamma, (2\bar{n}_L + 1)\kappa\}$ where \bar{n} and \bar{n}_L are the mirror and light bath mean occupancy. This condition means that the speed of coupling between the mirror and cavity ($g_0\alpha$) is faster than the rate of decoherence due to the baths.

Note that our floating mirror can never reach $\Delta = \Omega_M$ as it must be blue detuned $\Delta < 0$ to have stability.

Let us now perform a similar linearisation on our system and compare it to the standard theory.

6.7 Linearised Hamiltonian

In our system, the mirror can be said to be floating on a ‘bed’ of photons that act like a spring. The mirror is not naturally a harmonic oscillator; only the perturbations of the mirror around the steady state act like a harmonic oscillator. Recalling our previous definition for the linearisation $\mathcal{O} = \langle \mathcal{O} \rangle + \delta\mathcal{O}$, for small variations of p , q , a and a^\dagger , the variation of the Hamiltonian is

$$\begin{aligned} \delta H = & \underbrace{\frac{p}{m}}_{\text{steady state means}=0} + \underbrace{\left(-mg + \frac{\hbar\Omega_c^2 N_c}{j\pi c} \right)}_{\text{steady state means}=0} \delta q + \underbrace{\hbar\Delta \left(\alpha^* \delta a + \alpha \delta a^\dagger \right)}_{\text{Cancelled by terms in Langevin equations \& SS eqns}^*} \\ & \underbrace{\hspace{15em}}_{\text{no contribution to dynamics}} \\ & + \frac{1}{2m} \delta p^2 + \frac{\hbar\Omega_c^3 N_c}{(j\pi c)^2} \delta q^2 + \hbar\Delta \delta a^\dagger \delta a + \frac{\hbar\Omega_c^2}{j\pi c} \left(\alpha \delta a^\dagger + \alpha^* \delta a \right) \delta q, \end{aligned} \quad (6.42)$$

where $\Delta = \Omega_c - \Omega_L$. Let us define

$$\delta q = \sqrt{\frac{\hbar}{2m\Omega_M}} (\delta b + \delta b^\dagger) \quad (6.43)$$

$$\delta p = i\sqrt{\frac{\hbar m\Omega_M}{2}} (\delta b^\dagger - \delta b) \quad (6.44)$$

where

$$\Omega_M^2 = \frac{2\hbar\Omega_c^3 N_c}{m(j\pi c)^2} \quad (6.45)$$

and

$$\delta b = \frac{1}{2} \left(\sqrt{\frac{2m\Omega_M}{\hbar}} \delta q + i\sqrt{\frac{2}{\hbar m\Omega_M}} \delta p \right). \quad (6.46)$$

Assuming that $\alpha = \sqrt{N_c}$ is real (which is an arbitrary choice of phase reference), our Hamiltonian can be rewritten as

$$\delta H = \hbar\Delta\delta a^\dagger\delta a + \hbar\Omega_M\delta b^\dagger\delta b + \hbar g_c (\delta a + \delta a^\dagger) (\delta b + \delta b^\dagger). \quad (6.47)$$

Thus, the perturbations of the mirror (δb) now acts like a harmonic mechanical oscillator with a frequency Ω_M that couples to the perturbations of the intra-cavity field (δa) with coupling strength,

$$g_c = \frac{\Omega_c^2}{j\pi c} \sqrt{\frac{\hbar}{2m\Omega_M}} \alpha. \quad (6.48)$$

We see that Eq. (6.47) has the exact same form as Eq. (6.39). There are however, a few differences in how the parameters of the Hamiltonian behave. The first thing to notice is that the frequency for the mirror oscillator Eq. (6.45) and the coupling g_c Eq. (6.48) is dependent on the steady state solutions being a function of N_c and Ω_c . In contrast, in the standard optomechanical system, the frequency of the oscillator is a free parameter. The coupling $g_0\alpha$ in the standard case looks exactly the same as Eq. (6.48) but has a different dependence on steady state solution as Ω_M is a free parameter that is not dependent on N_c and Ω_c . The dependence of parameters on the steady state solutions and the requirement of stability means that we cannot control freely control the detuning. This is an important point of departure from normal optomechanics where the detuning is the most important parameter controlling the behaviour of the system. Not only does it control heating and cooling of the mechanical oscillator, much of the analytical results in Bowen & Milburn²⁰⁰ rely on the simplifying assumption of zero detuning. We are forbidden from this regime for reasons of design and stability, this will complicate our analysis later.

The Langevin equations are now modified to

$$\begin{aligned} \dot{O} = & \frac{1}{i\hbar} [O, \delta H] - [O, \delta a^\dagger] \left(\frac{\kappa}{2}\delta a - \sqrt{\kappa} \delta a_{\text{in}}(t) \right) + \left(\frac{\kappa}{2}\delta a^\dagger - \sqrt{\kappa} \delta a_{\text{in}}^\dagger(t) \right) [O, \delta a] \\ & - [O, \delta b^\dagger] \left(\frac{\Gamma}{2}\delta b - \sqrt{\Gamma} \delta b_{\text{in}}(t) \right) + \left(\frac{\Gamma}{2}\delta b^\dagger - \sqrt{\Gamma} \delta b_{\text{in}}^\dagger(t) \right) [O, \delta b]. \end{aligned} \quad (6.49)$$

* This term is the equivalent of the coherent driving term in the previous section

Dropping the δ s for convenience, this gives the equations of motion

$$\frac{d}{dt} \begin{pmatrix} b \\ b^\dagger \\ a \\ a^\dagger \end{pmatrix} = A \begin{pmatrix} b \\ b^\dagger \\ a \\ a^\dagger \end{pmatrix} + \begin{pmatrix} \sqrt{\Gamma} b_{\text{in}} \\ \sqrt{\Gamma} b_{\text{in}}^\dagger \\ \sqrt{\kappa} a_{\text{in}} \\ \sqrt{\kappa} a_{\text{in}}^\dagger \end{pmatrix}, \quad (6.50)$$

where

$$A = \begin{pmatrix} -\frac{\Gamma}{2} - i\Omega_M & 0 & -ig_c & -ig_c \\ 0 & -\frac{\Gamma}{2} + i\Omega_M & ig_c & ig_c \\ -ig_c & -ig_c & -\frac{\kappa}{2} - i\Delta & 0 \\ ig_c & ig_c & 0 & -\frac{\kappa}{2} + i\Delta \end{pmatrix}. \quad (6.51)$$

In contrast to the steady state parameters, the linearised theory parameters have slightly different parameter dependence. As before, the detuning can be written as $\Delta = \Delta(\tilde{P}, \Omega_L, L, \kappa)$, but the mechanical frequency and coupling have additional dependence on g : $\Omega_M = \Omega_M(\tilde{P}, \Omega_L, L, \kappa, g)$ and $g_c = g_c(\tilde{P}, \Omega_L, L, \kappa, g)$. While we do not indicate dependence on c and \hbar , those being constants of nature, we do indicate a dependence on g as this might be a parameter that could be changed by accelerating the system. I further note that we can easily show that $\Omega_M \propto \sqrt{g}$ and $g_c \propto g^{\frac{1}{4}}$. This can be seen by replacing $N_{\text{in}} = \frac{\tilde{P}mgc}{\hbar\Omega_L}$ in Eqs. (6.26) and (6.27). This shows that $\Omega_c = \Omega_c(\tilde{P}, \Omega_L, j, L, \kappa)$ and $N_c \propto g$. From Eqs. (6.45) and (6.48), we note that $\Omega_M \propto \sqrt{N_c}$ and $g_c \propto \sqrt{\frac{N_c}{\Omega_M}}$. Hence, $\Omega_M \propto \sqrt{g}$ and $g_c \propto g^{\frac{1}{4}}$.

6.8 Numerical study

As we will be considering a table top experiment, for the rest of this chapter, unless otherwise stated, we will set $L = 5$ cm, $g = 9.81$ ms⁻², $c = 3 \times 10^8$ m s⁻¹, $\lambda_L = 1050$ nm. The simplest parameter for the experimentalist to change is the laser power which is encapsulated by changes in dimensionless power. This has the added advantage of also visualising changes in the mass, as the steady state solutions are a function of \tilde{P} and not mass or laser power alone.

6.8.1 Stability

Being blue detuned does not ensure that the linearised equations are stable oscillations around the steady state. Furthermore, our analysis also cannot capture the free fall that happens in the red detuned case as we explicitly consider a steady state to exist. Our stability analysis therefore hinges on the fact that all instability is manifest in the linearised equations as exponential growth in the solutions for $a(t)$ and $b(t)$. As in classical mechanics, exponential growth in an explicitly linearised solution around a steady state implies instability of the steady state solutions. Such exponential growth comes from positive real parts of the eigenvalues of A in Eq. (6.51). While there are general formulas for the roots of a quartic function, they are not especially useful and I have elected to numerically analyse the stability. To do this, we numerically solve Eq. (6.51) for a range of parameters. This leads to four

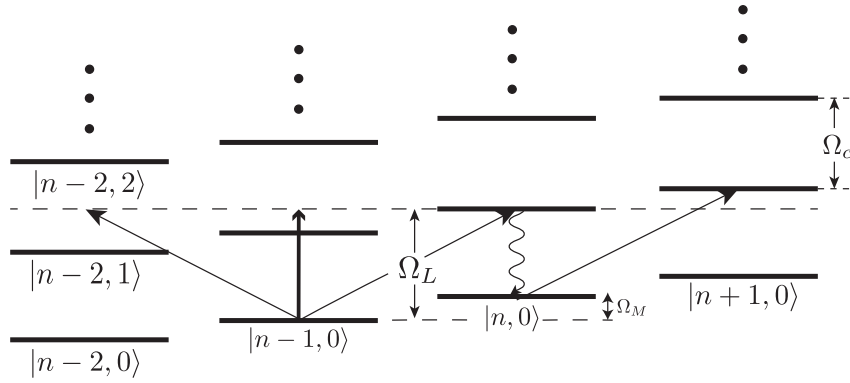


Figure 6.2: Energy level diagram for the floating mirror system. $|n, m\rangle$ is an n -phonon, m -photon state. This figure illustrates the energetically preferred heating of the mirror (increasing phonons) due to blue detuning $\Omega_c < \Omega_L$. Diagram inspired from a corresponding red detuned diagram from Bowen and Milburn²⁰⁰.

eigenvalues, $\lambda_1, \lambda_1^*, \lambda_2, \lambda_2^*$ where two of the eigenvalues are related to the two others by a complex conjugate. The system is only stable if the real parts of the eigenvalues are less than or equal to zero. What we see is that only the blue detuned solution is stable as per our earlier argument.

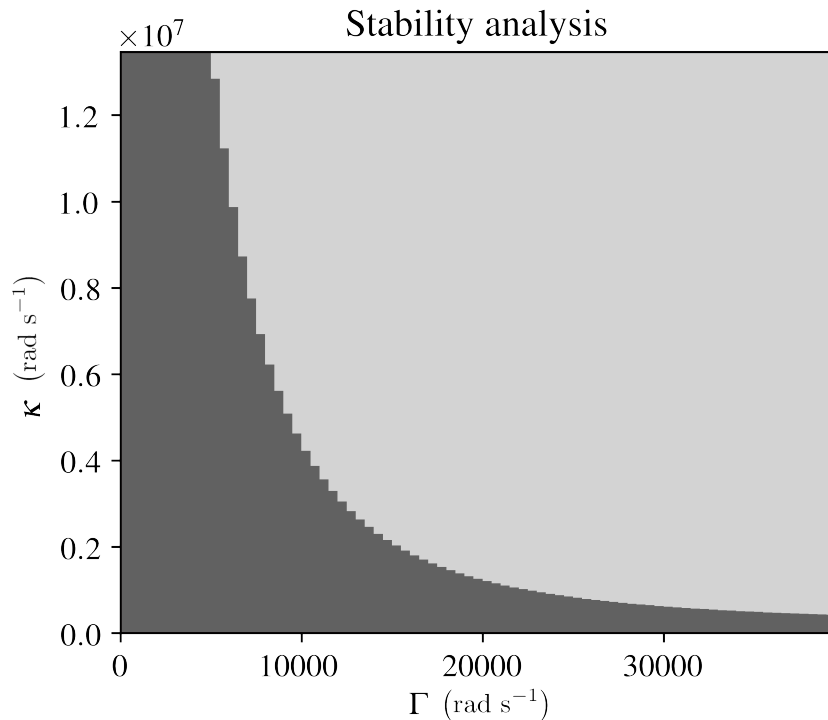


Figure 6.3: Light grey indicates stability while dark grey indicates instability. The dimensionless power is $\tilde{P} = 0.0017$.

Note in Fig. 6.3 that the system is unstable unless there is damping on the mirror, i.e. $\Gamma > 0$ the reason for this is because of the heating we described earlier. For stability we must be blue detuned, but that also means that we are heating up the mirror, which needs to be damped/‘cooled’. As long as $\Gamma \neq 0$, we can trade between κ and Γ to maintain stability. While we can control κ by adjusting the reflectivity, we do not have a similarly straightforward method for tuning the mirror radiative

damping. In principle radiative damping could be controlled by the physical properties of the mirror or by introducing a second cavity above the floating mirror to enhance radiation at particular frequencies.

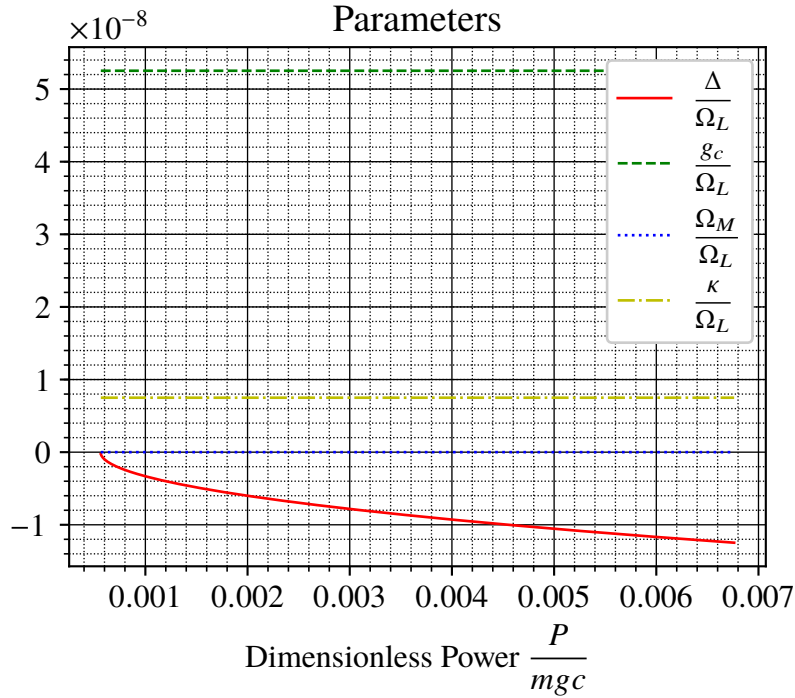


Figure 6.4: Steady state parameters of the floating mirror as a function of dimensionless power. There is some structure in g_c and Ω_M that is obscured by the scale in the figure. $F = 700, \Gamma = 0$.

Before we look at the damping as a function of dimensionless power \tilde{P} , let us qualitatively explore the system by looking at the order of magnitude of the parameters. We see in Fig. 6.4 that for large enough \tilde{P} , $-\Delta \sim g_c$ while in comparison, Ω_M is negligibly small. For $\tilde{P} > 0.001$, we are in a parameter regime where the mirror has a low frequency while it is coupling (g_c) at a high frequency to a high frequency cavity (Δ). This means that over one oscillation of the mirror, the coupling averages to zero. This is far from the case where $\Omega_M = \Delta$ and there is coherent exchange of excitations in Eq. (6.41).

For $\tilde{P} < 0.001$ we have $-\Delta \sim \Omega_M$, so we have one of the conditions for strong coupling. However, this occurs for very small frequencies, such that $-\Delta \ll \kappa$ and the dynamics of the problem are highly damped. Nonetheless, this pseudo-strong coupling regime does manifest itself in the eigenvalues of Eq. (6.51). We note, however, since $\Omega_M \propto \sqrt{g}$ and $g_c \propto g^{\frac{1}{4}}$, if we change g by accelerating the system or putting it on a different planet, we could potentially get to a regime where there is strong coupling.

In comparison, in the standard optomechanical case, g_c is a linearly proportional to \tilde{P} and Ω_M and Δ are independent of \tilde{P} .

6.8.2 Damping

We now plot the real part of the eigenvalues of Eq. (6.51)—which tell us the damping in the eigenstates (linear combinations of mirror and cavity excitations)—as a function of dimensionless power.

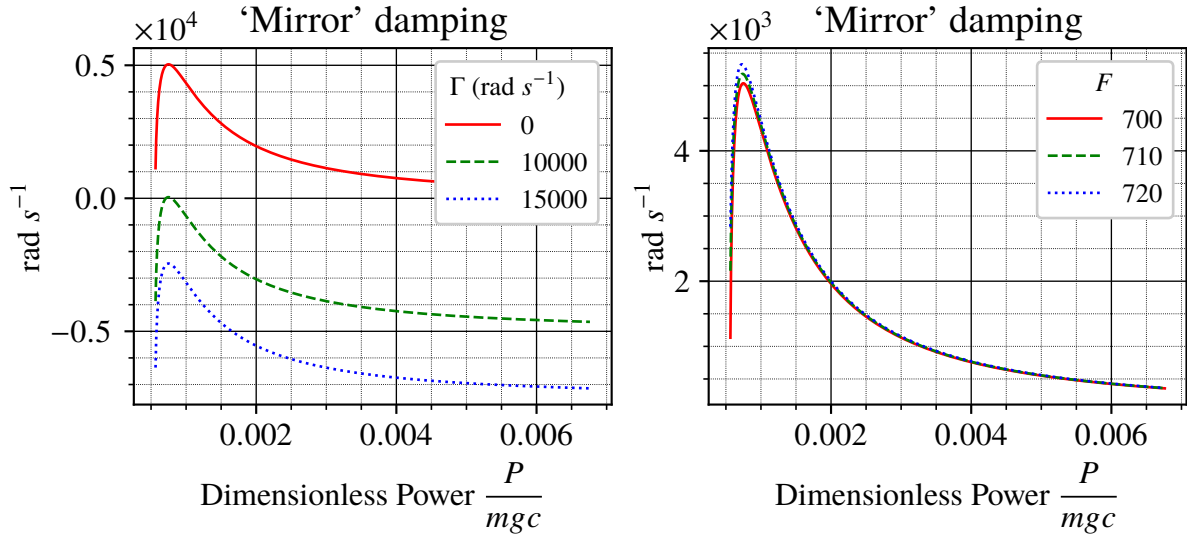
(a) $F = 700$ corresponds to a reflectivity of $\approx 99.1\%$ (b) $\Gamma = 0$

Figure 6.5: The ‘mirror’ damping as a function of dimensionless power.

In Fig. 6.5 we plot the real part of the first eigenvalue ($\Re(\lambda_1)$). If we compare the two figures, we see that λ_1 is dominated by mirror damping for $\tilde{P} > 0.001$. While there is significant contribution from F (equivalently κ) at $\tilde{P} < 0.001$ where we have pseudo-strong coupling, the cavity damping κ is dominant in this regime (Fig. 6.4). For this reason we have labelled the figure as ‘mirror’ damping. Note that the damping is positive for $\Gamma = 0$ which indicates anti-damping, or heating. This is another manifestation of the heating discussed before and confirms our conclusion that there can be no stability without non-zero Γ . We do see an interesting effect where the heating decreases as we go to higher powers. This is because the mirror and the cavity become more off-resonant at higher powers. Furthermore, we also see that the heating increases as the finesse increases which corresponds to a decrease in κ and shift towards stronger coupling. For comparison we plot the imaginary part of the first eigenvalue, that is, the frequency of the ‘mirror’ mode in Fig. 6.6

Fig. 6.7, plots the real part of the second eigenvalue as a function of dimensionless power. As you can see by comparing the two figures, the damping is dominated by cavity damping κ or, equivalently, F , hence we have labelled it ‘cavity’ damping. While it is difficult to see in Fig. 6.7, because there is some contribution from the mirror damping for $\tilde{P} < 0.001$, it is also weakly dependent on Γ .

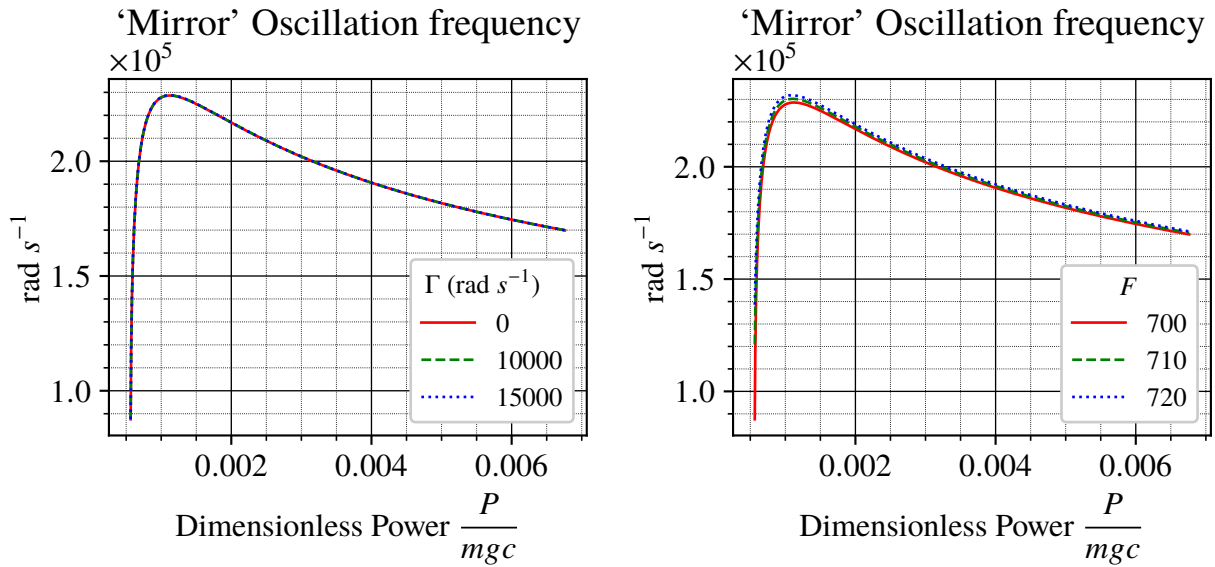
So we see that in the parameters that we have explored do not result in strong coupling. Either the mirror and the cavity are off-resonant for large powers \tilde{P} or we have $-\Delta \sim \Omega_M$ but $-\Delta \ll \kappa$.

6.9 Frequency space solution to linearised equations of motion

We want to find a solution to Eq. (6.50) in the frequency domain. We define our Fourier transforms by

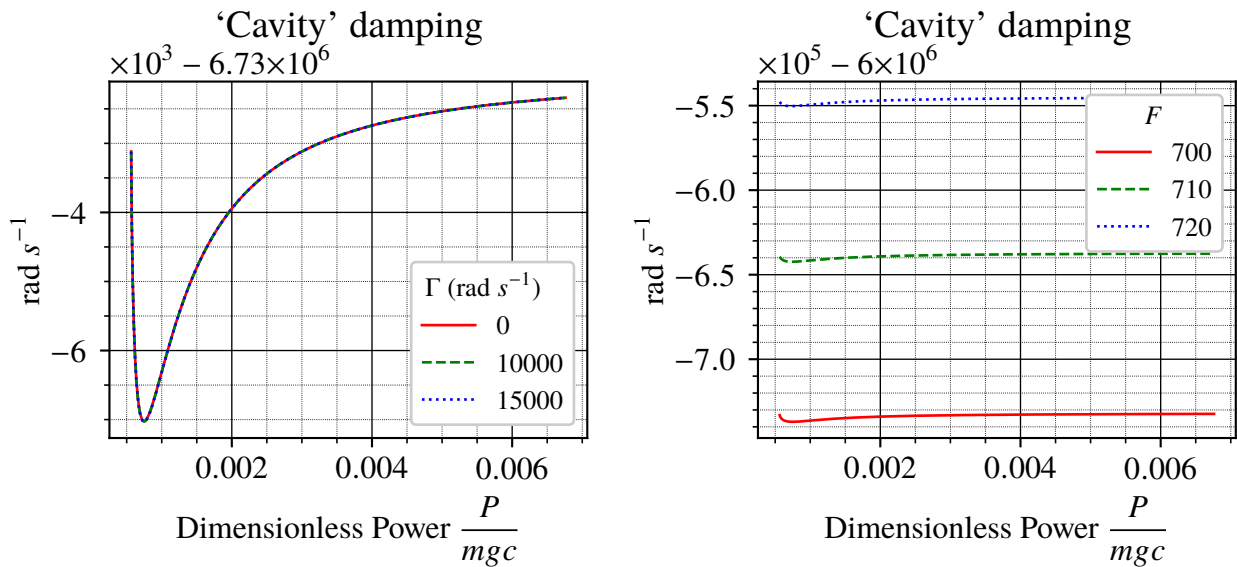
$$a(t) = \int_{-\infty}^{\infty} \frac{d\omega}{\sqrt{2\pi}} e^{-i\omega t} a(\omega), \quad (6.52)$$

$$a^\dagger(t) = \int_{-\infty}^{\infty} \frac{d\omega}{\sqrt{2\pi}} e^{-i\omega t} a^\dagger(\omega), \quad (6.53)$$


 (a) $F = 700$ corresponds to a reflectivity of $\approx 99.1\%$

 (b) $\Gamma = 0$

Figure 6.6: The 'mirror' frequency as a function of dimensionless power.


 (a) $F = 700$ corresponds to a reflectivity of $\approx 99.1\%$

 (b) $\Gamma = 0$

Figure 6.7: The 'cavity' damping as a function of dimensionless power.

and the corresponding reverse Fourier transforms are

$$a(\omega) = \int_{-\infty}^{\infty} \frac{dt}{\sqrt{2\pi}} e^{i\omega t} a(t), \quad (6.54)$$

$$a^\dagger(\omega) = \int_{-\infty}^{\infty} \frac{d\omega}{\sqrt{2\pi}} e^{i\omega t} a^\dagger(t). \quad (6.55)$$

$$(6.56)$$

In contrast, the conjugate of the Fourier transform, $a(\omega)^\dagger$ is defined by

$$a(\omega)^\dagger = \int_{-\infty}^{\infty} \frac{d\omega}{\sqrt{2\pi}} e^{-i\omega t} a^\dagger(t) = a^\dagger(-\omega). \quad (6.57)$$

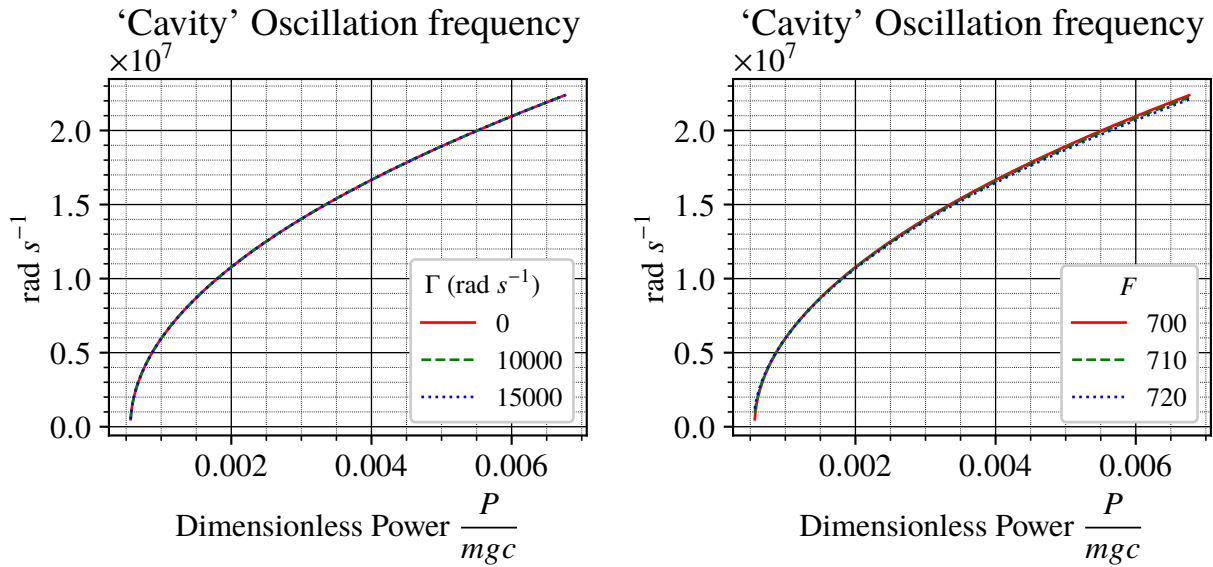
(a) $F = 700$ corresponds to a reflectivity of $\approx 99.1\%$ (b) $\Gamma = 0$

Figure 6.8: The ‘cavity’ frequency as a function of dimensionless power.

Note the placement of the Hermitian conjugate symbol. This is important because of the commutation relations (assuming the usual $[a(t), a^\dagger(t')] = \delta(t - t')$ in free space),

$$[a(\omega), a(\omega')^\dagger] = \delta(\omega - \omega') \quad (6.58)$$

$$[a(\omega), a^\dagger(\omega')] = \delta(\omega + \omega'). \quad (6.59)$$

However, the notation of the Fourier transform of the conjugate is useful in solving the coupled equations but also because, we usually define the quadratures thus,

$$X_\pm(\omega) = \int_{-\infty}^{\infty} \frac{dt}{\sqrt{2\pi}} e^{i\omega t} \frac{1}{\sqrt{2}} (a(t) \pm a(t)^\dagger) \quad (6.60)$$

$$= \frac{1}{\sqrt{2}} (a(\omega) \pm a(-\omega)^\dagger) \quad (6.61)$$

$$= \frac{1}{\sqrt{2}} (a(\omega) \pm a^\dagger(\omega)). \quad (6.62)$$

Note that this quadrature actually probes the upper (ω) and lower ($-\omega$) side-bands. Let us note that the time domain quadratures are Hermitian, from our definition of Fourier transforms, this means that,

$$X_\pm^\dagger(\omega) \equiv \int \frac{dt e^{i\omega t}}{\sqrt{2\pi}} X_\pm^\dagger(t) = \int \frac{dt e^{i\omega t}}{\sqrt{2\pi}} X_\pm(t) = X_\pm(\omega) \quad (6.63)$$

$$X_\pm(\omega)^\dagger \equiv \left(\int \frac{dt e^{i\omega t}}{\sqrt{2\pi}} X_\pm(t) \right)^\dagger = \int \frac{dt e^{-i\omega t}}{\sqrt{2\pi}} X_\pm(t) = X_\pm(-\omega). \quad (6.64)$$

Both notations should be considered when we calculate. For example, when we use the usual expression,

$$n(|\omega|) = \frac{1}{2} [|X_+(\omega)|^2 + |X_-(\omega)|^2 - \delta(0)] \quad (6.65)$$

$$= \frac{1}{2} (a(\omega)^\dagger a(\omega) + a(-\omega)^\dagger a(-\omega)). \quad (6.66)$$

Thus, in the frequency domain, we find that,

$$\begin{pmatrix} b \\ b^\dagger \\ a \\ a^\dagger \end{pmatrix} = T \begin{pmatrix} \sqrt{\Gamma} b_{\text{in}} \\ \sqrt{\Gamma} b_{\text{in}}^\dagger \\ \sqrt{\kappa} a_{\text{in}} \\ \sqrt{\kappa} a_{\text{in}}^\dagger \end{pmatrix} \quad (6.67)$$

, where

$$T = (-i\omega I - A)^{-1}. \quad (6.68)$$

From the input-output relations, we have,

$$a_{\text{out}}(\omega) = a_{\text{in}}(\omega) - \sqrt{\kappa} a(\omega), \quad (6.69)$$

$$b_{\text{out}}(\omega) = b_{\text{in}}(\omega) - \sqrt{\Gamma} b(\omega). \quad (6.70)$$

From our solutions we have,

$$a = T_{31} \sqrt{\Gamma} b_{\text{in}} + T_{32} \sqrt{\Gamma} b_{\text{in}}^\dagger + T_{33} \sqrt{\kappa} a_{\text{in}} + T_{34} \sqrt{\kappa} a_{\text{in}}^\dagger, \quad (6.71)$$

$$a^\dagger = T_{41} \sqrt{\Gamma} b_{\text{in}} + T_{42} \sqrt{\Gamma} b_{\text{in}}^\dagger + T_{43} \sqrt{\kappa} a_{\text{in}} + T_{44} \sqrt{\kappa} a_{\text{in}}^\dagger, \quad (6.72)$$

$$b = T_{11} \sqrt{\Gamma} b_{\text{in}} + T_{12} \sqrt{\Gamma} b_{\text{in}}^\dagger + T_{13} \sqrt{\kappa} a_{\text{in}} + T_{14} \sqrt{\kappa} a_{\text{in}}^\dagger, \quad (6.73)$$

$$b^\dagger = T_{21} \sqrt{\Gamma} b_{\text{in}} + T_{22} \sqrt{\Gamma} b_{\text{in}}^\dagger + T_{23} \sqrt{\kappa} a_{\text{in}} + T_{24} \sqrt{\kappa} a_{\text{in}}^\dagger \quad (6.74)$$

and we define our quadratures to be $X_a^\pm = \frac{1}{\sqrt{2}} (a \pm a^\dagger)$ which gives us the quadrature for the cavity

$$X_{a_{\text{out}}}^\pm = \frac{1}{\sqrt{2}} \left\{ - (T_{31} \pm T_{41}) \sqrt{\kappa\Gamma} b_{\text{in}} - (T_{32} \pm T_{42}) \sqrt{\kappa\Gamma} b_{\text{in}}^\dagger - [\kappa(T_{33} \pm T_{43}) - 1] a_{\text{in}} - [\kappa(T_{34} \pm T_{44}) \mp 1] a_{\text{in}}^\dagger \right\}, \quad (6.75)$$

and the quadrature for the mirror

$$X_{b_{\text{out}}}^\pm = \frac{1}{\sqrt{2}} \left\{ - [\Gamma(T_{11} \pm T_{21}) - 1] b_{\text{in}} - [\Gamma(T_{12} \pm T_{22}) \mp 1] b_{\text{in}}^\dagger - (T_{13} \pm T_{23}) \sqrt{\kappa\Gamma} a_{\text{in}} - (T_{14} \pm T_{24}) \sqrt{\kappa\Gamma} a_{\text{in}}^\dagger \right\}. \quad (6.76)$$

Let us change notation to keep track of the frequency dependence of our operators. Note that because $X^\pm(\omega) = a(\omega) \pm a(-\omega)^\dagger = \pm X^\pm(-\omega)^\dagger$. This motivates us to define the following functions,

$$B_{a_{\text{out}}}^\pm(\omega) = - (T_{31}(\omega) \pm T_{41}(\omega)) \sqrt{\kappa\Gamma}, \quad (6.77)$$

$$\pm B_{a_{\text{out}}}^\pm(-\omega)^* = - (T_{32}(\omega) \pm T_{42}(\omega)) \sqrt{\kappa\Gamma}, \quad (6.78)$$

$$A_{a_{\text{out}}}^\pm(\omega) = - [\kappa(T_{33}(\omega) \pm T_{43}(\omega)) - 1], \quad (6.79)$$

$$\pm A_{a_{\text{out}}}^\pm(-\omega)^* = - [\kappa(T_{34}(\omega) \pm T_{44}(\omega)) \mp 1], \quad (6.80)$$

$$B_{b_{\text{out}}}^\pm(\omega) = - [\Gamma(T_{11} \pm T_{21}) - 1], \quad (6.81)$$

$$\pm B_{b_{\text{out}}}^\pm(-\omega)^* = - [\Gamma(T_{12} \pm T_{22}) \mp 1], \quad (6.82)$$

$$A_{b_{\text{out}}}^\pm(\omega) = -\sqrt{\kappa\Gamma} (T_{13}(\omega) \pm T_{23}(\omega)), \quad (6.83)$$

$$\pm A_{b_{\text{out}}}^\pm(-\omega)^* = -\sqrt{\kappa\Gamma} (T_{14}(\omega) \pm T_{24}(\omega)). \quad (6.84)$$

The quadratures may now be defined as

$$X_{a_{\text{out}}}^{\pm} = \frac{1}{\sqrt{2}} \left\{ B_{a_{\text{out}}}^{\pm}(\omega) b_{\text{in}}(\omega) \pm B_{a_{\text{out}}}^{\pm}(-\omega)^* b_{\text{in}}(-\omega)^{\dagger} + A_{a_{\text{out}}}^{\pm}(\omega) a_{\text{in}}(\omega) \pm A_{a_{\text{out}}}^{\pm}(-\omega)^* a_{\text{in}}(-\omega)^{\dagger} \right\}, \quad (6.85a)$$

$$X_{b_{\text{out}}}^{\pm} = \frac{1}{\sqrt{2}} \left\{ B_{b_{\text{out}}}^{\pm}(\omega) b_{\text{in}}(\omega) \pm B_{b_{\text{out}}}^{\pm}(-\omega)^* b_{\text{in}}(-\omega)^{\dagger} + A_{b_{\text{out}}}^{\pm}(\omega) a_{\text{in}}(\omega) \pm A_{b_{\text{out}}}^{\pm}(-\omega)^* a_{\text{in}}(-\omega)^{\dagger} \right\}. \quad (6.85b)$$

Let us first introduce the notation $X_{i_{\text{out}}}^{\alpha}$, where $\alpha, \beta, \dots \in \{+, -\}$ indicate + or – and let $i, j, \dots \in \{a, b\}$ indicate the mode. Then we can combine the above equations into

$$X_{i_{\text{out}}}^{\alpha} = \frac{1}{\sqrt{2}} \left\{ B_{i_{\text{out}}}^{\alpha}(\omega) b_{\text{in}}(\omega) + \alpha B_{i_{\text{out}}}^{\alpha}(-\omega)^* b_{\text{in}}(-\omega)^{\dagger} + A_{i_{\text{out}}}^{\alpha}(\omega) a_{\text{in}}(\omega) + \alpha A_{i_{\text{out}}}^{\alpha}(-\omega)^* a_{\text{in}}(-\omega)^{\dagger} \right\}. \quad (6.86)$$

6.9.1 Covariance matrix

It is known that Hamiltonians that are bilinear in creation and annihilation operators preserve and create Gaussian states.^{203,204} Gaussian states are quantum states that are described by a Gaussian Wigner functions which are fully characterised by their covariance matrices. As our linearised Hamiltonian is bilinear in operators, we will characterise our system using covariance matrices. Covariance matrices are usually defined from the quadrature operators, however the frequency quadratures that we have used so far are only Hermitian when there is zero detuning. In the presence of detuning they are not directly measurable as they are not Hermitian. If we use homodyne detection, what we measure is the time domain quadratures $X_{i_{\text{out}}}^{\alpha}(t)$. For this section we will suppress the *out* subscript for legibility. To get the proper frequency quadratures, we mix-down the time domain quadratures with a cosine²⁰⁵ to get the symmetric, Hermitian quadrature,

$$\begin{aligned} X_i^{\alpha,C}(\omega) &= \sqrt{\frac{2}{\pi}} \int dt \frac{\cos(\omega t)}{\sqrt{2}} X_i^{\alpha}(t) \\ &= \frac{1}{\sqrt{2}} (X_i^{\alpha}(\omega) + X_i^{\alpha}(-\omega)), \end{aligned} \quad (6.87)$$

and the accompanying sine mix-down gives the antisymmetric, Hermitian quadrature,

$$\begin{aligned} X_i^{\alpha,S}(\omega) &= \sqrt{\frac{2}{\pi}} \int dt \frac{\sin(\omega t)}{\sqrt{2}} X_i^{\alpha}(t) \\ &= \frac{-i}{\sqrt{2}} (X_i^{\alpha}(\omega) - X_i^{\alpha}(-\omega)), \end{aligned} \quad (6.88)$$

which we naturally combine into one expression,

$$X_i^{\alpha,\aleph}(\omega) = \frac{1}{\sqrt{2}} (\aleph X_i^{\alpha}(\omega) + X_i^{\alpha}(-\omega)), \quad (6.89)$$

where $\aleph = \pm 1$, $X_i^{\alpha,C} = X_i^{\alpha,+}$ and $X_i^{\alpha,S} = iX_i^{\alpha,-}$. We now define the Q and P quadratures to be

$$Q_i^C(\omega) = \frac{1}{\sqrt{2}} (X_i^+(\omega) + X_i^+(-\omega)), \quad (6.90)$$

$$\begin{aligned} P_i^C(\omega) &= \frac{1}{\sqrt{2}} (-iX_i^-(\omega) + (-i)X_i^-(-\omega)) \\ &= \frac{-i}{\sqrt{2}} (X_i^-(\omega) + X_i^-(-\omega)), \end{aligned} \quad (6.91)$$

$$Q_i^S(\omega) = \frac{-i}{\sqrt{2}} (X_i^+(\omega) - X_i^+(-\omega)), \quad (6.92)$$

$$\begin{aligned} P_i^S(\omega) &= \frac{-i}{\sqrt{2}} (-iX_i^-(\omega) - (-i)X_i^-(-\omega)) \\ &= \frac{-1}{\sqrt{2}} (X_i^-(\omega) - X_i^-(-\omega)). \end{aligned} \quad (6.93)$$

To simplify notation, we define the vector

$$R_i(\omega) = \begin{pmatrix} Q_b^C(\omega) \\ P_b^C(\omega) \\ Q_b^S(\omega) \\ P_b^S(\omega) \\ Q_a^C(\omega) \\ P_a^C(\omega) \\ Q_a^S(\omega) \\ P_a^S(\omega) \end{pmatrix}, \quad (6.94)$$

from which we define the (real and symmetric) covariance matrix

$$\sigma_{ij}(\omega) = \frac{1}{2} \langle R_i(\omega)R_j(\omega) + R_j(\omega)R_i(\omega) \rangle - \langle R_i(\omega) \rangle \langle R_j(\omega) \rangle. \quad (6.95)$$

Let us now consider the case of an input vacuum. Note from the structure of Eq. (6.85), that $\langle 0 | R_i | 0 \rangle = 0$. Because the matrix is symmetric, the general form of the covariance matrix is given by,

$$\sigma = \begin{pmatrix} \sigma_b & \sigma_{\text{upper}} \\ \sigma_{\text{upper}}^T & \sigma_a \end{pmatrix}, \quad (6.96)$$

where σ_b and σ_a are symmetric submatrices of the mirror and cavity whose cross-correlations are given by σ_{upper} . The submatrix for b is,

$$\sigma_b = \left\langle 0 \left| \begin{pmatrix} Q_b^C Q_b^C & \frac{1}{2} (Q_b^C P_b^C + P_b^C Q_b^C) & \frac{1}{2} (Q_b^C Q_b^S + Q_b^S Q_b^C) & \frac{1}{2} (Q_b^C P_b^S + P_b^S Q_b^C) \\ & P_b^C P_b^C & \frac{1}{2} (P_b^C Q_b^S + Q_b^S P_b^C) & \frac{1}{2} (P_b^C P_b^S + P_b^S P_b^C) \\ & & Q_b^S Q_b^S & \frac{1}{2} (Q_b^S P_b^S + P_b^S Q_b^S) \\ & & & P_b^S P_b^S \end{pmatrix} \right| 0 \right\rangle, \quad (6.97)$$

while the submatrix for a is,

$$\sigma_a = \left\langle 0 \left[\begin{array}{cccc} Q_a^C Q_a^C & \frac{1}{2} (Q_a^C P_a^C + P_a^C Q_a^C) & \frac{1}{2} (Q_a^C Q_a^S + Q_a^S Q_a^C) & \frac{1}{2} (Q_a^C P_a^S + P_a^S Q_a^C) \\ & P_a^C P_a^C & \frac{1}{2} (P_a^C Q_a^S + Q_a^S P_a^C) & \frac{1}{2} (P_a^C P_a^S + P_a^S P_a^C) \\ & & Q_a^S Q_a^S & \frac{1}{2} (Q_a^S P_a^S + P_a^S Q_a^S) \\ & & & P_a^S P_a^S \end{array} \right] 0 \right\rangle. \quad (6.98)$$

The upper right matrix is

$$\sigma_{\text{upper}} = \frac{1}{2} \left\langle 0 \left[\begin{array}{cccc} Q_b^C Q_a^C + Q_a^C Q_b^C & Q_b^C P_a^C + P_a^C Q_b^C & Q_b^C Q_a^S + Q_a^S Q_b^C & Q_b^C P_a^S + P_a^S Q_b^C \\ P_b^C Q_a^C + Q_a^C P_b^C & P_b^C P_a^C + P_a^C P_b^C & P_b^C Q_a^S + Q_a^S P_b^C & P_b^C P_a^S + P_a^S P_b^C \\ Q_b^S Q_a^C + Q_a^C Q_b^S & Q_b^S P_a^C + P_a^C Q_b^S & Q_b^S Q_a^S + Q_a^S Q_b^S & Q_b^S P_a^S + P_a^S Q_b^S \\ P_b^S Q_a^C + Q_a^C P_b^S & P_b^S P_a^C + P_a^C P_b^S & P_b^S Q_a^S + Q_a^S P_b^S & P_b^S P_a^S + P_a^S P_b^S \end{array} \right] 0 \right\rangle. \quad (6.99)$$

Let us construct the matrix elements step by step. Firstly, the matrix elements are—modulo factors of $-i$ —composed of,

$$\begin{aligned} & \frac{1}{2} \left\langle X_{i_{\text{out}}}^{\alpha, \aleph}(\omega) X_{j_{\text{out}}}^{\beta, \beth}(\omega) + X_{j_{\text{out}}}^{\beta, \beth}(\omega) X_{i_{\text{out}}}^{\alpha, \aleph}(\omega) \right\rangle \quad (6.100) \\ &= \frac{1}{2} \left\{ \begin{array}{l} \beth \frac{1}{2} \left\langle X_{i_{\text{out}}}^{\alpha}(\omega) X_{j_{\text{out}}}^{\beta}(-\omega) + X_{j_{\text{out}}}^{\beta}(\omega) X_{i_{\text{out}}}^{\alpha}(-\omega) \right\rangle + \beth \frac{1}{2} \left\langle X_{i_{\text{out}}}^{\alpha}(-\omega) X_{j_{\text{out}}}^{\beta}(\omega) + X_{j_{\text{out}}}^{\beta}(-\omega) X_{i_{\text{out}}}^{\alpha}(\omega) \right\rangle, \quad \aleph = \beth \\ \beth \frac{1}{2} \left\langle -X_{i_{\text{out}}}^{\alpha}(\omega) X_{j_{\text{out}}}^{\beta}(-\omega) + X_{j_{\text{out}}}^{\beta}(\omega) X_{i_{\text{out}}}^{\alpha}(-\omega) \right\rangle + \beth \frac{1}{2} \left\langle X_{i_{\text{out}}}^{\alpha}(-\omega) X_{j_{\text{out}}}^{\beta}(\omega) - X_{j_{\text{out}}}^{\beta}(-\omega) X_{i_{\text{out}}}^{\alpha}(\omega) \right\rangle, \quad \aleph = -\beth \end{array} \right\}. \quad (6.101) \end{aligned}$$

We can now calculate the brackets inside, where we find that,

$$\frac{1}{2} \left\langle X_{i_{\text{out}}}^{\alpha}(\omega) X_{j_{\text{out}}}^{\beta}(-\omega) + X_{j_{\text{out}}}^{\beta}(\omega) X_{i_{\text{out}}}^{\alpha}(-\omega) \right\rangle = \frac{1}{2} \left\{ \begin{array}{l} \beta \aleph \left[B_{i_{\text{out}}}^{\alpha}(\omega) B_{j_{\text{out}}}^{\beta}(\omega)^* + A_{i_{\text{out}}}^{\alpha}(\omega) A_{j_{\text{out}}}^{\beta}(\omega)^* \right] \delta(0), \quad \alpha = \beta \\ i \beta \beth \left[B_{i_{\text{out}}}^{\alpha}(\omega) B_{j_{\text{out}}}^{\beta}(\omega)^* + A_{i_{\text{out}}}^{\alpha}(\omega) A_{j_{\text{out}}}^{\beta}(\omega)^* \right] \delta(0), \quad \alpha = -\beta \end{array} \right\}, \quad (6.102)$$

$$\frac{1}{2} \left\langle X_{i_{\text{out}}}^{\alpha}(\omega) X_{j_{\text{out}}}^{\beta}(-\omega) - X_{j_{\text{out}}}^{\beta}(\omega) X_{i_{\text{out}}}^{\alpha}(-\omega) \right\rangle = \frac{1}{2} \left\{ \begin{array}{l} i \beta \beth \left[B_{i_{\text{out}}}^{\alpha}(\omega) B_{j_{\text{out}}}^{\beta}(\omega)^* + A_{i_{\text{out}}}^{\alpha}(\omega) A_{j_{\text{out}}}^{\beta}(\omega)^* \right] \delta(0), \quad \alpha = \beta \\ \beta \aleph \left[B_{i_{\text{out}}}^{\alpha}(\omega) B_{j_{\text{out}}}^{\beta}(\omega)^* + A_{i_{\text{out}}}^{\alpha}(\omega) A_{j_{\text{out}}}^{\beta}(\omega)^* \right] \delta(0), \quad \alpha = -\beta \end{array} \right\}. \quad (6.103)$$

This then gives us,

$$\begin{aligned} & \frac{1}{2} \left\langle X_{i_{\text{out}}}^{\alpha, \aleph}(\omega) X_{j_{\text{out}}}^{\beta, \beth}(\omega) + X_{j_{\text{out}}}^{\beta, \beth}(\omega) X_{i_{\text{out}}}^{\alpha, \aleph}(\omega) \right\rangle \quad (6.104) \\ &= \frac{1}{4} \left\{ \begin{array}{l} \left\{ \beta \beth \aleph \left[B_{i_{\text{out}}}^{\alpha}(\omega) B_{j_{\text{out}}}^{\beta}(\omega)^* + A_{i_{\text{out}}}^{\alpha}(\omega) A_{j_{\text{out}}}^{\beta}(\omega)^* \right] + (\omega \rightarrow -\omega) \right\} \delta(0), \quad \alpha = \beta, \aleph = \beth \\ \left\{ i \beta \beth \beth \left[B_{i_{\text{out}}}^{\alpha}(\omega) B_{j_{\text{out}}}^{\beta}(\omega)^* + A_{i_{\text{out}}}^{\alpha}(\omega) A_{j_{\text{out}}}^{\beta}(\omega)^* \right] + (\omega \rightarrow -\omega) \right\} \delta(0), \quad \alpha = -\beta, \aleph = \beth \\ \left\{ -i \beta \beth \beth \left[B_{i_{\text{out}}}^{\alpha}(\omega) B_{j_{\text{out}}}^{\beta}(\omega)^* + A_{i_{\text{out}}}^{\alpha}(\omega) A_{j_{\text{out}}}^{\beta}(\omega)^* \right] - (\omega \rightarrow -\omega) \right\} \delta(0), \quad \alpha = \beta, \aleph = -\beth \\ \left\{ -\beta \beth \aleph \left[B_{i_{\text{out}}}^{\alpha}(\omega) B_{j_{\text{out}}}^{\beta}(\omega)^* + A_{i_{\text{out}}}^{\alpha}(\omega) A_{j_{\text{out}}}^{\beta}(\omega)^* \right] - (\omega \rightarrow -\omega) \right\} \delta(0), \quad \alpha = -\beta, \aleph = -\beth \end{array} \right\}. \quad (6.105) \end{aligned}$$

$(\omega \rightarrow -\omega)$ is taken to mean the previous term with ω replaced with $-\omega$. The actual matrix elements are listed in Chapter 8 with the factors of $-i$ restored.

6.9.2 Entropy of entanglement

For a bipartite pure Gaussian state, the Rényi-2 entropy of entanglement is defined as,²⁰⁴

$$\mathcal{E}_2(\sigma_{a:b}) = \frac{1}{2} \log_2 [\det(2\sigma_a)] \quad (6.106)$$

$$= \frac{1}{2} \log_2 [\det(2\sigma_b)]. \quad (6.107)$$

This characterises the entanglement between the two subsystems, a and b . Using our expressions for an input vacuum state, we can see the entanglement in Fig. 6.9. As we noted before, at larger \tilde{P} the coupling strength decreases; this is manifested in the decreasing entanglement at larger \tilde{P} . Furthermore, we see the maximum entanglement is at the peaks which are located at mirror frequency and decreases away from it. While we have strong entanglement between the mirror and the cavity, our simple theory does not provide for an easy way to access the mirror output. This could be remedied through additional interactions with the mirror. Earlier we suggested that a second cavity could be used to enhance mirror damping at certain frequencies, such a system has been shown to transfer the entanglement between the cavity and mirror to entanglement between two cavities²⁰⁶. We also note the result of Vanner *et al.* where mechanical state tomography has been shown to ‘cool-by-measurement’.²⁰⁷ Thus, accessing the mechanical state through additional interaction with the mirror could be useful in both controlling mirror damping and transfer of entanglement.

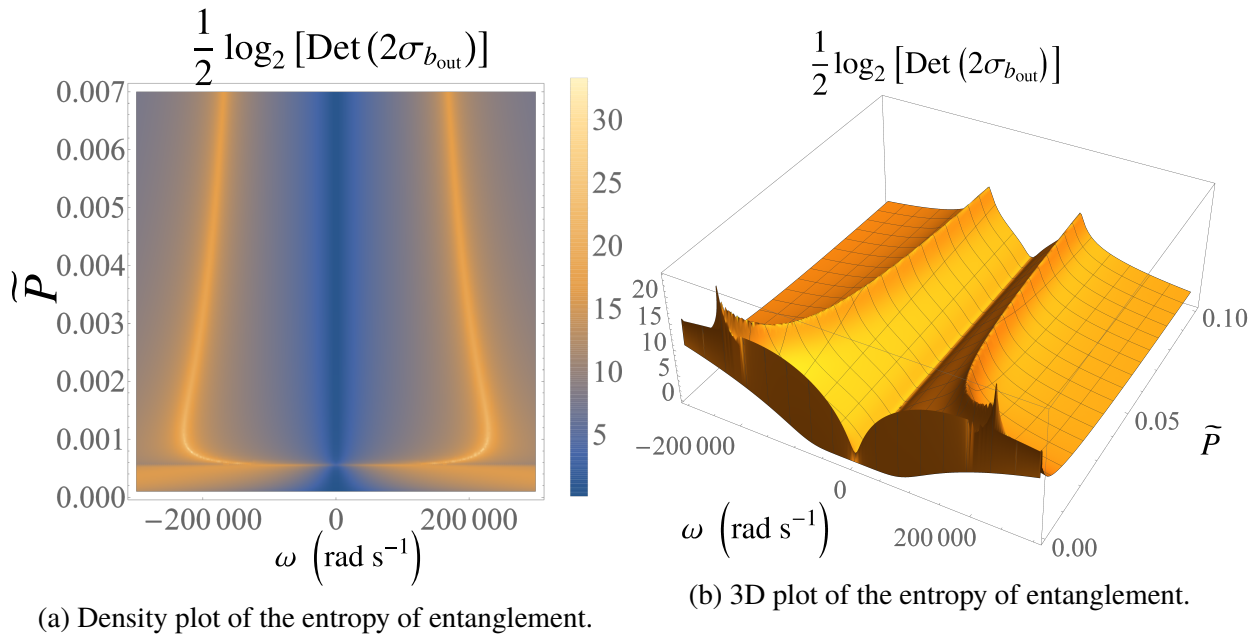


Figure 6.9: Entropy of entanglement between the mirror and the cavity. Note that there is a change in behaviour at $\tilde{P} \approx 0.0005$ where the steady state solution goes from imaginary to real. Around this point there are also sharp spikes which are due to numerical error. The peaks of the entanglement at a given \tilde{P} is at the mirror oscillation frequency. ω is in units of radians per second, $\kappa = 1.35 \times 10^7 \text{ rad s}^{-1}$ and $\Gamma = 1 \times 10^4 \text{ rad s}^{-1}$

6.9.3 Diagonalisation of the Covariance matrix

For a given ω and steady state parameters, the submatrices σ_a and σ_b have off-diagonal terms. These off-diagonal terms indicate coupling between the symmetric and antisymmetric (cosine and sine) side-bands. While it is difficult to derive an closed-form expression, the two matrices can be independently diagonalised leading to two independent side-bands formed from linear combinations of the symmetric and antisymmetric side-bands. This leads to a covariance matrix with diagonal blocks $\sigma_{b,D}$ and $\sigma_{a,D}$ given by,

$$\begin{pmatrix} \sigma_{b,D} & \sigma_{\text{upper},D} \\ \sigma_{\text{upper},D}^T & \sigma_{a,D} \end{pmatrix} = \begin{pmatrix} U^{-1} & 0 \\ 0 & V^{-1} \end{pmatrix} \begin{pmatrix} \sigma_b & \sigma_{\text{upper}} \\ \sigma_{\text{upper}}^T & \sigma_a \end{pmatrix} \begin{pmatrix} U & 0 \\ 0 & V \end{pmatrix} \quad (6.108)$$

$$= \begin{pmatrix} U^{-1} & 0 \\ 0 & V^{-1} \end{pmatrix} \begin{pmatrix} \sigma_b U & \sigma_{\text{upper}} V \\ \sigma_{\text{upper}}^T U & \sigma_a V \end{pmatrix} \quad (6.109)$$

$$= \begin{pmatrix} U^T \sigma_b U & U^T \sigma_{\text{upper}} V \\ V^T \sigma_{\text{upper}}^T U & V^T \sigma_a V \end{pmatrix} \quad (6.110)$$

With $\sigma_{b,D}$ ($\sigma_{a,D}$) being the diagonal matrix of eigenvalues of σ_b (σ_a) and U (V) consisting of columns that are the right eigenvectors of σ_b (σ_a). Because the covariance matrix is real and symmetric the inverse of U and V is equal to their transpose, i.e., $U^{-1} = U^T$ and $V^{-1} = V^T$. In this basis, the entropy is simply the logarithm of the product of the eigenvalues of σ_b or σ_a , $\mathcal{E}_2 = \frac{1}{2} \log_2 [\det (2\sigma_{a,D})]$.

6.9.4 Quadrature variances

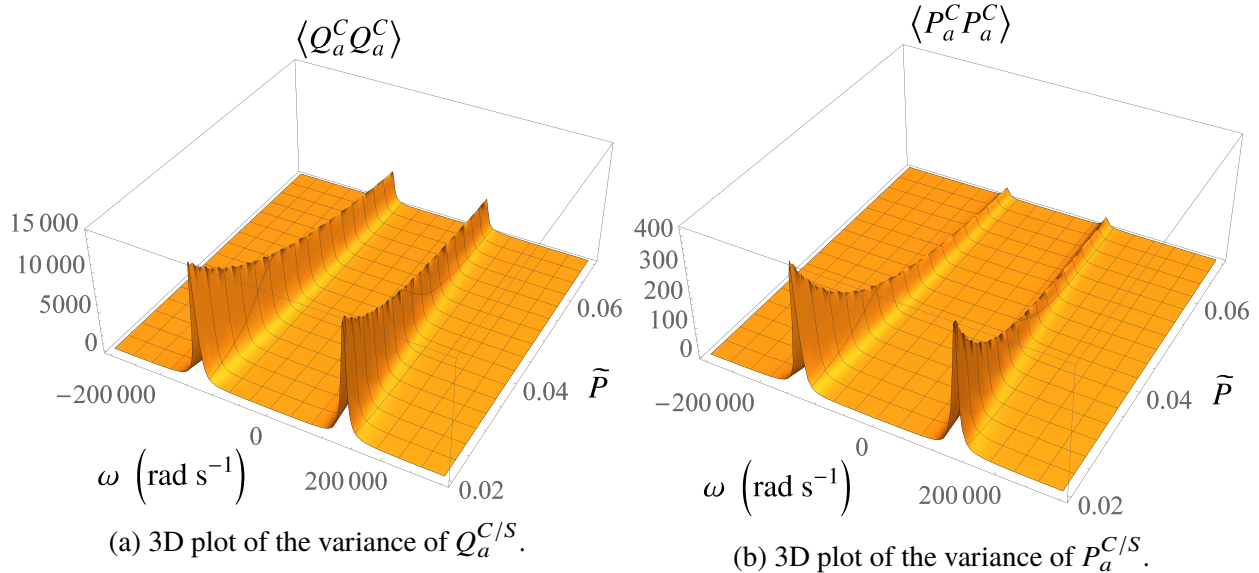


Figure 6.10: 3D plots of the variance of cavity Q and P quadratures with $\Gamma = 1 \times 10^4 \text{ rad s}^{-1}$, $F = 700$. The central location of the peaks is of a similar order to the mirror frequency.

Now let us consider the variance of the quadrature variances of a and b . We do not need to consider the cosine and sine quadratures separately, as can be seen in Chapter 8, the variance of the cosine quadratures are the same as the sine quadratures. While not as obvious as the entropy of entanglement

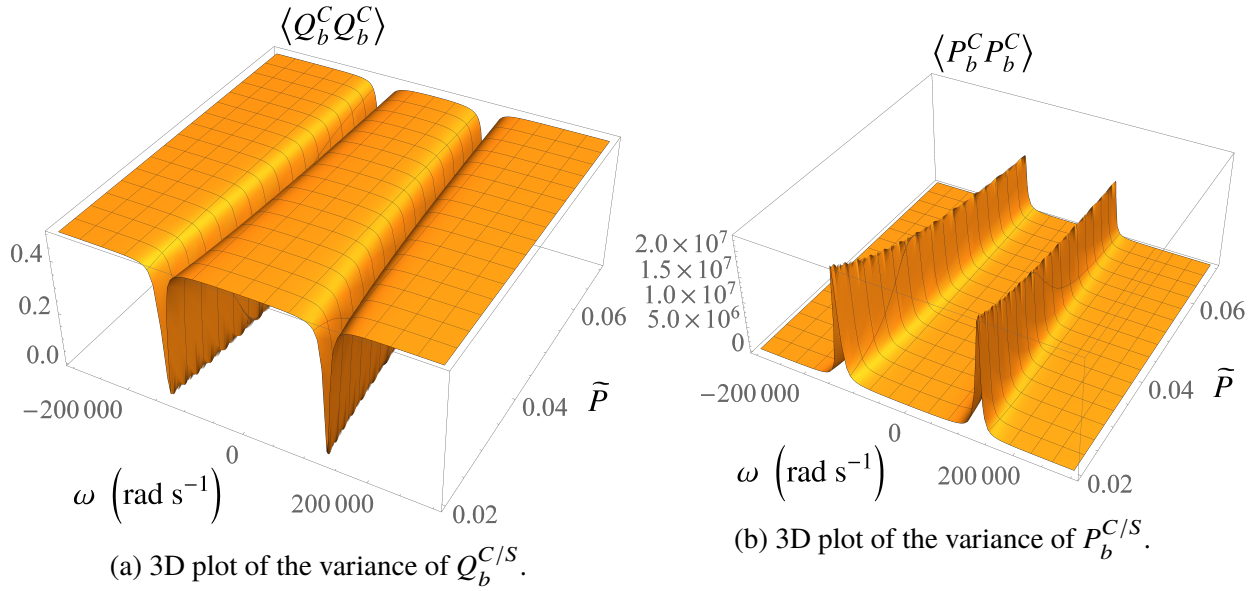


Figure 6.11: 3D plots of the variance of mirror Q and P quadratures with $\Gamma = 1 \times 10^4 \text{ rad s}^{-1}$, $F = 700$. The central location of the peaks is of a similar order to the mirror frequency.

plot, as was the case before, the central location of the peaks in Fig. 6.10 are approximately located at the mirror frequency for a given \tilde{P} and its behaviour tracks the mirror frequency's behaviour. In Fig. 6.11 (a) and (b), we can see that the variance of Q_b dip below $\frac{1}{2}$ which indicates squeezing. The maximum squeezing is seen at some linear combination of the cosine and sine quadratures and given by the eigenvalues of σ_b . However, for our particular parameters, the detuning is small so while there is some coupling between the cosine and sine quadratures, there is less than 0.1% difference between our plots and the maximum squeezing.

6.10 Conclusion

In the floating mirror, the acceleration of the mirror is due to a quantum source. From the close relationship between gravity and acceleration, the study of the noise in the acceleration could conceivably be understood as quantum noise from a quantum source of gravity. This was initially the motivation of the research, but the understanding of the dynamics of the floating mirror proved to be more complex than initially thought. We have seen how the floating mirror behaves for some table top experimental parameters. The mirror is only stable for blue detuning which necessitates damping on the mirror. For accelerations/gravity on earth $g = 9.8 \text{ ms}^{-2}$, the cavity frequency is much larger than the mirror's frequency ($-\Delta \gg \Omega_M$) which means 'weak' coupling between the cavity and the mirror. We also found that $\Omega_M \propto \sqrt{g}$, consequently, with large accelerations, it is possible that we could reach a regime where $\Delta \sim \Omega_M$. Despite the 'weak' coupling, we found entanglement between the output of the mirror and cavity and characterised it with the Rényi entropy of entanglement, finding maximal entanglement at the frequency of the mirror. Our study of the quadratures of the system found the presence of squeezing in the output position of the mirror.

Chapter 7

Conclusion

Through our exploration of Quantum Field Theory on Curved Spacetime, we have seen how particles and vacuums are fundamentally observer dependent and how an infinite number quantisation methods leads to the problem of unitary inequivalence. While QFTCS has predicted novel physics such as Hawking radiation and helped illuminate the essential and inessential features of QFT, it has left us with more questions than answers. The black hole information paradox is a clear case of the limitation of our analysis, not only do we lack a formalised theory of backreaction—being often treated in an ad-hoc manner—the very formalism of modes implies a global structure and our lack of a unique vacuum state to understand the dynamics greatly hinders any quantitative prediction. While the problem remains unresolved, the arguments from the firewall and unitary inequivalence prompted us to propose that an initial vacuum state around a collapsing black hole evolves into a modified Boulware vacuum state. In Chapter 3, we see that our black hole field theory has firewall as predicted by Almheiri *et al.* In addition to addressing the information paradox that the firewall argument makes, we have seen how the proposal also avoids the problem of unitary inequivalence between the Boulware vacuum and Unruh vacuum. While we characterised our firewall, we note that it results from a UV cutoff representing our ignorance of high energy physics. It is entirely possible that a future theory of quantum fields around black holes might significantly modify Hawking radiation and remove the need for a firewall entirely.

Despite how the firewall illuminates the limitations, of QFTCS, it continues to surprise. While the creation of particles by black holes and colliding gravitational waves has long been known to cause particle creation, none of them have been so far observable. In Chapter 4, we saw how particles cannot be created by linear gravitational waves on flat spacetime through a Feynman diagrams and summarised our discovery that quasi-normal modes (damped gravitational waves around a ringing black hole) couple with a scalar field to produce particles for a faraway observer. The quasi-normal modes act as a multi-mode squeezing Hamiltonian which act on an arbitrary initial state to produce particles. With the detection of merging black holes, our discovery could have major implications for the current detection and understanding of black hole mergers.

While there is physics left to discover within QFTCS, it is clear that we must go beyond it. The nascent attempts by string theory and loop quantum gravity to build a new foundation have proven to be

conceptually intriguing, but computationally intractable. The field of relativistic quantum information has taken another tack, building on and extending from the solid foundations of quantum physics and general relativity. In particular, the process matrix formalism attempts to extend quantum physics to processes with no causal order. Unfortunately, we found in Chapter 5 that it seems to be incomplete. The problem of localisation in QFT means concepts such as closed labs and ‘particles’ need to be carefully defined in QFT and that leads to a major difficulty in constructing background-independent definition of causal relations in QFT.

We investigated the dynamics of a laser-floated mirror in Chapter 6, looking for an analogy between a quantum source of acceleration and gravity. The initial idea was to consider a quantum source of gravity and thereby study feedback effects that QFTCS excludes. The physics of the floating mirror proved to be richer than previously expected. The mirror is only stable when it is blue detuned: that is when the steady state solution is such that the coupling between the mirror and the cavity leads to ‘heating’ of the mirror. While according to optomechanical theory, the different frequency of the mirror and the cavity would imply weak coupling, under realistic laboratory parameters we find there is significant (14-20 ebit) entanglement between the output of the mirror and the cavity.

In seeking to use QFTCS to understand the deeper principles required in a quantum theory of gravity, we have seen the limits of QFTCS. It is clear that QFTCS must be extended and modified to understand these problems. Whether by extending quantum physics to no situations with no causal order or by studying the floating mirrors, relativistic quantum information holds great promise in introducing new techniques and perspectives to understanding the intersection of quantum physics and gravity.

Bibliography

1. Ho, C. M., Su, D., Mann, R. B. & Ralph, T. C. Black hole field theory with a firewall in two spacetime dimensions. *Physical Review D* **94**, 081502 (Oct. 10, 2016).
2. Su, D., Ho, C. M., Mann, R. B. & Ralph, T. C. Black hole squeezers. *Physical Review D* **96**, 065017 (Sept. 25, 2017).
3. Ho, C. T. M., Costa, F., Giarmatzi, C. & Ralph, T. C. Violation of a causal inequality in a spacetime with definite causal order. *arXiv:1804.05498 [quant-ph]*. arXiv: 1804.05498 (Apr. 16, 2018).
4. Su, D., Ho, C. T. M., Mann, R. B. & Ralph, T. C. Quantum circuit model for non-inertial objects: a uniformly accelerated mirror. *New Journal of Physics* **19**, 063017 (2017).
5. Kiefer, C. *Quantum Gravity* 2nd edition. 376 pp. (Oxford University Press, Oxford : New York, Apr. 19, 2007).
6. Griffiths, D. *Introduction to Elementary Particles* (Wiley-VCH, Weinheim, 2005).
7. Peskin, M. E. & Schroeder, D. V. *An Introduction to Quantum Field Theory* (Addison-Wesley Publishing Company, Reading, 1995).
8. Arnowitt, R., Deser, S. & Misner, C. W. Republication of: The dynamics of general relativity. *General Relativity and Gravitation* **40**, 1997–2027 (Aug. 8, 2008).
9. *Approaches to Quantum Gravity: Toward a New Understanding of Space, Time and Matter* (ed Oriti, D.) (Cambridge University Press, Cambridge, England ; New York, Apr. 27, 2009). 604 pp.
10. Zee, A. *Einstein Gravity in a Nutshell* 889 pp. (Princeton University Press, May 5, 2013).
11. Birrell, N. D. & Davies, P. C. W. *Quantum Fields in Curved Space* (Cambridge University Press, 1984).
12. Fröhlich, J. *Non-Perturbative Quantum Field Theory: Mathematical Aspects and Applications* (WORLD SCIENTIFIC, Apr. 1992).
13. Benedetti, D., Machado, P. F. & Saueressig, F. Asymptotic safety in higher-derivative gravity. *Modern Physics Letters A* **24**, 2233–2241 (Sept. 14, 2009).

14. Lauscher, O. & Reuter, M. Fractal spacetime structure in asymptotically safe gravity. *Journal of High Energy Physics* **2005**, 050 (Oct. 1, 2005).
15. Douglas, M. R. The statistics of string/M theory vacua. *Journal of High Energy Physics* **2003**, 046 (May 1, 2003).
16. Rovelli, C. A dialog on quantum gravity. *International Journal of Modern Physics D* **12**, 1509–1528 (Oct. 1, 2003).
17. Nicolai, H., Peeters, K. & Zamaklar, M. Loop quantum gravity: an outside view. *Classical and Quantum Gravity* **22**, R193 (Oct. 7, 2005).
18. Fulling, S. A. Nonuniqueness of Canonical Field Quantization in Riemannian Space-Time. *Physical Review D* **7**, 2850–2862 (May 15, 1973).
19. Davies, P. C. W. Scalar production in Schwarzschild and Rindler metrics. *Journal of Physics A: Mathematical and General* **8**, 609 (Apr. 1, 1975).
20. Hawking, S. W. Particle creation by black holes. *Communications in Mathematical Physics* **43**, 199–220 (Aug. 1975).
21. Gerlach, U. H. The mechanism of blackbody radiation from an incipient black hole. *Physical Review D* **14**, 1479–1508 (Sept. 15, 1976).
22. Unruh, W. G. Notes on black-hole evaporation. *Physical Review D* **14**, 870–892 (Aug. 1976).
23. Ford, L. H. Quantum Field Theory in Curved Spacetime. *arXiv:gr-qc/9707062*. arXiv: gr-qc/9707062 (July 30, 1997).
24. 't Hooft, G. The black hole interpretation of string theory. *Nuclear Physics B* **335**, 138–154 (Apr. 30, 1990).
25. Banks, T., O’Loughlin, M. & Strominger, A. Black hole remnants and the information puzzle. *Physical Review D* **47**, 4476–4482 (May 1993).
26. Hawking, S. W. Information loss in black holes. *Physical Review D* **72**, 084013 (Oct. 2005).
27. Mann, R. B. & Ralph, T. C. Relativistic quantum information. *Classical and Quantum Gravity* **29**, 220301 (2012).
28. Oreshkov, O., Costa, F. & Brukner, Č. Quantum correlations with no causal order. *Nature Communications* **3**, 1092 (Oct. 2012).
29. Olson, S. J. & Ralph, T. C. Entanglement between the Future and the Past in the Quantum Vacuum. *Physical Review Letters* **106**, 110404 (Mar. 2011).
30. Pozas-Kerstjens, A. & Martín-Martínez, E. Harvesting correlations from the quantum vacuum. *Physical Review D* **92**, 064042 (Sept. 24, 2015).
31. Knetter, C. G. Effective Lagrangians with higher derivatives and equations of motion. *Physical Review D* **49**, 6709–6719 (June 15, 1994).

32. Simon, J. Z. Higher-derivative Lagrangians, nonlocality, problems, and solutions. *Physical Review D* **41**, 3720–3733 (June 15, 1990).
33. Hollands, S. & Wald, R. M. Quantum fields in curved spacetime. *Physics Reports. Quantum fields in curved spacetime* **574**, 1–35 (Apr. 2015).
34. Nicolis, A., Rattazzi, R. & Trincherini, E. Galileon as a local modification of gravity. *Physical Review D* **79**, 064036 (Mar. 31, 2009).
35. Clifton, T., Ferreira, P. G., Padilla, A. & Skordis, C. Modified gravity and cosmology. *Physics Reports. Modified Gravity and Cosmology* **513**, 1–189 (Mar. 2012).
36. Kobayashi, T., Yamaguchi, M. & Yokoyama, J. Generalized G-Inflation —Inflation with the Most General Second-Order Field Equations—. *Progress of Theoretical Physics* **126**, 511–529 (Sept. 1, 2011).
37. Pagani, E., Tecchiolli, G. & Zerbini, S. On the problem of stability for higher-order derivative Lagrangian systems. *Letters in Mathematical Physics* **14**, 311–319 (Nov. 1, 1987).
38. Srednicki, M. *Quantum Field Theory* 1st edition. 660 pp. (Cambridge University Press, Cambridge ; New York, Feb. 5, 2007).
39. Takagi, S. Vacuum Noise and Stress Induced by Uniform Acceleration Hawking-Unruh Effect in Rindler Manifold of Arbitrary Dimension. *Progress of Theoretical Physics Supplement* **88**, 1–142 (Mar. 1986).
40. Carroll, S. M. *Spacetime and Geometry: An Introduction to General Relativity* (Addison-Wesley Longman, Incorporated, 2004).
41. Parker, L. & Toms, D. *Quantum Field Theory in Curved Spacetime: Quantized Fields and Gravity* 1 edition (Cambridge University Press, Cambridge, UK ; New York, Sept. 2009).
42. Sakurai, J. J & Napolitano, J. J. *Modern quantum mechanics* (Pearson Education, 2009).
43. Schwinger, J. The Theory of Quantized Fields. I. *Physical Review* **82**, 914–927 (June 15, 1951).
44. Zee, A. *Quantum field theory in a nutshell* (Princeton Univ. Press, Princeton, 2003).
45. Wald, R. M. *Quantum Field Theory in Curved Spacetime and Black Hole Thermodynamics* 1st edition (University of Chicago Press, Chicago, Nov. 1994).
46. Jacobson, T. Introduction to Quantum Fields in Curved Spacetime and the Hawking Effect. *arXiv:gr-qc/0308048*. arXiv: gr-qc/0308048 (Aug. 14, 2003).
47. Brout, R., Massar, S., Parentani, R. & Spindel, P. A primer for black hole quantum physics. *Physics Reports* **260**, 329–446 (Sept. 1995).
48. Wald, R. M. *General Relativity* (University of Chicago Press, June 1984).
49. Fuentes-Schuller, I. & Mann, R. B. Alice Falls into a Black Hole: Entanglement in Noninertial Frames. *Physical Review Letters* **95**, 120404 (Sept. 2005).

50. Isham, C. J. *Modern Differential Geometry for Physicists* 2nd edition. 289 pp. (World Scientific Pub Co Inc, Singapore ; River Edge, N.J, June 1999).
51. Crispino, L. C. B., Higuchi, A. & Matsas, G. E. A. The Unruh effect and its applications. *Rev. Mod. Phys.* **80**, 787–838 (2008).
52. Hodgkinson, L., Louko, J. & Ottewill, A. C. Static detectors and circular-geodesic detectors on the Schwarzschild black hole. *Physical Review D* **89**, 104002 (May 1, 2014).
53. Misner, C. W., Thorne, K. S. & Wheeler, J. A. *Gravitation* 1st edition (W. H. Freeman, San Francisco, Sept. 1973).
54. Vázquez, M. R., del Rey, M., Westman, H. & León, J. Local quanta, unitary inequivalence, and vacuum entanglement. *Annals of Physics* **351**, 112–137 (Dec. 2014).
55. Wallace, D. In Defence of Naiveté: The Conceptual Status of Lagrangian Quantum Field Theory. *Synthese* **151**, 33–80 (July 2006).
56. Itzykson, C. & Zuber, J.-B. *Quantum Field Theory* Google-Books-ID: 4MwsAwAAQBAJ. 756 pp. (Courier Corporation, Feb. 24, 2006).
57. Fredenhagen, K. & Rejzner, K. Perturbative algebraic quantum field theory. *arXiv:1208.1428 [hep-th, physics:math-ph]*. arXiv: 1208.1428 (Aug. 7, 2012).
58. Hawking, S. W. Breakdown of predictability in gravitational collapse. *Physical Review D* **14**, 2460–2473 (Nov. 1976).
59. Banks, T., Susskind, L. & Peskin, M. E. Difficulties for the evolution of pure states into mixed states. *Nuclear Physics B* **244**, 125–134 (Sept. 24, 1984).
60. Unruh, W. G. & Wald, R. M. Evolution laws taking pure states to mixed states in quantum field theory. *Physical Review D* **52**, 2176–2182 (Aug. 15, 1995).
61. Susskind, L., Thorlacius, L. & Uglum, J. The stretched horizon and black hole complementarity. *Physical Review D* **48**, 3743–3761 (Oct. 1993).
62. Hossenfelder, S. & Smolin, L. Conservative solutions to the black hole information problem. *Physical Review D* **81**, 064009 (Mar. 2010).
63. Aharonov, Y., Casher, A. & Nussinov, S. The unitarity puzzle and Planck mass stable particles. *Physics Letters B* **191**, 51–55 (June 1987).
64. Mann, R. B. in *Black Holes: Thermodynamics, Information, and Firewalls* 1–95 (Springer International Publishing, 2015).
65. Braunstein, S. L. & Pati, A. K. Quantum Information Cannot Be Completely Hidden in Correlations: Implications for the Black-Hole Information Paradox. *Physical Review Letters* **98**, 080502 (Feb. 2007).
66. Almheiri, A., Marolf, D., Polchinski, J. & Sully, J. Black holes: complementarity or firewalls? *Journal of High Energy Physics* **2013**, 1–20 (Feb. 2013).

67. Braunstein, S. L., Pirandola, S. & Życzkowski, K. Better Late than Never: Information Retrieval from Black Holes. *Physical Review Letters* **110**, 101301 (Mar. 2013).
68. Bousso, R. Complementarity Is Not Enough. *Physical Review D* **87**, 124023 (June 20, 2013).
69. Susskind, L. The Transfer of Entanglement: The Case for Firewalls. *arXiv:1210.2098 [gr-qc, physics:hep-th, physics:quant-ph]*. arXiv: 1210.2098 (Oct. 7, 2012).
70. Kim, W. & Son, E. J. Freely Falling Observer and Black Hole Radiation. *Modern Physics Letters A* **29**, 1450052 (Apr. 10, 2014).
71. Berenstein, D. & Dzienkowski, E. Numerical Evidence for Firewalls. *arXiv:1311.1168 [hep-th]*. arXiv: 1311.1168 (Nov. 21, 2013).
72. Mathur, S. D. The fuzzball proposal for black holes: an elementary review. *Fortschritte der Physik* **53**, 793–827 (July 15, 2005).
73. Mathur, S. D. & Turton, D. The flaw in the firewall argument. *Nuclear Physics B* **884**, 566–611 (July 1, 2014).
74. Avery, S. G., Chowdhury, B. D. & Puhm, A. Unitarity and fuzzball complementarity: Alice fuzzes but may not even know it! *Journal of High Energy Physics* **2013**, 12 (Sept. 3, 2013).
75. Golovnev, A. Smooth horizons and quantum ripples. *The European Physical Journal C* **75**, 185 (May 2015).
76. Freivogel, B. Energy and Information Near Black Hole Horizons. *Journal of Cosmology and Astroparticle Physics* **2014**, 041–041 (July 21, 2014).
77. Maldacena, J. & Susskind, L. Cool horizons for entangled black holes. *Fortschritte der Physik* **61**, 781–811 (Sept. 2, 2013).
78. Giddings, S. B. Nonviolent nonlocality. *Physical Review D* **88**, 064023 (Sept. 10, 2013).
79. Iizuka, N. & Terashima, S. Brick Walls for Black Holes in AdS/CFT. *arXiv:1307.5933 [gr-qc, physics:hep-th]*. arXiv: 1307.5933 (Dec. 31, 2014).
80. Pullin, J. Matters of Gravity, the newsletter of the Topical Group in Gravitation of APS. *arXiv:gr-qc/0510021*. arXiv: gr-qc/0510021 (Oct. 5, 2005).
81. Ashtekar, A. & Bojowald, M. Black hole evaporation: a paradigm. *Classical and Quantum Gravity* **22**, 3349 (Aug. 21, 2005).
82. Ashtekar, A. & Bojowald, M. Quantum geometry and the Schwarzschild singularity. *Classical and Quantum Gravity* **23**, 391 (2006).
83. Jacobson, T. Boundary Unitarity and the Black Hole information paradox. *International Journal of Modern Physics D* **22**, 1342002 (July 5, 2013).
84. Preskill, J. Do Black Holes Destroy Information? *arXiv:hep-th/9209058*. arXiv: hep-th/9209058 (Sept. 16, 1992).

85. Bena, I., El-Showk, S. & Vercoocke, B. *Black Holes in String Theory in Black Objects in Supergravity* (ed Bellucci, S.) (Springer International Publishing, 2013), 59–178.
86. Perez, A. Black holes in loop quantum gravity. *Reports on Progress in Physics* **80**, 126901 (Oct. 2017).
87. Bekenstein, J. D. Black Holes and Entropy. *Physical Review D* **7**, 2333–2346 (Apr. 15, 1973).
88. Rovelli, C. Notes for a brief history of quantum gravity. *arXiv:gr-qc/0006061*. arXiv: gr-qc/0006061 (June 16, 2000).
89. Mathur, S. D. in *The Universe: Visions and Perspectives* (eds Dadhich, N. & Kembhavi, A.) 201–212 (Springer Netherlands, Dordrecht, 2000). doi:10.1007/978-94-011-4050-8_19.
90. Singleton, D. & Wilburn, S. Hawking Radiation, Unruh Radiation, and the Equivalence Principle. *Physical Review Letters* **107**, 081102 (Aug. 2011).
91. Candelas, P. Vacuum polarization in Schwarzschild spacetime. *Physical Review D* **21**, 2185–2202 (Apr. 1980).
92. Israel, W. in *Current Trends in Relativistic Astrophysics* (eds Fernández-Jambrina, D. L. & González-Romero, P. L. M.) *Lecture Notes in Physics* 617, 15–49 (Springer Berlin Heidelberg, 2003).
93. Boulware, D. G. Quantum field theory in Schwarzschild and Rindler spaces. *Physical Review D* **11**, 1404–1423 (Mar. 1975).
94. Thorne, K. S., Price, R. H. & MacDonald, D. A. *Black Holes: The Membrane Paradigm* (Yale University Press, 1986).
95. Wipf, A. in *Black Holes: Theory and Observation* (eds Hehl, F. W., Kiefer, C. & Metzler, R. J. K.) *Lecture Notes in Physics* 514, 385–415 (Springer Berlin Heidelberg, 1998).
96. Fabbri, A., Farese, S., Navarro-Salas, J., Olmo, G. J. & Sanchis-Alepuz, H. Semiclassical zero-temperature corrections to Schwarzschild spacetime and holography. *Physical Review D* **73**, 104023 (May 2006).
97. Celotti, A., Miller, J. C. & Sciamia, D. W. Astrophysical evidence for the existence of black holes. *Classical and Quantum Gravity* **16**, A3 (Dec. 1999).
98. Christensen, S. M. & Fulling, S. A. Trace anomalies and the Hawking effect. *Physical Review D* **15**, 2088–2104 (Apr. 1977).
99. Wald, R. M. On particle creation by black holes. *Communications in Mathematical Physics* **45**, 9–34 (Feb. 1975).
100. Kempf, A., Chatwin-Davies, A. & Martin, R. T. W. A fully covariant information-theoretic ultraviolet cutoff for scalar fields in expanding Friedmann Robertson Walker spacetimes. *Journal of Mathematical Physics* **54**, 022301 (Feb. 1, 2013).
101. Juárez-Aubry, B. A. & Louko, J. Onset and decay of the 1 + 1 Hawking–Unruh effect: what the derivative-coupling detector saw. *Classical and Quantum Gravity* **31**, 245007 (2014).

102. Crispino, L. C. B., Higuchi, A. & Matsas, G. E. A. Comment on “Hawking Radiation, Unruh Radiation, and the Equivalence Principle”. *Physical Review Letters* **108**, 049001 (Jan. 2012).
103. Singleton, D. & Wilburn, S. Singleton and Wilburn Reply: *Physical Review Letters* **108**, 049002 (Jan. 2012).
104. Louko, J. & Satz, A. Transition rate of the Unruh–DeWitt detector in curved spacetime. *Classical and Quantum Gravity* **25**, 055012 (Mar. 2008).
105. Louko, J. Unruh-DeWitt detector response across a Rindler firewall is finite. *J. High Energy Phys.* **2014**, 1–22 (Sept. 2014).
106. Martín-Martínez, E. & Louko, J. (1+1)D Calculation Provides Evidence that Quantum Entanglement Survives a Firewall. *Physical Review Letters* **115**, 031301 (July 14, 2015).
107. Sakharov, A. D. The Initial Stage of an Expanding Universe and the Appearance of a Nonuniform Distribution of Matter. *Soviet Journal of Experimental and Theoretical Physics* **22**, 241 (Jan. 1, 1966).
108. Mukhanov, V. F., Feldman, H. A. & Brandenberger, R. H. Theory of cosmological perturbations. *Physics Reports* **215**, 203–333 (June 1, 1992).
109. Zeldovich, \. Y. B. & Starobinsky, A. A. Particle production and vacuum polarization in an anisotropic gravitational field. *Sov. Phys. JETP* **34**, 1159–1166 (1972).
110. Misner, C. W. Interpretation of Gravitational-Wave Observations. *Physical Review Letters* **28**, 994–997 (Apr. 10, 1972).
111. Unruh, W. G. Second quantization in the Kerr metric. *Physical Review D* **10**, 3194–3205 (Nov. 15, 1974).
112. LIGO Scientific Collaboration and Virgo Collaboration *et al.* Observation of Gravitational Waves from a Binary Black Hole Merger. *Physical Review Letters* **116**, 061102 (Feb. 11, 2016).
113. Gibbons, G. W. Vacuum polarization and the spontaneous loss of charge by black holes. *Communications in Mathematical Physics* **44**, 245–264 (Oct. 1, 1975).
114. Deser, S. Plane waves do not polarize the vacuum. *Journal of Physics A: Mathematical and General* **8**, 1972 (1975).
115. Garriga, J. & Verdaguer, E. Scattering of quantum particles by gravitational plane waves. *Physical Review D* **43**, 391–401 (Jan. 15, 1991).
116. Sorge, F. Do gravitational waves create particles? *Classical and Quantum Gravity* **17**, 4655 (2000).
117. Schwinger, J. On Gauge Invariance and Vacuum Polarization. *Physical Review* **82**, 664–679 (June 1, 1951).
118. Arcos, H., Krssak, M. & Pereira, J. G. Exploring Higher-Order Gravitational Waves. *arXiv:1504.07817 [gr-qc, physics:hep-th]*. arXiv: 1504.07817 (Apr. 29, 2015).

119. Aldrovandi, R., Pereira, J. G., Rocha, R. d. & Vu, K. H. Nonlinear Gravitational Waves: Their Form and Effects. *International Journal of Theoretical Physics* **49**, 549–563 (Jan. 5, 2010).
120. Yurtsever, U. Quantum field theory in a colliding plane-wave background. *Physical Review D* **40**, 360–371 (July 15, 1989).
121. Dorca, M. & Verdaguer, E. Quantum fields interacting with colliding plane waves: particle creation. *Nuclear Physics B* **403**, 770–808 (1993).
122. Hubbell, J. H. Electron positron pair production by photons: A historical overview. *Radiation Physics and Chemistry* **75**, 614–623 (June 1, 2006).
123. LIGO Scientific Collaboration and Virgo Collaboration *et al.* GW151226: Observation of Gravitational Waves from a 22-Solar-Mass Binary Black Hole Coalescence. *Physical Review Letters* **116**, 241103 (June 15, 2016).
124. LIGO Scientific and Virgo Collaboration *et al.* GW170104: Observation of a 50-Solar-Mass Binary Black Hole Coalescence at Redshift 0.2. *Physical Review Letters* **118**, 221101 (June 1, 2017).
125. Lehner, L. Numerical relativity: a review. *Classical and Quantum Gravity* **18**, R25 (2001).
126. Price, R. H. Nonspherical Perturbations of Relativistic Gravitational Collapse. II. Integer-Spin, Zero-Rest-Mass Fields. *Physical Review D* **5**, 2439–2454 (May 15, 1972).
127. Chan, J. S. F. & Mann, R. B. Scalar wave falloff in asymptotically anti-de Sitter backgrounds. *Physical Review D* **55**, 7546–7562 (June 15, 1997).
128. Nollert, H.-P. Quasinormal modes: the characteristic ‘sound’ of black holes and neutron stars. *Classical and Quantum Gravity* **16**, R159 (1999).
129. Kokkotas, K. D. & Schmidt, B. G. Quasi-Normal Modes of Stars and Black Holes. *Living Reviews in Relativity* **2**, 2 (Sept. 16, 1999).
130. Berti, E., Cardoso, V. & Starinets, A. O. Quasinormal modes of black holes and black branes. *Classical and Quantum Gravity* **26**, 163001 (2009).
131. Konoplya, R. A. & Zhidenko, A. Quasinormal modes of black holes: From astrophysics to string theory. *Reviews of Modern Physics* **83**, 793–836 (July 11, 2011).
132. Regge, T. & Wheeler, J. A. Stability of a Schwarzschild Singularity. *Physical Review* **108**, 1063–1069 (Nov. 15, 1957).
133. Zerilli, F. J. Gravitational Field of a Particle Falling in a Schwarzschild Geometry Analyzed in Tensor Harmonics. *Physical Review D* **2**, 2141–2160 (Nov. 15, 1970).
134. Pankow, C., Chase, E. A., Coughlin, S., Zevin, M. & Kalogera, V. Improvements in Gravitational-wave Sky Localization with Expanded Networks of Interferometers. *The Astrophysical Journal Letters* **854**, L25 (2018).

135. LIGO Scientific Collaboration and Virgo Collaboration *et al.* GW170817: Observation of Gravitational Waves from a Binary Neutron Star Inspiral. *Physical Review Letters* **119**, 161101 (Oct. 16, 2017).
136. Hardy, L. Towards quantum gravity: a framework for probabilistic theories with non-fixed causal structure. *Journal of Physics A: Mathematical and Theoretical* **40**, 3081–3099 (Mar. 2007).
137. Brukner, Č. Quantum causality. *Nature Physics* **10**, 259–263 (Apr. 2014).
138. Chiribella, G., D’Ariano, G. M., Perinotti, P. & Valiron, B. Quantum computations without definite causal structure. *Physical Review A* **88**, 022318 (Aug. 2013).
139. Chiribella, G. Perfect discrimination of no-signalling channels via quantum superposition of causal structures. *Physical Review A* **86**, 040301 (Oct. 2012).
140. Araújo, M., Costa, F. & Brukner, Č. Computational Advantage from Quantum-Controlled Ordering of Gates. *Physical Review Letters* **113**, 250402 (Dec. 2014).
141. Feix, A., Araújo, M. & Brukner, Č. Quantum superposition of the order of parties as a communication resource. *Physical Review A* **92**, 052326 (Nov. 2015).
142. Guérin, P. A., Feix, A., Araújo, M. & Brukner, Č. Exponential Communication Complexity Advantage from Quantum Superposition of the Direction of Communication. *Physical Review Letters* **117**, 100502 (Sept. 2016).
143. Ebler, D., Salek, S. & Chiribella, G. Enhanced Communication with the Assistance of Indefinite Causal Order. *Physical Review Letters* **120**, 120502 (Mar. 22, 2018).
144. Procopio, L. M. *et al.* Experimental superposition of orders of quantum gates. *Nature Communications* **6**, 7913 (2015).
145. Rubino, G. *et al.* Experimental verification of an indefinite causal order. *Science Advances* **3**, e1602589 (2017).
146. Rubino, G. *et al.* Experimental Entanglement of Temporal Orders. *arXiv:1712.06884 [quant-ph]*. arXiv: 1712.06884 (Dec. 19, 2017).
147. Goswami, K. *et al.* Indefinite Causal Order in a Quantum Switch. *arXiv:1803.04302 [quant-ph]* (Mar. 2018).
148. Oreshkov, O. & Giarmatzi, C. Causal and causally separable processes. *New Journal of Physics* **18**, 093020 (Sept. 2016).
149. Branciard, C., Araújo, M., Feix, A., Costa, F. & Brukner, Č. The simplest causal inequalities and their violation. *New Journal of Physics* **18**, 013008 (2016).
150. Abbott, A. A., Giarmatzi, C., Costa, F. & Branciard, C. Multipartite causal correlations: Polytopes and inequalities. *Physical Review A* **94**, 032131 (Sept. 2016).
151. Oreshkov, O. On the whereabouts of the local operations in physical realizations of quantum processes with indefinite causal order. *arXiv:1801.07594 [quant-ph]*. arXiv: 1801.07594 (Jan. 23, 2018).

152. Feynman, R. P., Hibbs, A. R. & Styer, D. F. *Quantum mechanics and path integrals* (Dover Publications, Mineola, N.Y., 2010).
153. De la Madrid, R. Localization of non-relativistic particles. *arXiv:quant-ph/0601161*. arXiv:quant-ph/0601161 (Jan. 23, 2006).
154. Schroer, B. Localization and the interface between quantum mechanics, quantum field theory and quantum gravity I: The two antagonistic localizations and their asymptotic compatibility. *Studies in History and Philosophy of Science Part B: Studies in History and Philosophy of Modern Physics* **41**, 104–127 (May 2010).
155. Balachandran, A. P. Localization in quantum field theory. *International Journal of Geometric Methods in Modern Physics* **14**, 1740008 (May 11, 2017).
156. Knight, J. M. Strict Localization in Quantum Field Theory. *Journal of Mathematical Physics* **2**, 459–471 (1961).
157. Licht, A. L. Strict Localization. *Journal of Mathematical Physics* **4**, 1443–1447 (1963).
158. Rohde, P. P., Maurerer, W. & Silberhorn, C. Spectral structure and decompositions of optical states, and their applications. *New Journal of Physics* **9**, 91 (2007).
159. Eckstein, A., Brecht, B. & Silberhorn, C. A quantum pulse gate based on spectrally engineered sum frequency generation. *Optics Express* **19**, 13770 (July 2011).
160. Yanagisawa, M. & Hope, J. J. Self-consistent input-output formulation of quantum feedback. *Physical Review A* **82**, 062109 (Dec. 10, 2010).
161. Combes, J., Kerckhoff, J. & Sarovar, M. The SLH framework for modeling quantum input-output networks. *Advances in Physics: X* **2**, 784–888 (2017).
162. Hegerfeldt, G. C. Remark on causality and particle localization. *Physical Review D* **10**, 3320–3321 (Nov. 1974).
163. Summers, S. J. & Werner, R. The vacuum violates Bell’s inequalities. *Physics Letters A* **110**, 257–259 (1985).
164. Bombelli, L., Koul, R. K., Lee, J. & Sorkin, R. D. Quantum source of entropy for black holes. *Physical Review D* **34**, 373–383 (July 1986).
165. Summers, S. J. & Werner, R. Bell’s inequalities and quantum field theory. II. Bell’s inequalities are maximally violated in the vacuum. *Journal of Mathematical Physics* **28**, 2448–2456 (1987).
166. Redhead, M. More ado about nothing. *Foundations of Physics* **25**, 123–137 (Jan. 1995).
167. Halvorson, H. & Clifton, R. Generic Bell correlation between arbitrary local algebras in quantum field theory. *Journal of Mathematical Physics* **41**, 1711–1717 (2000).
168. Reznik, B. Entanglement from the Vacuum. *Found. Phys.* **33**, 167–176 (Jan. 2003).
169. Calabrese, P. & Cardy, J. Entanglement entropy and quantum field theory. *Journal of Statistical Mechanics: Theory and Experiment* **2004**, P06002 (2004).

170. Zych, M., Costa, F., Kofler, J. & Brukner, Č. Entanglement between smeared field operators in the Klein-Gordon vacuum. *Physical Review D* **81**, 125019 (June 2010).
171. Ibnouhsein, I., Costa, F. & Grinbaum, A. Renormalized entropy of entanglement in relativistic field theory. *Physical Review D* **90**, 065032 (Sept. 2014).
172. Su, D. & Ralph, T. C. Spacetime diamonds. *Physical Review D* **93**, 044023 (Feb. 2016).
173. Newton, T. D. & Wigner, E. P. Localized States for Elementary Systems. *Reviews of Modern Physics* **21**, 400–406 (July 1949).
174. Fleming, G. N. Covariant Position Operators, Spin, and Locality. *Physical Review* **137**, B188–B197 (Jan. 1965).
175. Segal, I. E. & Goodman, R. W. Anti-Locality of Certain Lorentz-Invariant Operators. *Journal of Mathematics and Mechanics* **14**, 629–638 (1965).
176. Fleming, G. N. Reeh-Schlieder Meets Newton-Wigner. *Philosophy of Science* **67**, S495–S515 (2000).
177. Halvorson, H. Reeh-Schlieder Defeats Newton-Wigner: On Alternative Localization Schemes in Relativistic Quantum Field Theory. *Philosophy of Science* **68**, 111–133 (2001).
178. Piazza, F. & Costa, F. *Volumes of space as subsystems* in *Proceedings of From Quantum to Emergent Gravity: Theory and Phenomenology* (PoS(QG-Ph)032, Trieste, Italy, 2007).
179. Costa, F. & Piazza, F. Modeling a particle detector in field theory. *New Journal of Physics* **11**, 113006 (2009).
180. Cacciatori, S. L., Costa, F. & Piazza, F. Renormalized thermal entropy in field theory. *Physical Review D* **79**, 025006 (Jan. 2009).
181. Schroeren, D. P. Is Quantum Field Theory ontologically interpretable? On localization, particles and fields in relativistic Quantum Theory. *arXiv:1007.0664 [math-ph, physics:quant-ph]*. arXiv: 1007.0664 (July 5, 2010).
182. Baumann, V. & Brukner, Č. Appearance of causality in process matrices when performing fixed-basis measurements for two parties. *Physical Review A* **93**, 062324 (June 2016).
183. Marino, F., Cataliotti, F. S., Farsi, A., de Cumis, M. S. & Marin, F. Classical Signature of Ponderomotive Squeezing in a Suspended Mirror Resonator. *Physical Review Letters* **104**, 073601 (Feb. 16, 2010).
184. Safavi-Naeini, A. H. *et al.* Squeezed light from a silicon micromechanical resonator. *Nature* **500**, 185–189 (Aug. 2013).
185. Gröblacher, S. *et al.* Demonstration of an ultracold micro-optomechanical oscillator in a cryogenic cavity. *Nature Physics* **5**, 485–488 (July 2009).
186. Tsang, M. Quantum metrology with open dynamical systems. *New Journal of Physics* **15**, 073005 (July 2013).

187. Carmon, T., Rokhsari, H., Yang, L., Kippenberg, T. J. & Vahala, K. J. Temporal Behavior of Radiation-Pressure-Induced Vibrations of an Optical Microcavity Phonon Mode. *Physical Review Letters* **94**, 223902 (June 10, 2005).
188. Sun, X., Zheng, J., Poot, M., Wong, C. W. & Tang, H. X. Femtogram Doubly Clamped Nanomechanical Resonators Embedded in a High-Q Two-Dimensional Photonic Crystal Nanocavity. *Nano Letters* **12**, 2299–2305 (May 9, 2012).
189. Corbitt, T., Ottaway, D., Innerhofer, E., Pelc, J. & Mavalvala, N. Measurement of radiation-pressure-induced optomechanical dynamics in a suspended Fabry-Perot cavity. *Physical Review A* **74**, 021802 (Aug. 15, 2006).
190. Corbitt, T. & Mavalvala, N. Review: Quantum noise in gravitational-wave interferometers. *Journal of Optics B: Quantum and Semiclassical Optics* **6**, S675–S683 (July 2004).
191. Großardt, A., Bateman, J., Ulbricht, H. & Bassi, A. Optomechanical test of the Schrödinger-Newton equation. *Physical Review D* **93**, 096003 (May 4, 2016).
192. Gan, C., Savage, C. & Scully, S. Optomechanical tests of a Schrödinger-Newton equation for gravitational quantum mechanics. *Physical Review D* **93**, 124049 (June 20, 2016).
193. Arvanitaki, A. & Geraci, A. A. Detecting High-Frequency Gravitational Waves with Optically Levitated Sensors. *Physical Review Letters* **110**, 071105 (Feb. 14, 2013).
194. Libbrecht, K. G. & Black, E. D. Toward quantum-limited position measurements using optically levitated microspheres. *Physics Letters A* **321**, 99–102 (Jan. 26, 2004).
195. Guccione, G. *et al.* Scattering-Free Optical Levitation of a Cavity Mirror. *Physical Review Letters* **111**, 183001 (Oct. 29, 2013).
196. Michimura, Y., Kuwahara, Y., Ushiba, T., Matsumoto, N. & Ando, M. Optical levitation of a mirror for reaching the standard quantum limit. *Optics Express* **25**, 13799–13806 (June 12, 2017).
197. Nation, P. D. & Blencowe, M. P. The trilinear Hamiltonian: a zero-dimensional model of Hawking radiation from a quantized source. *New Journal of Physics* **12**, 095013 (2010).
198. Alsing, P. M. Parametric down conversion with a depleted pump as a model for classical information transmission capacity of quantum black holes. *Classical and Quantum Gravity* **32**, 075010 (2015).
199. Alsing, P. M. & Fanto, M. L. Spontaneous parametric down conversion with a depleted pump as an analogue for black hole evaporation/particle production. *arXiv:1507.00429 [gr-qc, physics:hep-th, physics:quant-ph]*. arXiv: 1507.00429 (July 2, 2015).
200. Bowen, W. P. & Milburn, G. J. *Quantum Optomechanics* (CRC Press, Boca Raton, FL, Dec. 2015).

201. Gardiner, C. W. & Collett, M. J. Input and output in damped quantum systems: Quantum stochastic differential equations and the master equation. *Physical Review A* **31**, 3761–3774 (June 1985).
202. Bachor, H.-A. & Ralph, T. C. *A Guide to Experiments in Quantum Optics* 2nd edition (Wiley, Mar. 2004).
203. Schumaker, B. L. Quantum mechanical pure states with gaussian wave functions. *Physics Reports* **135**, 317–408 (Apr. 1, 1986).
204. Adesso, G., Ragy, S. & Lee, A. R. Continuous Variable Quantum Information: Gaussian States and Beyond. *Open Systems & Information Dynamics* **21**, 1440001 (Mar. 12, 2014).
205. Ralph, T. C., Huntington, E. H. & Symul, T. Single-photon side bands. *Physical Review A* **77**, 063817 (June 11, 2008).
206. Huan, T., Zhou, R. & Ian, H. Dynamic entanglement transfer in a double-cavity optomechanical system. *Physical Review A* **92**, 022301 (Aug. 3, 2015).
207. Vanner, M. R., Hofer, J., Cole, G. D. & Aspelmeyer, M. Cooling-by-measurement and mechanical state tomography via pulsed optomechanics. *Nature Communications* **4**, 2295 (Aug. 15, 2013).

Chapter 8

Floating Mirror covariance matrix elements

For brevity, Eq. (6.105) had extremely compressed notation. By design, the notational excluded factors of i in the sine quadratures and the P quadratures. In this appendix, I have restored the factors of i and explicitly written the covariance matrix elements down.

$$\begin{aligned}
& \frac{1}{2} \left\langle Q_{i_{\text{out}}}^C(\omega) Q_{j_{\text{out}}}^C(\omega) + Q_{j_{\text{out}}}^C(\omega) Q_{i_{\text{out}}}^C(\omega) \right\rangle \\
&= \frac{1}{2} \left\langle Q_{i_{\text{out}}}^S(\omega) Q_{j_{\text{out}}}^S(\omega) + Q_{j_{\text{out}}}^S(\omega) Q_{i_{\text{out}}}^S(\omega) \right\rangle \\
&= \frac{1}{4} \left\{ \Re \left[B_{i_{\text{out}}}^+(\omega) B_{j_{\text{out}}}^+(\omega)^* + A_{i_{\text{out}}}^+(\omega) A_{j_{\text{out}}}^+(\omega)^* \right] + (\omega \rightarrow -\omega) \right\} \delta(0)
\end{aligned} \tag{8.1}$$

$$\begin{aligned}
& \frac{1}{2} \left\langle Q_{i_{\text{out}}}^C(\omega) Q_{j_{\text{out}}}^S(\omega) + Q_{j_{\text{out}}}^S(\omega) Q_{i_{\text{out}}}^C(\omega) \right\rangle \\
&= -\frac{1}{2} \left\langle Q_{i_{\text{out}}}^S(\omega) Q_{j_{\text{out}}}^C(\omega) + Q_{j_{\text{out}}}^C(\omega) Q_{i_{\text{out}}}^S(\omega) \right\rangle \\
&= \frac{1}{4} \left\{ -\Im \left[B_{i_{\text{out}}}^+(\omega) B_{j_{\text{out}}}^+(\omega)^* + A_{i_{\text{out}}}^+(\omega) A_{j_{\text{out}}}^+(\omega)^* \right] - (\omega \rightarrow -\omega) \right\} \delta(0)
\end{aligned} \tag{8.2}$$

$$\begin{aligned}
& \frac{1}{2} \left\langle P_{i_{\text{out}}}^C(\omega) P_{j_{\text{out}}}^C(\omega) + P_{j_{\text{out}}}^C(\omega) P_{i_{\text{out}}}^C(\omega) \right\rangle \\
&= \frac{1}{2} \left\langle P_{i_{\text{out}}}^S(\omega) P_{j_{\text{out}}}^S(\omega) + P_{j_{\text{out}}}^S(\omega) P_{i_{\text{out}}}^S(\omega) \right\rangle \\
&= \frac{1}{4} \left\{ \Re \left[B_{i_{\text{out}}}^-(\omega) B_{j_{\text{out}}}^-(\omega)^* + A_{i_{\text{out}}}^-(\omega) A_{j_{\text{out}}}^-(\omega)^* \right] + (\omega \rightarrow -\omega) \right\} \delta(0)
\end{aligned} \tag{8.3}$$

$$\begin{aligned}
& \frac{1}{2} \left\langle P_{i_{\text{out}}}^C(\omega) P_{j_{\text{out}}}^S(\omega) + P_{j_{\text{out}}}^S(\omega) P_{i_{\text{out}}}^C(\omega) \right\rangle \\
&= -\frac{1}{2} \left\langle P_{i_{\text{out}}}^S(\omega) P_{j_{\text{out}}}^C(\omega) + P_{j_{\text{out}}}^C(\omega) P_{i_{\text{out}}}^S(\omega) \right\rangle \\
&= \frac{1}{4} \left\{ -\Im \left[B_{i_{\text{out}}}^-(\omega) B_{j_{\text{out}}}^-(\omega)^* + A_{i_{\text{out}}}^-(\omega) A_{j_{\text{out}}}^-(\omega)^* \right] - (\omega \rightarrow -\omega) \right\} \delta(0)
\end{aligned} \tag{8.4}$$

$$\begin{aligned}
& \frac{1}{2} \left\langle Q_{i_{\text{out}}}^C(\omega) P_{j_{\text{out}}}^C(\omega) + P_{j_{\text{out}}}^C(\omega) Q_{i_{\text{out}}}^C(\omega) \right\rangle \\
&= \frac{1}{2} \left\langle Q_{i_{\text{out}}}^S(\omega) P_{j_{\text{out}}}^S(\omega) + P_{j_{\text{out}}}^S(\omega) Q_{i_{\text{out}}}^S(\omega) \right\rangle \\
&= \frac{1}{4} \left\{ -\Im \left[B_{i_{\text{out}}}^+(\omega) B_{j_{\text{out}}}^-(\omega)^* + A_{i_{\text{out}}}^+(\omega) A_{j_{\text{out}}}^-(\omega)^* \right] + (\omega \rightarrow -\omega) \right\} \delta(0)
\end{aligned} \tag{8.5}$$

$$\begin{aligned}
& \frac{1}{2} \left\langle Q_{i_{\text{out}}}^C(\omega) P_{j_{\text{out}}}^S(\omega) + P_{j_{\text{out}}}^S(\omega) Q_{i_{\text{out}}}^C(\omega) \right\rangle \\
&= -\frac{1}{2} \left\langle Q_{i_{\text{out}}}^S(\omega) P_{j_{\text{out}}}^C(\omega) + P_{j_{\text{out}}}^C(\omega) Q_{i_{\text{out}}}^S(\omega) \right\rangle \\
&= \frac{1}{4} \left\{ -\Re \left[B_{i_{\text{out}}}^+(\omega) B_{j_{\text{out}}}^-(\omega)^* + A_{i_{\text{out}}}^+(\omega) A_{j_{\text{out}}}^-(\omega)^* \right] - (\omega \rightarrow -\omega) \right\} \delta(0)
\end{aligned} \tag{8.6}$$

$$\begin{aligned}
& \frac{1}{2} \left\langle P_{i_{\text{out}}}^C(\omega) Q_{j_{\text{out}}}^C(\omega) + Q_{j_{\text{out}}}^C(\omega) P_{i_{\text{out}}}^C(\omega) \right\rangle \\
&= \frac{1}{2} \left\langle P_{i_{\text{out}}}^S(\omega) Q_{j_{\text{out}}}^S(\omega) + Q_{j_{\text{out}}}^S(\omega) P_{i_{\text{out}}}^S(\omega) \right\rangle \\
&= \frac{1}{4} \left\{ \Im \left[B_{i_{\text{out}}}^-(\omega) B_{j_{\text{out}}}^+(\omega)^* + A_{i_{\text{out}}}^-(\omega) A_{j_{\text{out}}}^+(\omega)^* \right] + (\omega \rightarrow -\omega) \right\} \delta(0)
\end{aligned} \tag{8.7}$$

$$\begin{aligned}
& \frac{1}{2} \left\langle P_{i_{\text{out}}}^C(\omega) Q_{j_{\text{out}}}^S(\omega) + Q_{j_{\text{out}}}^S(\omega) P_{i_{\text{out}}}^C(\omega) \right\rangle \\
&= -\frac{1}{2} \left\langle P_{i_{\text{out}}}^S(\omega) Q_{j_{\text{out}}}^C(\omega) + Q_{j_{\text{out}}}^C(\omega) P_{i_{\text{out}}}^S(\omega) \right\rangle \\
&= \frac{1}{4} \left\{ \Re \left[B_{i_{\text{out}}}^-(\omega) B_{j_{\text{out}}}^+(\omega)^* + A_{i_{\text{out}}}^-(\omega) A_{j_{\text{out}}}^+(\omega)^* \right] - (\omega \rightarrow -\omega) \right\} \delta(0)
\end{aligned} \tag{8.8}$$

To our fellow citizens
Who, for love of truth,
Take from their own wants
By taxes and gifts,
And now and then send forth
One of themselves
As dedicated servant,
To forward the search
Into the mysteries and marvelous simplicities
Of this strange and beautiful Universe,
Our home.

Charles Misner, Kip Thorne and John Wheeler,
Gravitation 1st edition (W. H. Freeman, San Francisco, Sept. 1973)